

Aus der Fakultät für Chemie und Pharmazie
Lehrstuhl für Pharmazeutische Biologie und Biotechnologie
Ludwig-Maximilians-Universität München

angefertigt unter der Leitung von Herrn Univ. Prof. Dr. Ernst Wagner

Vorgelegt an der
Tierärztlichen Fakultät
Department für Veterinärwissenschaften
Lehrstuhl für Molekulare Tierzucht und Biotechnologie
der Ludwig-Maximilians-Universität München
(Vorstand: Univ. Prof. Dr. med. vet. Eckard Wolf)

**In vivo bioluminescence imaging for monitoring of
siRNA mediated luciferase knockdown
in tumor models**

Inaugural-Dissertation
zur Erlangung der tiermedizinischen Doktorwürde
der Tierärztlichen Fakultät der
Ludwig-Maximilians-Universität München

von
Gelja Maiwald
aus
Bielefeld

München 2009

Gedruckt mit Genehmigung der Tierärztlichen Fakultät der
Ludwig-Maximilians-Universität München

Dekan: Univ.-Prof. Dr. Braun

Berichterstatter: Univ.-Prof. Dr. Wolf

Korreferent/en: Priv.-Doz. Dr. Breuer

Tag der Promotion: 13. Februar 2010

Meinen Eltern

The most exciting phrase to hear in science,
the one that heralds new discoveries, is not
'Eureka!' (I found it!) but 'That's funny ...'.

Isaac Asimov
(1920 – 1992)

1	Introduction	1
1.1	Nucleic acid-based therapy	1
1.2	Delivery of nucleic acids	2
1.2.1	OEI – HD1	4
1.2.2	bPEI Succ 10	5
1.2.3	Tf-PLL-DMMAAn-Mel-ss-siRNA	5
1.2.4	PLL50-PEG-DMMAAn-Mel / PLL185-PEG-DMMAAn-Mel	5
1.3	Assessment of nucleic acid transfer systems	5
1.3.1	Toxicity	6
1.3.2	Distribution	6
1.3.3	Efficacy	6
1.4	<i>In vivo</i> bioluminescence imaging for siRNA efficacy studies	9
1.4.1	Integration of luciferase into the HIF-pathway	11
1.5	Aim of this thesis	13
2	Material and Methods	15
2.1	Materials	15
2.1.1	Bacterial culture	15
2.1.2	Molecular biology	16
2.1.2.1	Vector cloning and amplification	16
2.1.2.1.1	Restriction enzymes	17
2.1.2.2	Western blot	17
2.1.2.2.1	Antibodies	18
2.1.2.3	PCR	18
2.1.3	Cell culture	19
2.1.4	<i>In vitro/in vivo</i> transfection experiments	20
2.1.4.1	Synthetic siRNA vectors	21
2.1.4.2	siRNA	22
2.1.4.3	Plasmids	22
2.1.4.4	Laboratory animals	22
2.1.5	Instruments	23
2.1.6	Software	23
2.2	Amplification of plasmids	23
2.3	Cloning of the SV40 promoter into the pGL4.16 plasmid	24
2.4	Western blot	24
2.5	RtQPCR	24
2.6	Cell culture	25
2.6.1	Maintenance of cultured cells	25

2.6.2	Luciferase reporter gene assay	25
2.6.3	VHL protein expression in Neuro 2a	25
2.6.4	Creation of transgenic luciferase expressing Neuro 2a cell clones	26
2.6.5	Preparation of primary ODD Luc expressing fibroblasts.....	26
2.6.6	Luciferase gene silencing.....	26
2.7	Animal experiments.....	27
2.7.1	Characterization of subcutaneous tumor mouse models	27
2.7.2	siRNA delivery experiments	27
2.7.2.1	Polyplex mediated siRNA delivery	27
2.7.2.2	Hydrodynamic siRNA delivery	28
2.7.3	Implantation of tumor fragments.....	29
2.7.4	Transgenic cell injection into wildtype tumor tissue.....	29
2.7.5	Luciferin kinetic studies	29
3	Results	31
3.1	Generation of different monoclonal Luc transgenic Neuro 2a cells.....	31
3.1.1	Cloning of plasmid GL4.16SV40.....	31
3.1.2	Evaluation of expression intensities of luciferase encoding plasmids	32
3.1.3	Expression intensities of stably luciferase expressing Neuro 2a cell clones.....	32
3.2	Characterization and optimisation of subcutaneous tumor mouse models.....	34
3.2.1	Characterization of the different Luc transgenic cell clones	34
3.2.2	Influence of luciferin distribution on the bioluminescence signal	37
3.2.3	Influence of animal positioning on the bioluminescence signal	39
3.2.4	Influence of transgenic cell number on the bioluminescence signal.....	40
3.3	Utilization of mouse models for detection of effective siRNA delivery	42
3.3.1	Utilization of the negative readout system (Neuro 2a Luc+)	42
3.3.1.1	Tf-PLL-DMMAn-Mel-ss-siRNA	42
3.3.1.2	OEI-HD1/Tf-OEI-HD1 (90/10).....	45
3.3.1.3	bPEI Succ 10	48
3.3.1.4	PEI (22 kDa).....	53
3.3.1.5	PLL50- PEG-DMMAn-Mel / PLL185- PEG-DMMAn-Mel	55
3.3.2	Utilization of the positive readout system (Neuro 2a ODD Luc).....	59
3.3.2.1	A/J Neuro 2a ODD Luc tumor mouse model	59
3.3.2.2	ODD Luc transgenic mouse strain.....	60
4	Discussion.....	63
4.1	Generation of different monoclonal Luc transgenic Neuro 2a cell lines.....	63
4.2	Characterization and optimization of subcutaneous tumor mouse models.....	64
4.3	Utilization of mouse models for detection of effective siRNA delivery	68

4.3.1	Utilization of the negative readout system (Luc+).....	68
4.3.1.1	Impact of the transfer vector.....	69
4.3.1.2	Impact of the measurement method.....	71
4.3.2	Utilization of the positive readout system (ODD Luc).....	73
4.3.2.1	A/J Neuro 2a ODD Luc tumor mouse model.....	73
4.3.2.2	ODD Luc transgenic mouse strain.....	73
5	Summary.....	76
6	Zusammenfassung.....	78
7	Appendix.....	80
7.1	Supplements.....	80
7.2	Abbreviations.....	82
7.3	Publications.....	84
8	References.....	85
9	Acknowledgement.....	96

1 Introduction

1.1 Nucleic acid-based therapy

Nucleic acid-based therapy holds tremendous promise in the treatment of many genetic and acquired diseases by delivering therapeutic nucleic acids into patients. In general it exhibits the possibility to compensate a genetic defect or to indirectly mediate a therapeutic effect (“gain of function”) or to silence target genes, which are either pathogenic or essential for cell viability (“loss of function”).

Meanwhile more than 1500 clinical trials on nucleic acid-based therapeutics have been or still are conducted. The indications cover as diverse fields as inherent genetic diseases (e.g. cystic fibrosis, severe combined immunodeficiency (SCID)) and acquired diseases (e.g. infectious diseases, neuropathological diseases). Nevertheless cancer therapy is the main focus (> 60%) (1). Therapeutic effects in cancer treatment are mainly achieved by knocking out genes that facilitate tumor growth, or by introducing therapeutic genes that – when expressed – antagonize tumor growth or cause apoptosis in tumor cells (2, 3).

Standard gene therapy is based on the integration of genes into the target cells genome to correct or mediate the expression of certain proteins. New approaches mainly utilize small interfering RNA (siRNA), which can be used to posttranscriptionally silence protein expression by specific degradation of messenger RNA (mRNA) (4). The mechanism of siRNA mediated gene silencing is adopted from the naturally occurring phenomenon of RNA interference. This is based on double stranded RNA (dsRNA) molecules which are proposed to function as a mechanism for regulation of gene expression on the posttranscriptional level. While delivery of dsRNA to mammalian cells provokes an interferon response and apoptosis, small synthetic dsRNA, so called siRNA does not evoke such effects but is equally effective (5). Within the cytosol siRNA is cleaved into single strands and the antisense strand is incorporated into the RNA induced silencing complex (RISC). If the nucleotide sequence of the antisense strand resembles a sequence within the mRNA of a target gene, this mRNA is cleaved in the middle by RISC. Cleavage of the mRNA leads to reduction of translation and therefore silencing of the targeted gene (6) (Figure 1).

This technology became increasingly important not only in research due to the possibility to create specific knock-down systems for basic research and determination of new therapeutic targets, but also due to its impact as a new therapeutic tool in nucleic acid-based therapy.

Consequently in 2006 Andrew Fire and Craig Mello won the Nobel Prize for their work on RNA interference in *Caenorhabditis elegans* which was published in the year 1998 (7).

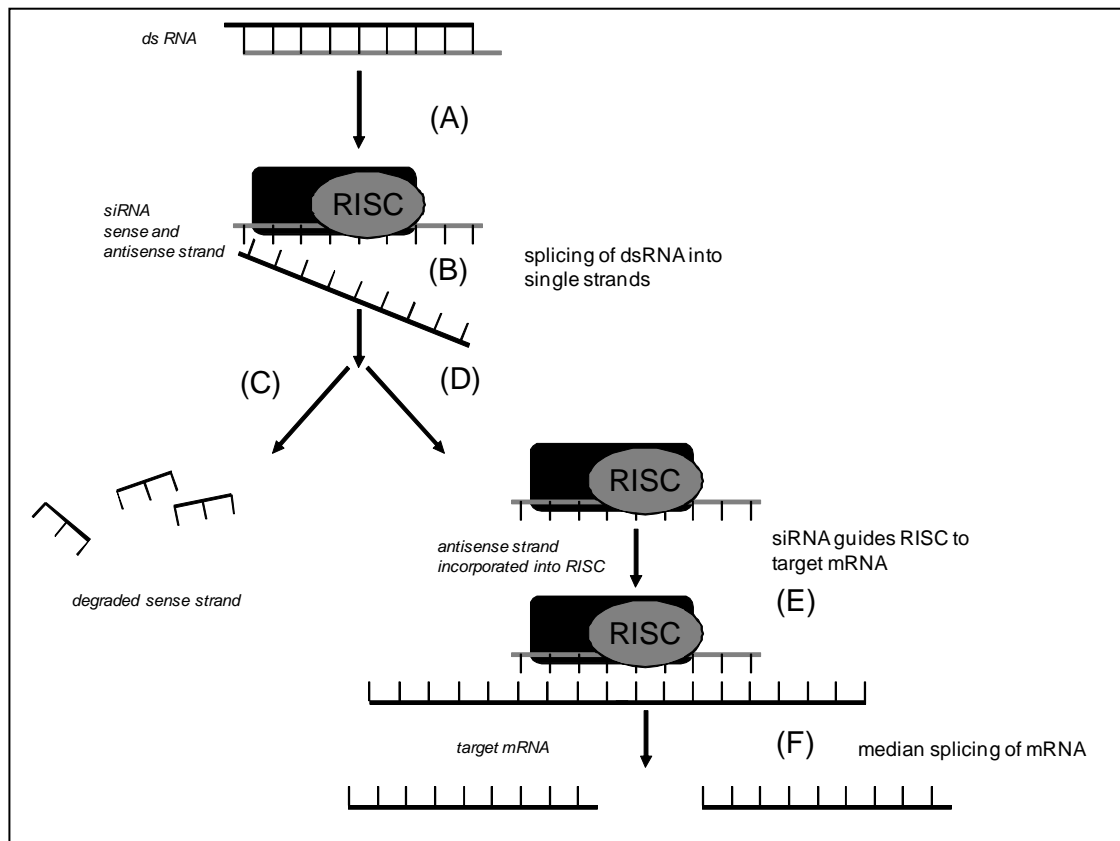


Figure 1: Processing of dsRNA to effective siRNA.

- (A) In the cytosol dsRNA is incorporated into RISC.
- (B) The dsRNA is spliced into single strands.
- (C) The sense strand is degraded.
- (D) The antisense strand remains incorporated in RISC.
- (E) Complementary mRNA sequences are bound by the antisense strand.
- (F) This guides RISC to splice the target mRNA. The corresponding protein is silenced.

Despite these promising data nucleic acid-based therapy still holds a lot of challenges. Nucleic acids naturally are highly hydrophilic and therefore cannot permeate lipid cell membranes. Additionally they are subject to fast degradation by nucleases mainly in the blood stream (8-11). Only for a few applications, like intramuscular injection, electroporation or hydrodynamic injection, naked pDNA led to effective gene transfection (12-15), naked siRNA based therapy was successfully shown in the treatment of age related macula degeneration in mice (16) and has already been applied in humans in clinical trials (17). But for the broad range of indications nucleic acids have to be transported to their target tissues.

1.2 Delivery of nucleic acids

Generally, nucleic acid delivery systems can be divided into two main categories: viral vectors and synthetic transfer systems. Viral vectors are most commonly used in clinical trials due to their high transfection ability (1). Nevertheless their performance is hampered by toxicity, potential of insertional mutagenesis, immunogenicity, low transgene loading size, high costs and low adaptability of design (18, 19). These problems can be overcome by the development

of synthetic gene delivery systems. Such delivery systems are designed to provoke less immunogenicity, to offer a higher loading capacity and to be easily and rather cheaply synthesized. Additionally they implicate the advantage to be easily adaptable to specific needs. On the other hand the major drawback of synthetic vectors is their limited efficacy compared to viral vectors after *in vivo* application. Amongst the synthetic nucleic acid delivery systems the most distinguished subgroups are liposomal formulations and cationic polymers (20, 21). Liposomal formulations are based on cationic lipids, which are amphiphilic molecules. This structure leads in aqueous solutions after condensation of the positively charged head-group with the negatively charged nucleic acids to spontaneous assemblies into nanospheric lipoplexes thereby protecting the nucleic acids from degradation (22). Like cationic lipids, cationic polymers show as well high potential to condense nucleic acids. In the line of cationic polymers polyethylenimine (PEI) has an outstanding position due to its superior transfection efficacy (23-25). Nevertheless its toxicity, which is caused by the positive surface charge, the non-degradability of the polymer and a variety of undesired, unspecific interactions with the biological environment has to be considered (26, 27). Accordingly in the field of cationic polymers as nucleic acid delivery systems the major challenge is to decrease toxicity and simultaneously hold or even increase transfection efficacy compared to the gold standard PEI. Peracute toxicity *in vivo* is mainly caused by the surface charge of the polyplexes leading already in the blood stream either to aggregation with erythrocytes causing embolism or to uptake by macrophages and therefore rapid removal (26, 28-30). Toxicity and rapid clearance can be diminished by shielding of the polyplexes e.g. with polyethylenglycol (PEG), or reduction of their surface charge (31-33). Acute toxicity is also due to accumulation of the polymers in reticular organs such as lung or liver because of their non-degradability (34). This problem can be overcome by using biodegradable polymers, which ideally exhibit high stability in the extracellular surrounding whereas after delivering their payload they degrade to non-toxic metabolites in the intracellular environment (35, 36).

To enhance the transfection efficacy at least two bottle necks have to be taken into consideration. These are specific uptake of the polyplexes by the targeted cells and endosomal release. To allow for specific cellular uptake, polyplexes have on the one hand to be stable in the blood stream (37, 38), on the other hand targeting ligands are needed to enhance the uptake by specific tissues (39). Ligands are as diverse as antibodies (40), peptides (41), transferrin (42), sugars (43), mannuronic acid (44), folate (45) and growth factors such as EGF (46). For effective endosomal release disruption of the endosomal membrane is necessary. Some polycations (e.g. PEI) naturally possess considerable buffering properties below the physiological pH, leading to the so called "proton sponge effect" (47). Briefly explained buffering of the protons by PEI leads to endosomal accumulation of hydrated chloride ions, which subsequently results in osmotic effects leading to swelling and disruption of the

endosome (48). As another possibility to mediate endosomal escape the polymer is conjugated to endosomolytic peptides. Those peptides are either adopted from naturally occurring sequences (e.g. peptides derived from viruses) (49, 50), from the bee venom (51, 52) or artificially synthesized (e.g. GALA) (53).

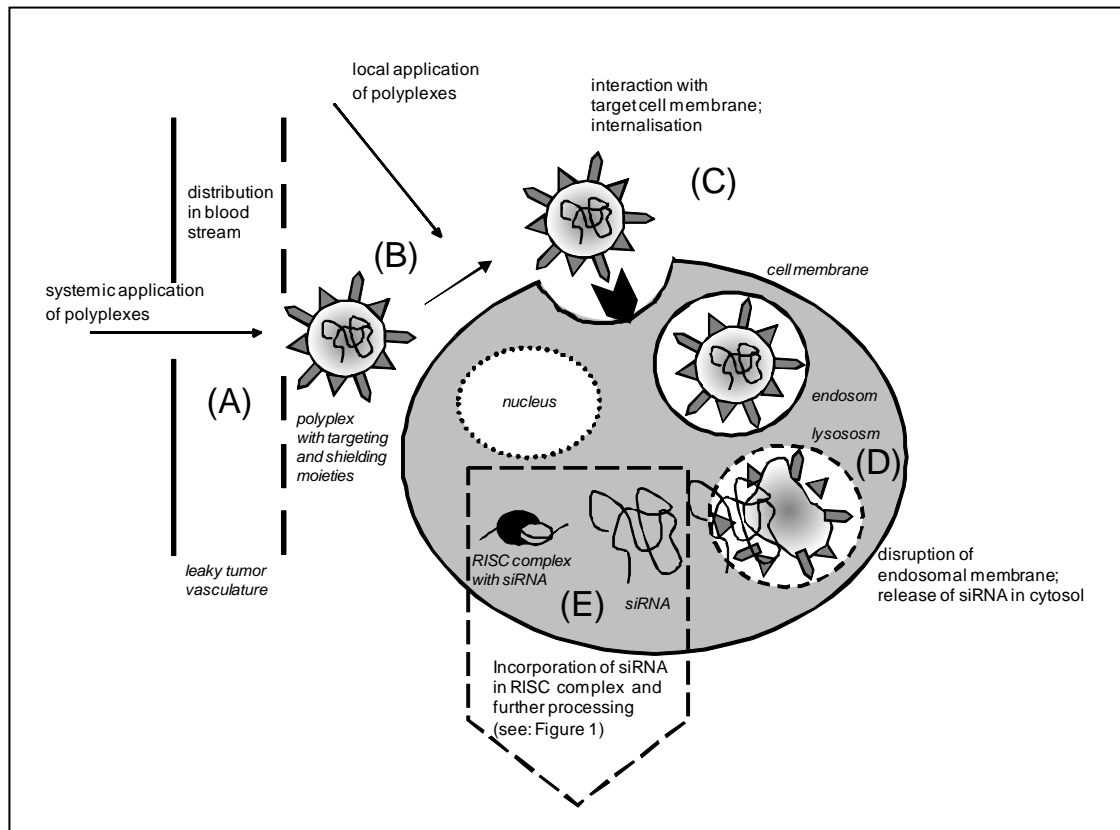


Figure 2: Optimized delivery of nucleic acids from application to action side.

- (A) After systemic application polyplexes are distributed by the bloodstream. Leaky tumor vasculature favours extravasation into extracellular environment. Shielding and diminished surface charge hinder undesired interaction with blood components or aggregation.
- (B) By local application polyplexes directly reach the extracellular environment.
- (C) Polyplexes bind to the cells. Targeting ligands mediate a selective uptake by target cells.
- (D) Polyplexes cause disruption of the endosomal membrane. siRNA cargo is released into the cytosol.
- (E) siRNA is further processed by RISC (see: Figure 1)

The following sections will focus on synthetic vectors used in the present work. For more details on recent developments in the design of nucleic acid delivery systems see Schaffert *et al.* (54) and Meyer *et al.* (55).

1.2.1 OEI – HD1

The polymer is synthesized using oligoethylenimine 800 Da (OEI) and 1, 6-hexanedioldiacrylate (HD) as a linker, resulting in a biodegradable polymer with branched

structure (56). To enhance the specific uptake by tumor cells and provide shielding, OEI-HD1 was further modified adding Transferrin (Tf) as a targeting and shielding ligand (Tf-OEI-HD1). It was shown that a mixture of OEI-HD1 with Tf-OEI-HD1 (w/w: 90/10) is able to promote a specific silencing of the targeted gene in tumor cells *in vitro* and *in vivo* without unspecific toxicity (57). This formulation is subsequently referred to as OEI-HD1/Tf-OEI-HD1 (90/10).

1.2.2 bPEI Succ 10

bPEI Succ 10 is synthesized by succinylation of 10% of the amines of branched PEI 25 kDa (bPEI). This modification decreases the positive charge of the polymer resulting in high transfection efficacy for siRNA and less toxicity in murine neuroblastoma cells (Neuro 2a) *in vitro* compared to PEI (33).

1.2.3 Tf-PLL-DMMAAn-Mel-ss-siRNA

Tf-PLL-DMMAAn-Mel is an analog of the poly-L-lysine (PLL) conjugate described in Meyer *et al.* (58) containing Transferrin (Tf) and melittin peptide (Mel) acylated with 2,3-dimethylmaleic anhydride (DMMAAn). The modification with Tf mediates an effective shielding and a receptor targeting function, and the melittin peptide masked by DMMAAn provides pH-sensitive endosomolytic properties. Extracellular stability is generated by covalent attachment of the siRNA. Therefore this conjugate exhibits high biocompatibility and transfection efficacy *in vitro*.

1.2.4 PLL50-PEG-DMMAAn-Mel / PLL185-PEG-DMMAAn-Mel

PLL50-PEG-DMMAAn-Mel and PLL85-PEG-DMMAAn-Mel were synthesized as PLL-PEG-DMMAAn-Mel (58), but PLL molecules with a defined chain length (PLL 50 and PLL 185) were used. The numbers (50 and 185) thereby refer to the number of lysines in the PLL chain. Thereby the polydispersity of the polymers is diminished and the biocompatibility is enhanced.

1.3 Assessment of nucleic acid transfer systems

Modification of nucleic acid transfer systems in order to decrease toxicity and increase efficacy requires an appropriate assessment of performance. First tests include evaluation of toxicity and efficacy *in vitro*. As a next step toxicity, distribution and efficacy of nucleic acid transfer systems are assessed *in vivo*. *In vivo* applicable methods bear much more challenges as *in vitro* methods. They should allow for consecutive measurements as well as fast and easy analysis, be highly sensitive and specific, facilitate statistically significant results and not at least be compatible with animal welfare. Taken together literally no *in vivo* method so far

fulfils all these demands. The following chapters focus on *in vivo/ex vivo* methods with a special emphasis on methods for efficacy testing.

1.3.1 Toxicity

Preclinical toxicity testing of potential drug candidates for application in clinical trials is excessive. It includes observation of acute and chronic toxicity as well as reproductive and teratogenic toxicity (59). Nevertheless first toxicity tests mainly concentrate on peracute and acute adverse reactions. In case of polycationic transfer systems those are predominantly caused by interference of the polyplexes with blood components, liver or lung tissue (26, 28-30, 34). To predict the interaction of polyplexes with blood components, *ex vivo* erythrocyte leakage assays and blood aggregation assays are performed (36, 58). Affection of liver and lung tissue can be visualized by histopathology of the respective organs. Light microscopic as well as fluorescence microscopic pictures can reveal pathological changes such as adverse metabolism, apoptosis or necrosis (34, 57). Measurement of the blood levels of certain liver enzymes such as aspartate aminotransferase (AST or SGOT) and alanine aminotransferase (ALT or SGPT) illustrate toxic damage to liver cells (57). Additionally in small rodents decreased body weight as a consequence of inappetence is a fast and easy remarkable parameter.

1.3.2 Distribution

Assessment of drug distribution patterns is an essential step to forecast possible side as well as desired effects. It is mainly performed by tagging the drug with a reporter molecule, which can be easily detected. Well established methods are based on fluorescent dyes or quantum dots (Fluorescence Imaging) or radioisotopes (Positron Emission Tomography (PET), Single Photon Emission Computed Tomography (SPECT)) (60, 61). Additionally determination of drug levels in body fluids (e.g. blood, serum, urine, faeces) is facilitated. Nevertheless drug distribution must not be confused with drug efficacy. Even accumulation of the drug in certain tissues does not necessarily implicate efficacy of the drug at this specific side. For example polycations as nucleic acid transfer vector systems are typically distributed over the blood stream throughout the whole body when administered intravenously. Often their side of accumulation differs substantially from the side of action depending on the targeting, thereby making it necessary to equally prove efficacy as well as distribution (34, 62).

1.3.3 Efficacy

In case of nucleic acid delivery the provoked effect that has to be proven is for DNA the expression of a gene resulting in the translation of the encoded protein, and for siRNA the specific silencing of a gene by interaction with the corresponding mRNA resulting in a stop of

protein translation. Therefore efficacy in delivering nucleic acids can for DNA as well as siRNA be shown on the protein as well as on the nucleic acid level.

One of the most sensitive techniques for nucleic acid detection and quantification currently available is Real Time Quantitative Polymerase Chain Reaction (rtQPCR) (63). Messenger RNA is reverse transcribed to cDNA. The specific amplification of cDNA by thermostable DNA polymerase is assessed by fluorescence measurements over the exponential phase of the PCR. The fluorescence signal is generated by using fluorescent dyes that intercalate with double-stranded DNA or sequence specific DNA oligonucleotide probes that fluoresce when being cleaved due to the nuclease activity of DNA polymerase. Therefore the fluorescence signal is proportional to the increasing amount of DNA copies. Values of target mRNA are normalized to mRNA values of a housekeeper, that is unaffected by the therapy.

In the present study, beside Luciferase, Ran was used as target gene. It served as a positive control, because it was already used successfully in our lab as a target for siRNA mediated silencing *in vivo* (57). Ran protein was recently identified from an RNAi based screen as possible target in cancer therapy, as its knockdown with siRNA leads to apoptosis (64). It is a small GTPase and has been implicated in a large number of nuclear processes including regulation of nuclear transport and formation and organisation of the microtubule network (65, 66).

Despite of being a very valuable tool for efficacy testing the above mentioned method bears the disadvantage of relying on single point evaluations *ex vivo*. This implicates that drug kinetics within the same animal cannot be displayed. This consequently leads to higher numbers of animals per experiment, which is problematic due to ethical as well as commercial reasons and moreover does not result in the same level of confidence. With *in vivo* imaging methods these disadvantages can be equalised. There are several methods available at the moment that meet the demands discussed above, for example computer tomography (CT), magnetic resonance imaging (MRI), positron emission tomography (PET), single photon emission tomography (SPECT) and fluorescence as well as bioluminescence imaging (67, 68). CT imaging relies on the different absorption of X-rays by various tissues, thereby allowing for high anatomical resolution imaging (but with relatively low soft tissue contrast) of small animals (69, 70). MRI is based on nuclear magnetic resonance. Unpaired nuclear spins, which are usually hydrogen atoms, align themselves when placed in a magnetic field. They thereby form a net effect called magnetic dipole. The dipoles can be disturbed by using a radio-frequency pulse. When the system thereafter relaxes back to its equilibrium state, the relaxation time corresponds to the physicochemical environment. Due to the differences in magnetic susceptibility of certain tissues MR images with high spatial resolution, versatile contrasts and clear tissue delineation can be obtained. However a drawback lies within the long acquisition and processing time and the low contrast (CT) or sensitivity (MRI),

respectively. In nuclear acid-based therapy CT and MRI can be used to measure therapeutic effects, e.g. the volume of a treated tumor (71). Further effort has been made to improve the contrast (72) and the sensitivity (73-79). PET relies on isotopes emitting positrons (e.g. ^{15}O , ^{13}N , ^{11}C , ^{18}F). The positrons undergo annihilation with nearby electrons, thereby resulting in two gamma-rays. Those gamma-rays are subsequently detected, converted into visible light and displayed as a PET image. In contrast, isotopes for SPECT imaging (e.g. ^{123}I , $^{99\text{m}}\text{Tc}$) directly emit gamma-rays. This technique makes it less sensitive and specific as PET but on the other hand bears the advantage of a longer half-life of the isotopes accompanied by lower costs. For PET as well as SPECT the imperative to apply radiation to the animal is a major drawback and has to be taken into consideration. Marker genes that have been used with PET/SPECT imaging in nucleic acid-based therapy include the thymidine kinase transgene from HSV (HSV-tk) and its mutant version HSV-sr39tk (80-83), which trap their radiolabeled substrates in the cells by phosphorylation. Also other enzyme-based reporter systems (84, 85) and extracellular receptors for transport of radiolabeled molecules into the cell have been facilitated (86). Another widely used marker gene is the human sodium iodine symporter (human NIS) (87, 88), which allows for PET as well as SPECT imaging by mediating cellular uptake of ^{123}I -iodine or $^{99\text{m}}\text{Tc}$ respectively.

Despite the numerous successful experiments that have been performed with the imaging methods described above, *in vivo* optical imaging is more convenient, because it is highly sensitive, relatively cheap, does not rely on radiation and allows for rapid analysis due to its fast acquisition and processing time. Additionally the use of the same marker gene *in vitro* and *in vivo* is possible, which is beneficial. Taken together optical imaging fulfils nearly all demands for a suitable *in vivo* screening system. Still it has to be mentioned that also optical imaging methods have their challenge which mainly lies in attenuation of the signal with increasing signal depth. Optical imaging can be divided into two categories, fluorescence imaging and bioluminescence imaging, and in general employs the detection of light emission by a charge-coupled device (CCD) camera.

In fluorescence imaging light is emitted by a fluorochrome after excitation by an external light source of a different wavelength. For this purpose there are several fluorochromes available. The most prominent are green fluorescent protein (GFP) with an emission wavelength of 509 nm and its variants, e.g. eGFP, which has a longer emission wavelength and is brighter than the wildtyp (89, 90); red fluorescent protein (RFP) (emission wavelength: 574 nm) and its variants offer greater stability and longer emission wavelength (91, 92).

Within nucleic acid-based therapy direct expression of these reporter genes in target tissue or fusion of the reporter to a therapeutic gene are possible opening the way for a broad spectrum of experimental designs (93-95). Nevertheless there are restrictions to fluorescence imaging which originate from a high signal-to-noise ratio due to tissue autofluorescence and absorption

by hemoglobin. To overcome this problem fluorochromes emitting light of a wavelength longer than 600 nm should be used (96), hence tissue penetration can be maximised and autofluorescence diminished (97, 98). In this context the use of quantum dots (QD) which fluorescence brightly up to the near infrared (NIR) spectrum is beneficial (99). But then the toxicity of QD is discussed diversely (100).

In contrast to fluorescence imaging, bioluminescence imaging creates virtually no background light noise as light output is restricted to the expression sites of the luciferase enzymes. These enzymes can catalyze the emission of photons. A major challenge is given by the fact that this enzymatic reaction is depending on the availability of the substrate and in certain cases also on the presence of other co-factors and/or oxygen. Nevertheless bioluminescence imaging has evolved into the most employed technique for detection of effective nucleic acid transfer, including the transfer of siRNA.

1.4 *In vivo* bioluminescence imaging for siRNA efficacy studies

As mentioned above successful siRNA delivery in living subjects will consequently lead to the knockdown of the targeted protein. Protein depletion can be assessed directly by bioluminescence imaging, if the luciferase enzyme itself or a protein that influences the expression of luciferase (e.g. by promoting transcription of luciferase gene) is targeted, or indirectly, if the siRNA mediates death of luciferase expressing cells.

Heidel *et al.* showed reduction of tumor growth by targeting ribonucleotide reductase M2 subunit in transgenic neuroblastoma xenografts with siRNA (101). In order to test the functionality of this siRNA *in vivo*, a cotransfection was performed by high pressure tail vein coinjection of pDNA encoding for a fusion protein of ribonucleotide reductase M2 subunit and luciferase together with the siRNA. This injection technique leads by pressure induced reversion of the blood flow within the liver to highly efficient delivery of nucleic acids to the hepatocytes. Bioluminescence imaging thereafter revealed the silencing of the fusion protein. Pre-treatment of luciferase transgenic neuroblastoma cells with this siRNA before injection into the mice mediated a reduction in tumor growth. High pressure tail vein coinjection was as well used to compare the efficacy of siRNA and shRNA (102). Coinjection of pDNA and siRNA was also conducted in a mouse skin model. Herein siRNA targeted a mRNA bicistronically fused to luciferase mRNA (103). Although a significant siRNA mediated effect could be visualized by bioluminescence imaging, coinjection of pDNA encoding for the target gene together with the siRNA does not represent settings of gene therapy in human beings. Therefore the animal models and test procedures have to be further adapted to more closely mirror therapeutic situations.

Bisanz *et al.* developed a metastatic prostate xenograft mouse model and showed growth retardation of luciferase expressing bone metastases by intratumoral injection of siRNA

targeting alpha-v integrin (104). By establishing a subcutaneous luciferase transgenic neuroblastoma model in A/J mice, Bartlett *et al.* for the first time proved successful siRNA delivery to tumor tissue by directly targeting luciferase (62, 105). This working group also identified parameters within treatment that influence the outcome of siRNA delivery studies (106). Thereby it was shown that there are multiple parameters to be considered to obtain optimized results, such as dosage regimen of siRNA, cell doubling time and half-life of the target protein. Beside these treatment derived factors there are even more aspects to taken into account that originate from bioluminescence imaging itself. As mentioned above bioluminescence imaging relies on the quantification of photons. These photons are emitted due to an enzymatic reaction which depends not only on amount, character and activity of the enzyme, but also on the abundance of substrate, oxygen and energy. Additionally the detection of emitted photons can be hampered by tissue specific attenuation due to absorption and scattering of light by haemoglobin or melanin (107). The intensity of photons in the visible spectrum, such as that produced by luciferases, are attenuated approximately 10-fold per cm of tissue.

Coming along with the importance of luciferases as reporter enzymes there are several different luciferases available. The most commonly used luciferase is derived from *Photinus pyralis* (firefly luciferase). It oxidizes its substrate, luciferin, to oxyluciferin thereby producing light with a broad emission spectrum and a peak at approximately 560 nm (108). This reaction depends on energy (ATP) and oxygen. Click beetle green and click beetle red luciferases, which were isolated from *Pyrophorus plagiophtalamus* and subsequently optimised for different wavelengths (544 and 611 nm, respectively) rely on the same enzymatic reaction (109). At 37 ° C, and taking attenuation into account, light emission from click beetle and firefly luciferases is comparable.

Luciferases from *Renilla reniformis* and *Gaussia princes* react with a different substrate, coelenterazine, thereby producing light with an emission peak at approximately 480 nm (110-113). Albeit being oxygen dependent, this reaction is independent of ATP. The utility of renilla and gaussia luciferases for *in vivo* imaging is hampered by their short wavelength and higher background signals caused by auto-oxidation of coelenterazine. On the other hand their independency of energy as well as the fact, that gaussia luciferase is secreted, makes them interesting tools for imaging studies. Therefore currently efforts are undergone to create renilla and gaussia luciferases with longer wavelengths (113). In addition to the enzymes, lux operons from bacteria, such as *Photorhabdus luminescence*, emit blue light without the need for an exogenous substrate. This effect has been used to monitor bacterial infections by bioluminescence imaging. However there has been insufficient research to determine if transfer of this operon to mammalian cells would be possible.

Alongside with optimization of the wavelength there is high effort put into alteration of the enzymes stability. Firefly luciferase has a half-life of approximately 3 – 4 hours, which should not limit the quantitative bioluminescence determination when performed as daily measurements. Nevertheless, destabilization motifs (e.g. PEST or tetra-ubiquitin) are used to shorten the half-life of luciferase (114, 115). Another approach is the identification of luciferase mutants with improved pH, thermal, and/or proteolysis resistance (116-118).

Beside the luciferase enzyme itself, biodistribution and pharmacology of the substrates are critical parameters and have to be standardized for reproducible quantification of bioluminescence.

In case of luciferin typically 150 mg/kg body weight are applied systemically by intraperitoneal injection. It has been reported that this concentration does not always lead to a maximal bioluminescence signal. Higher luciferin concentrations as well as local application increased the signal output dramatically with dependence on anatomic localization of the reporter (119). This is further supported by the finding, that ¹²⁵I-labeled luciferin is not distributed equally throughout the animal body with lower amounts in tissues such as bone, heart, skeletal muscle or brain (120). This result might however partly rely on the label itself.

Coelenterazine typically is injected directly into the circulation, either through tail vein or intracardiac injection. This route of application is more cumbersome and additionally the substrate distribution is hampered by active transport out of the tissue (121, 122). In addition to the above mentioned auto-oxidation these are severe drawbacks for this substrate and consecutively for renilla and gaussia luciferase.

Another parameter that strongly influences the measurements is the kinetic of bioluminescence. While renilla and gaussia luciferase produce flash kinetics with a peak 1 – 2 minutes after injection (110), kinetic is prolonged for firefly and click beetle luciferase with peaks after approximately 10 – 20 minutes. Therefore models that are based on renilla or gaussia luciferase are more likely to be affected by variations in timing between substrate injection and image acquisition. But even measurements using firefly and click beetle luciferase depend on exact time management.

Independently of the utilized luciferase further modifications are possible to adapt bioluminescence imaging to special needs. An often performed option is the control of luciferase expression by a physiological cellular pathway. An example that was as well facilitated in the present work is the hypoxia inducible factor (HIF) pathway.

1.4.1 Integration of luciferase into the HIF-pathway

The transcription complex hypoxia inducible factor (HIF) plays a central role in the maintenance of the oxygen (O₂) homeostasis, which is essential for cell survival (123). HIF is tightly regulated in an O₂-dependent manner by hydroxylation of one of the three HIF subunits

(HIF1, HIF2, and HIF3) (124, 125). In well oxygenated cells (normoxia), the hydroxylation of two proline residues by the HIF-prolyl hydroxylases (prolyl hydroxylase domains (PHDs)) allows the specific recognition and polyubiquitination by the von Hippel-Lindau protein (pVHL) E3-ligase complex, leading to proteasomal degradation (126). Moreover, the hydroxylation of an asparagine residue by the factor inhibiting HIF (FIH) prevents binding of the coactivator p300/CBP and hence blocks HIF transcriptional activity (127). In contrast, restricted O₂ availability by preventing HIF hydroxylation results in HIF stabilization and activation of the HIF transcriptional complex. Like FIH, the PHDs belong to the super family of iron- and 2-oxoglutarate-dependent dioxygenases, which, by using O₂ as a cosubstrate, provide the molecular basis for their O₂-sensing function (128). In mammalian cells, three PHD isoforms have been identified (PHD1, PHD2, and PHD3) and have been shown to hydroxylate HIF1 (129). It was reported that PHD2 has a dominant role, as it is the rate-limiting enzyme that sets the low steady-state level of HIF1 in normoxia (130, 131).

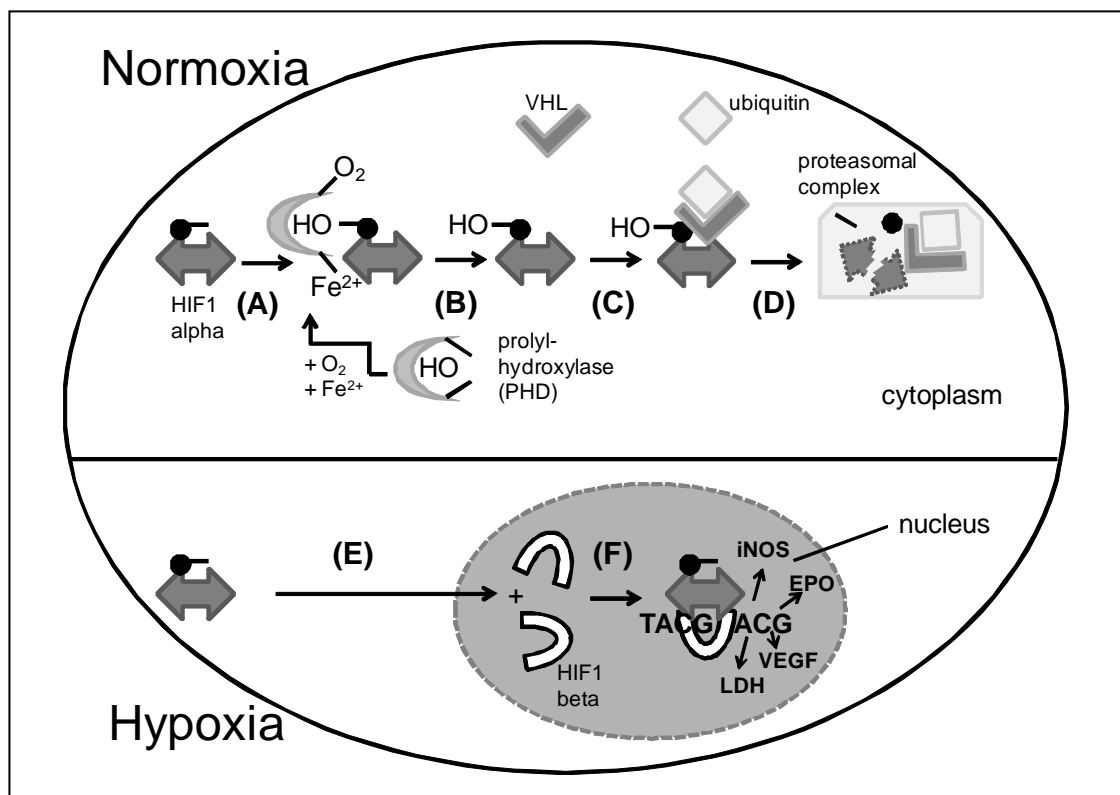


Figure 3: HIF pathway under normoxic or hypoxic conditions.

(A) – (D) Normoxic conditions. (E) – (F) Hypoxic conditions.

- (A) Proline residues of HIF1 alpha subunit are hydroxylated by PHD enzymes in an oxygen and iron dependent reaction.
- (B) Hydroxylated HIF1 alpha is recognized by VHL
- (C) and subsequently polyubiquitinated.
- (D) Ubiquitination leads to degradation of HIF1 alpha subunit.
- (E) HIF1 alpha subunit translocates into the nucleus.
- (F) HIF1 alpha and HIF 1 beta form a dimer, which activates transcription of HIF dependent genes such as erythropoietin (EPO), vascular endothelial growth factor (VEGF), inducible nitric oxide synthase (iNOS) or lactate dehydrogenase (LDH).

Luciferase can be set under the control of the HIF-pathway by different approaches. Gillespie *et al.* for example used tumor cells expressing luciferase under the control of a modified thymidine kinase promoter. Therefore it was consistently expressed in a hypoxia- and HIF-1–dependent manner (132). By targeting HIF1 with siRNA mediated treatment they were able to show a substantially decrease of luciferase by bioluminescence imaging in a tumor mouse model.

Another approach is the employment of a fusion protein of HIF and luciferase (133). Applicability of this construct for hypoxia detection and tests of small molecule PHD inhibitors was shown *in vitro* as well as *in vivo*.

Taken together these data implicate that with bioluminescence imaging highly sensitive images of siRNA mediated protein knockdown can be obtained. But for every single purpose a highly specific animal model and measurement protocol has to be tailored, which exactly meets the needs.

1.5 Aim of this thesis

The imperative to specifically tailor a mouse model for successful evaluation of siRNA delivery was pointed out above. Accordingly, the aim of this thesis is the generation, characterization and utilization of a mouse model for *in vivo* evaluation of siRNA delivery by synthetic vectors to tumor tissue. As bioluminescence imaging is the most advantageous *in vivo* imaging method it was therefore chosen for the experimental design. Beside the traditional method that relies on a reduction of bioluminescent signal as the readout (reducible, negative readout system) the development of a method that shows an induction of bioluminescent signal in case of successful siRNA delivery (inducible, positive readout system) was aimed.

The negative readout transgenic tumor cell clones were established based on some subtypes of firefly luciferase that differed in expression intensity and protein half-life (Luc, Luc+, Luc2). Such transgenes are designed to lead to increasing expression intensities. In order to decrease the enzyme half-life, Luc2 was equipped with two degradation sequences (CL1-PEST) (134). The positive readout transgenic tumor cell clones rest upon a fusion construct of one of the oxygen depending domains (ODD) of HIF1alpha and firefly luciferase (ODD Luc). Thereby luciferase expression is directly controlled by the HIF pathway (133).

As tumor cell line the murine neuroblastoma cell line Neuro 2a was chosen. Neuro 2a cells are known to overexpress the Tf-receptor, which allows for proper cell targeting by Tf-containing siRNA particles, and to reliably form well vascularized subcutaneous tumors in A/J as well as SCID mice, which is beneficial for systemic delivery (35, 57, 135). Additionally good

correlation between *in vitro* and *in vivo* tests was anticipated because these cells have as well been used for *in vitro* experiments.

The newly derived transgenic cell clones were characterized *in vitro* and *in vivo* by evaluation of bioluminescent signal and growth kinetics. Additionally the tumor mouse models had to be specifically optimized according to the demands of siRNA delivery studies. This was done by ruling out the influence of certain parameters on the bioluminescent readout. The best performing tumor mouse models were selected for further implementation in siRNA delivery studies. In addition to the ODD luciferase transgenic tumor mouse model transgenic mice expressing ODD luciferase in all tissues were utilized for siRNA treatment. SiRNA treatments were performed *in vitro* as well as *in vivo*.

2 Material and Methods

2.1 Materials

Materials were purchased/prepared as stated below.

2.1.1 Bacterial culture

LB-plates	<ul style="list-style-type: none"> - Bacto-Trypton (AppliChem, Darmstadt, Germany): 10g - Yeast Extract (AppliChem, Darmstadt, Germany): 5g - NaCl (Merck, Darmstadt, Germany): 5g - Agar (AppliChem, Darmstadt, Germany): 15 g - ad 1 liter with aqua bidest
-----------	--

LB-medium	<ul style="list-style-type: none"> - Bacto-Trypton (AppliChem, Darmstadt, Germany): 10g - Yeast Extract (AppliChem, Darmstadt, Germany): 5g - NaCl (Merck Darmstadt, Germany): 5g - ad 1 liter with aqua bidest
-----------	---

Ampicillin	SIGMA-Aldrich (Steinheim, Germany)
------------	------------------------------------

TfbI	<ul style="list-style-type: none"> - 30 mM KAc (Merck, Darmstadt, Germany): 0.29 g - 50 mM MnCl₂ (Merck, Darmstadt, Germany): 0.99 g - 100 mM KCl (Merck, Darmstadt, Germany): 0.75 g - 10 mM CaCl₂ (Merck, Darmstadt, Germany): 0.11 g - 15% Glycine (Merck, Darmstadt, Germany): 15 mL - ad 100 mL with aqua bidest - adjust on pH 5,8 with acetic acid
------	--

TfbII	<ul style="list-style-type: none"> - 10 mM Na MOPS (Fluka, Steinheim, Germany): 0.21 g - 75 mM CaCl₂ (Merck, Darmstadt, Germany): 0.83 g - 10 mM KCl (Merck, Darmstadt, Germany): 0.075 g - 15% Glycine (Merck, Darmstadt, Germany): 15 mL - ad 100 mL with aqua bidest
-------	---

Comp. E. coli (Dh5 alpha)	<ul style="list-style-type: none"> - incubate 50 µL DH5alpha in 1 mL LB medium without antibiotics overnight - cultivate 1 mL of overnight culture in 100 mL medium
---------------------------	---

until OD550 reaches 0.5

- centrifuge with 3500 rpm at 4 °C for 5 minutes
- resuspend pellet in 40 mL icecooled TfbI buffer
- incubate on ice for 20 minutes
- centrifuge with 2500 rpm at 4 °C for 5 minutes
- resuspend pellet in 4 mL TfbII

2.1.2 Molecular biology

2.1.2.1 Vector cloning and amplification

T4 DNA ligase	Promega (Mannheim, Germany)
T4 DNA ligation buffer	Promega (Mannheim, Germany)
Restriction buffers	New England BioLabs (Ipswich, U.S.A.) / Promega (Mannheim, Germany)
BSE	New England BioLabs (Ipswich, U.S.A.) / Promega (Mannheim, Germany)
EndoFree plasmid kits (Mini/Maxi/Mega/Giga)	Quiagen (Hilden, Germany)
10x TBE elektrophorese buffer	<ul style="list-style-type: none"> - Tris base (SIGMA-Aldrich, Steinheim, Germany): 108 g - Boric acid (Merck, Darmstadt, Germany): 55g - ad 700 mL with aqua bidest - 0.5 M EDTA (SIGMA-Aldrich, Steinheim, Germany)): 40 mL - adjust with NaOH (VWR International, Darmstadt, Germany) on pH 8 - ad 1 liter with aqua bidest
Agarose	Invitrogen (Karlsruhe, Germany)
Ethidiumbromide	SIGMA-Aldrich (Steinheim, Germany)
DNA-marker	Peqlab Biotechnologie (Erlangen, Germany)

2.1.2.1.1 Restriction enzymes

Apa L1	BioLabs (Ipswich, U.S.A.)
Nhe I	BioLabs (Ipswich, U.S.A.)/Promega (Mannheim, Germany)
Hind III	BioLabs (Ipswich, U.S.A.)/Promega (Mannheim, Germany)
Avr II	BioLabs (Ipswich, U.S.A.)
Sal I	BioLabs (Ipswich, U.S.A.)
Bgl II	Promega (Mannheim, Germany)

2.1.2.2 Western blot

Blotting membrane (PVDF)	Macherey-Nagel (Düren, Germany)
BSA	Invitrogen (Karlsruhe, Germany)
Pierce protein detection kit	Thermo Scientific (Bonn, Germany)
1.5 M Tris pH 8.8	- Tris base (SIGMA-Aldrich (Steinheim, Germany)) - add 70 mL Aqua bidest - correct on pH 8.8 - ad 100 mL with aqua bidest
Acrylbis (30%)	Bio-Rad (München, Germany)
SDS (10%)	- SDS (Roth, Karlsruhe, Germany): 10g - ad 100 mL with aqua bidest
TEMED	Promega (Mannheim, Germany)
APS (10%)	- Ammoniumpersulfat (SIGMA-Aldrich, Germany): 1 g - ad 100 mL with aqua bidest
Precision plus protein dual color standards	Bio-Rad (München, Germany)
Methanol	ACROS (Geel, Belgium)
Transferbuffer	- 25 mM Tris base (Fluka , Steinheim, Germany): 3.03 g - 192 mM Glycine (Merck, Darmstadt, Germany): 14.4 g - solve in 400 mL aqua bidest - add 100 mL Methanol (ACROS, Geel, Belgium)
10 x TBS buffer	- Tris base (Fluka, Steinheim, Germany): 24.2 g

- NaCl (VWR International, Darmstadt, Germany): 80 g
- solve in 800 mL aqua bidest
- correct pH with HCl (SIGMA-Aldrich, Steinheim, Germany) on pH 7.6
- ad 1 liter with aqua bidest

Blocking buffer	<ul style="list-style-type: none"> - 10 x TBS Buffer: 15 mL - milk powder: 7.5 g - aqua bidest: 135 mL - Tween-20 (SIGMA-Aldrich, Steinheim, Germany): 150 µL
Washing buffer	<ul style="list-style-type: none"> - 10 x TBS Buffer: 100 mL - aqua bidest: 900 mL - Tween-20 (SIGMA-Aldrich, Steinheim, Germany): 1mL
ECL spray	Upstate Cell Signaling Solutions (Billerica, U.S.A.)

2.1.2.2.1 Antibodies

antiVHL antibody	Cell Signaling (Frankfurt a.M., Germany)
anti alpha tubulin antibody	SIGMA-Aldrich (Steinheim, Germany)
2nd antibodies	Vector Laboratories (Burlingame, U.S.A.)

2.1.2.3 PCR

Sequences in 5' – 3' direction are stated following the purchasing company.

oligo-dT-primers	MWG Biotech (Eberberg, Germany)
DNA extraction kit (Wizard Promega)	Promega (Mannheim, Germany)
PCR buffer	Promega (Mannheim, Germany)
Q-solution	Promega (Mannheim, Germany)
MgCl ₂	Promega (Mannheim, Germany)
dNTPs	Promega (Mannheim, Germany)
High pure RNA tissue kit	Roche Diagnostics (Mannheim, Germany)
Primers (Luciferase)	Roche Diagnostics (Mannheim, Germany)

	L: TGAGTACTTCGAAATGTCCGTTC R: GTATTCAGCCCATATCGTTTCAT
Primers (Ran)	Roche Diagnostics (Mannheim, Germany) L: ACCCGCTCGTCTTCCATAC R: ATAATGGCACACTGGGCTTG
Lysis buffer	Roche Diagnostics (Mannheim, Germany)
Transcriptor high fidelity cDNA synthesis kit	Roche Diagnostics (Mannheim, Germany)
Random hexamer primers	Roche Diagnostics (Mannheim, Germany)
Universal probe library hydrolysis probe #2/#29	Roche Diagnostics (Mannheim, Germany)
Mouse GADP gene assay	Roche Diagnostics (Mannheim, Germany)
Mouse BACT gene assay	Roche Diagnostics (Mannheim, Germany)
2.1.3 Cell culture	
Murine neuroblastoma Neuro 2a cells	LGC Standards (ATCC CCI-131)
Neuro 2a eGFP Luc cells	Neuro 2a cells stably expressing a fusion protein of eGFP and Photinus pyralis luciferase were constructed in our lab by Jaroslav Pelisek.
DMEM 1 g glucose	- DMEM, 4.5 g Glucose/L, with L-Glutamin, without NaHCO ₃ (Biochrom, Berlin, Germany): 10.15 g - NaHCO ₃ p.A.: 3.7 g - ad 1 liter with aqua bidest
OptiMEM	Invitrogen (Karlsruhe, Germany)
Penicillin-Streptomycin	Biochrom (Berlin, Germany)
FBS	Invitrogen (Karlsruhe, Germany)
L-alanyl-L-glutamine	Biochrom (Berlin, Germany)
G418	Invitrogen (Karlsruhe, Germany)
Puromycin	SIGMA-Aldrich (Steinheim, Germany)
Hygromycin	SIGMA-Aldrich (Steinheim, Germany)

Cell culture plates	TPP (Trasadingen, Switzerland)
Cell culture flasks	TPP (Trasadingen, Switzerland)
TE	Biochrom (Berlin, Germany)
PBS	- Phosphat buffered saline (Biochrom, Berlin, Germany): 9.55g - ad 1 liter with aqua bidest
Clon ring	SIGMA-Aldrich (Steinheim, Germany)
Rich cream	SIGMA-Aldrich (Steinheim, Germany)
Amphotericin B	SIGMA-Aldrich (Steinheim, Germany)

2.1.4 *In vitrolin vivo* transfection experiments

HBS	- HEPES (Biomol, Hamburg, Germany): 2.38 g - ad 300 mL with aqua bidest - adjust with NaOH (VWR International, Darmstadt, Germany) on pH 7.1 - NaCl (VWR International, Darmstadt, Germany): 4.383 g - check pH, ad 500 mL with aqua bidest
HBG	- HEPES (Biomol, Hamburg, Germany): 2.38 g - ad 300 mL with aqua bidest - correct with NaOH (VWR International, Darmstadt, Germany) on pH 7.1 - Glucose-Monohydrat (Merck, Darmstadt, Germany): 27.5 g - check pH, ad 500 mL with aqua bidest
HBS 0,5	HBS/HBG: 1/1
Recombinant luciferase	Promega (Mannheim, Germany)
Luciferase cell culture lysis reagent	Promega (Mannheim, Germany)
Luciferin	Promega (Mannheim, Germany)
LAR	- 1 M Glycylglycin (Merck, Darmstadt, Germany): 2 mL - 100 mM MgCl (Carl Roth, Karlsruhe, Germany): 1mL

- 500 mM EDTA (SIGMA-Aldrich, Steinheim, Germany): 20 μ L
- DTT (SIGMA-Aldrich, Steinheim, Germany): 50.8 mg
- ATP (Roche, Mannheim, Germany): 27.8 mg
- Coenzym A (SIGMA-Aldrich, Steinheim, Germany): 0.5 mL
- ad 100 mL with aqua bidest
- adjust with NaOH (VWR International, Darmstadt, Germany) on pH 8 – 8.5

Deferoxamine	SIGMA-Aldrich (Steinheim, Germany)
Isoflurane ®	cp Pharma (Burgdorf, Germany)
Bepanthere®	Roche (Grenzach-Whylen, Germany)
Ketavet® 100 mg/mL	Pfizer, Pharmacia GmbH (Karlsruhe, Germany)
Rompun® 2%	Bayer Vital GmbH (Leverkusen, Germany)
Syringes	Heiland (Hamburg, Germany)
Needles	Heiland (Hamburg, Germany)
Isotonic sodiumchloride solution	B Braun Melsungen AG (Melsungen, Germany)

2.1.4.1 Synthetic siRNA vectors

Linear PEI 22 kDa	PEI (22 kDa) was synthesized by acidcatalysed deprotection of poly(2-ethyl-2-oxazoline) (50 kDa, Aldrich) in analogous form as described in Brissault <i>et al.</i> (136) and is also available from Polyplus Transfections (Strasbourg, France).
OEI-HD 1	OEI-HD 1 was synthesized by crosslinking of oligoethylenimines 800 (OEI) with 1,6-hexanedioldiacrylate (HD) as described in Kloeckner <i>et al.</i> (56).
bPEI Succ 10	PEI Succ 10 was synthesized by succinylation of LPEI as described in Zintchenko <i>et al.</i> (33).
Lipofectamine	Invitrogen (Karlsruhe, Germany)
Tf-PLL- DMMAAn- Mel /	PLL- DMMAAn-Mel was synthesized by modification of PLL according to Meyer <i>et al.</i> (58).

PLL50-PEG-DMMA_n-Mel / Tf was integrated (Tf-PLLDMMAn-Mel) or PLL of a defined
 PLL185-PEG-DMMA_n-Mel chain length (PLL50, PLL185) were used (PLL50-PEG-
 DMMA_n-Mel, PLL185-PEG-DMMA_n-Mel).

2.1.4.2 siRNA

Sequences of the sense strand in 5' – 3' direction are stated following the purchasing company.

Control #3	Eurofins MWG Operon (Ebersberg, Germany) AUGUAUUGGCCUGUAUUAGUUDtT
------------	--

Luc	Eurofins MWG Operon (Ebersberg, Germany) CUUACGCUGAGUACUUCGAdTtT
-----	---

VHL #50	Ambion (Darmstadt, Germany) #50: GGACUUCUGGUUAACCAAAdTtT
---------	---

PHD2	Eurofins MWG Operon (Ebersberg, Germany) GAACUCAAGCCCAAUUCAG dTtT
------	--

2.1.4.3 Plasmids

pCMV Luc	Plasmid Factory (Bielefeld, Germany). The plasmid design is described in Plank <i>et al.</i> (137).
----------	--

pC1	The plasmid was kindly provided by the working group of R. Haase, LMU Munich, München, Germany).
-----	--

pCDNA3 ODD Luc / pCDNA3 Luc	Both plasmids were kindly provided by the working group of W. G. Kaelin, Harvard Medical School, Boston, U.S.A.. The plasmid designs are described in Safran <i>et al.</i> (133).
--------------------------------	--

pGL3 contr.	Promega (Mannheim, Germany)
-------------	-----------------------------

pGL4.16	Promega (Mannheim, Germany)
---------	-----------------------------

2.1.4.4 Laboratory animals

A/JOl _a Hsd (A/J)	Harlan-Winkelmann (Borchen, Germany)
------------------------------	--------------------------------------

NMRI-nu (nu/nu)	Janvier (Le Genest-St-Isle, France)
-----------------	-------------------------------------

FVB.129S6-Gt(ROSA)26Sor CharlesRiver Laboratories (JacksonLab) (Kisslegg, Germany)
 <t mice (FVB ODD Luc)

FVB N/J (FVB) CharlesRiver Laboratories (JacksonLab) (Kisslegg, Germany)

2.1.5 Instruments

Luminometer Lumat LB Berchtold (Tuttlingen, Germany)
 9507

Luminometer Centro LB 960 Berchtold (Tuttlingen, Germany)

Tecan SpectraFlour Plus Tecan (Crailsheim, Germany)

IVIS Lumina Caliper Life Science (Rüsselsheim, Germany)

Shaver Philishave C486 Philips (Hamburg, Germany)

Caliper Digi-Met Peisser (Gammertingen, Germany)

PX2 Thermal Cycler Thermo electron corporation (Karlsruhe, Germany)

Light Cycler 480 Roche Diagnostics (Mannheim, Germany)

2.1.6 Software

MikroWin 2000 Berchtold (Tuttlingen, Germany)

ImageJ National Institute of Health (Bethesda, U.S.A.)

Graph Pad Prism 4 software Graph Pad Software (San Diego, U.S.A.)

Living Image 3.0 Caliper Life Science (Rüsselsheim, Germany)

ProbeFinder 2.44 software Roche Diagnostics (Mannheim, Germany)

2.2 Amplification of plasmids

All plasmids used were amplified in heat shock transformed E.coli. Competent E. coli were defrosted on ice before plasmid DNA was added. Thereafter the bacterial solution was kept on ice for 30 minutes, put into a 42° C water bath for 90 seconds and stored again on ice for 2 minutes. After heat shock transformation overnight colonies were grown using LB plates with ampicillin as selection pressure. Positive colonies were further amplified by overnight culturing in LB medium and plasmid DNA was purified using the EndoFree Plasmid Kits.

2.3 Cloning of the SV40 promoter into the pGL4.16 plasmid

The SV40 promoter was excised from the pGL3 control plasmid using Hind III and Nhe I as restriction enzymes and ligated into the pGL4.16 plasmid, which had been cut with the same enzymes, using T4 DNA ligase in an overnight reaction. (Restriction digest and ligation according to manufacturers protocols.) Thereafter the new vector was transferred into E.coli, propagated and the plasmid was isolated. Bacterial clones expressing the desired pGL4.16SV40 plasmid were identified by restriction digest of purified plasmid DNA with Avr II as restriction enzyme. (Restriction digest was performed according to manufacturers protocol.) Correctly ligated constructs are cut twice, whereas empty pGL4.16 plasmid is cut only once. Positive colonies were further amplified and pGL4.16SV40 plasmid was harvested (see: 2.2). The functionality of this newly generated plasmid was proven by transfection of Neuro 2a cells (see: 2.6.2).

2.4 Western blot

Proteins were extracted from wildtype Neuro 2a cells as described in 2.6.3. 50 µg protein per lane was separated by SDS-PAGE under reducing conditions. Proteins were then transferred on a PVDF membrane and blocked with 5 % fat-free milk powder for one hour at room temperature. Immunostaining was performed using primary murine VHL antibody diluted 1:1000 in blocking buffer over night at 4°C according to manufacturers protocol and peroxidase labelled anti-rabbit-IgG diluted 1:2000 in blocking buffer as the secondary antibody for two hours. VHL protein was visualized using ECL western blotting detection spray. In addition, to allow for normalization of protein expression, detection of the housekeeping protein alpha-tubulin was performed using primary murine antibody for one hour following incubation with anti-mouse HRP-secondary antibody for another hour. For quantification, VHL protein expression of each sample was normalized for the expression of the housekeeping protein alpha-tubulin by quantification using ImageJ.

2.5 RtQPCR

In order to prepare the tumor tissue samples for rtQPCR analysis, the samples were frozen in liquid nitrogen and crushed using a mortar. Twenty mg of the crushed tissues were incubated for 10 min with 400 µL lysis buffer. RNA was isolated using the High Pure RNA Tissue Kit according to the manufacturers protocol. RNA concentration was determined by absorbance at 260 nm. Two hundred ng of total RNA was used as template for cDNA synthesis using the Transcriptor High Fidelity cDNA Synthesis Kit according to manufacturer's protocol. For the reverse transcriptase reaction Random Hexamer Primers were used. For polymerase chain reaction 5 µL of cDNA dilution 1:5 in aqua bidest was used and PCR was performed with primers for luciferase or Ran together with Universal ProbeLibrary hydrolysis probe # 29 (for

Luc) or # 2 (for Ran) respectively. Primers and probes were designed using the ProbeFinder 2.44 software. Furthermore, glyceraldehyde-3-phosphate dehydrogenase (GAPDH) and beta-Actin (BACT) were used as internal standard. Dual-colour Multiplex real-time analysis was performed on the Light Cycler 480, data were acquired using the advanced relative quantification method. PCR was performed at 95°C for 10 minutes denaturation prior to amplification by 45 cycles with 10 seconds (sec) at 95 °C, 30 sec at 60 °C, 1 sec at 72°C and a final cooling step of 30 sec at 40°C.

2.6 Cell culture

2.6.1 Maintenance of cultured cells

All cultured cells were grown at 37 °C in 5% CO₂ humidified atmosphere. Wildtype murine neuroblastoma Neuro 2a cells and primary ODD Luc fibroblasts (preparation: see: 2.6.5) were cultured in DMEM (1 g/L glucose) supplemented with 10% FCS and 1% Penicillin-Streptomycin. Transgenic murine neuroblastoma Neuro 2a cells were cultured in DMEM (1 g/L glucose) supplemented with 10% FCS, 1% Penicillin-Streptomycin and selection antibiotic (Neuro 2a eGFP Luc, Neuro 2a Luc, Neuro 2a Luc+, Neuro 2a ODD Luc: G418 (2,25 mg/mL medium); Neuro 2a Luc2: Hygromycin (1,5 mg/mL medium)).

2.6.2 Luciferase reporter gene assay

For the evaluation of expression efficacy of the different luciferase encoding plasmids the luciferase activity was measured in 96-well plates with pCMV Luc as a reference. 24 h prior to transfection Neuro 2a cells were seeded at a density of 1×10^4 cells in 200 µL medium per well. At the time point of transfection cells reached a confluency of 60% to 80%. Transfections were performed by using polyplexes of LPEI and 200 ng plasmid DNA at a w/w ratio of 0.8/1 in HBS 0.5. Medium was exchanged against 90 µL fresh medium, 10 µL of polyplex solutions were added directly to the cells and after 4 h medium was exchanged against 100 µL fresh one. After 24 hours, cells were washed once with PBS and were subsequently lysed with 50 µL of 1:5 diluted cell culture lysis reagent per well. Luciferase activity was determined from 20 µL samples of the lysates using the luciferase assay system at the luminometer. Two nanograms of recombinant luciferase correspond to 10^7 light units.

2.6.3 VHL protein expression in Neuro 2a

For the evaluation of the expression of VHL, wildtype Neuro 2a cells were grown in cell culture flasks up to 70% confluence, cells were washed once with ice cooled PBS and were subsequently lysed with 200 µL of 1:5 diluted cell culture lysis reagent containing protease inhibitor cocktail. Thereafter a Western Blot was performed (see: 2.4). Protein extracted from murine liver tissue served as a positive control.

2.6.4 Creation of transgenic luciferase expressing Neuro 2a cell clones

To create monoclonal transgenic cell clones expressing different types of photinus pyralis luciferase, wildtype Neuro 2a cells were seeded in 96-well plates at a density of 1×10^3 cells in 200 μ L medium.

At the time point of the first transfection cells reached a confluency of 10%.

24 and 72 h after seeding cells were transfected using LPEI polyplexes (w/w ratio of 0.8/1 in HBS 0.5). 200 ng plasmid DNA per well were used. Medium was exchanged against 90 μ L fresh medium, 10 μ L of polyplex solutions were added directly to the cells and after 4 h medium was exchanged against 100 μ L fresh one. 24 h after the second transfection selection antibiotic was added to the medium (concentration as indicated in 2.6.1). After 3 days under selection pressure wells were washed carefully with PBS to remove dead cells and supplemented with selection antibiotic containing medium. Wells were allowed to reach 70% confluency before splitting of each well into two wells. One well was checked for gene expression (see: 2.6.2), the other one remained as backup.

The backups of those wells tested positive for luciferase expression were maintained further and finally all wells containing cells transgenic for the same type of luciferase were pooled to get one polyclonal cell line.

This cell line was subsequently splitted to a very low density (approximately 5 cells/mL medium) in 96-well-plates in order to generate wells containing only a single cell to derive a cell clone from. Those cell clones were maintained in the wells until they reached a confluency of 70 %, thereafter transferred to cell culture flasks for further maintenance and finally seeded in 96-well-plates at a density of 1×10^4 cells and after 24 h checked for expression efficacy (see: 2.6.2).

2.6.5 Preparation of primary ODD Luc expressing fibroblasts

A newborn heterozygous FVB ODD Luc donor mouse was sacrificed under sterile conditions by cervical dislocation. Small pieces of the ear were sliced, subsequently washed in 70% ethanol for several times and finally put in a cell culture dish containing DMEM (1 g/L glucose) supplemented with 10% FCS, 2% Penicillin-Streptomycin and Amphotericin B (0.25 μ g/mL). Fibroblasts were grown at 37 °C in 5% CO₂ humidified atmosphere until the separated from the ear tissue. During the first splitting ear tissue was removed carefully. Thereafter primary fibroblasts were maintained as described in 2.6.1.

2.6.6 Luciferase gene silencing

To check on the functionality of the newly created transgenic cell clones cells were seeded in 96-well plates using 1×10^4 cells per well 24 h prior to siRNA delivery. At the time point of treatment cells reached a confluency of 60% to 80%. Polyplexes containing 0.25 or 0.5 μ g siRNA per well and the indicated amount of polymers respectively were prepared in 20 mL

HBG per well and after a complexation time of 30 minutes added to cells in 80 μ L medium. Lipoplexes containing 0.25 or 0.5 μ g siRNA per well and the indicated amount of Lipofectamine were prepared in 20 mL OptiMEM per well, after a complexation time of 30 minutes added to cells in 80 μ L serum free medium, and after 4 hours medium was exchanged against 200 μ l fresh serum containing medium. 24 to 72 h after treatment medium was removed and cells were lysed in 50 μ L cell lysis reagent in order to measure the luciferase activity as described in 2.6.2.

2.7 Animal experiments

Animal experiments were performed according to guidelines of the German law of protection of animal life and were approved by the local animal experiments ethical committee. Mice were kept under specific pathogen free conditions in isolated ventilated cages with 5 animals per cage. Cages were equipped with wood shaving litter, a wooden rodent tunnel, cellulose bedding and a mouse house. Autoclaved standard breeding chow and water were provided *ad libitum*. A 12 h day/night cycle, 21° celsius room temperature and 60% humidity were kept. Mice were allowed to adapt to the housing conditions for at least one week before experiments were started.

2.7.1 Characterization of subcutaneous tumor mouse models

A/J mice, female, 6 – 10 weeks old were used (n = 10 per group).

Tumor cells were grown in cell culture as described above, despite being kept in antibiotic free medium for one week prior to injection. To harvest the cells they were trypsinated, washed several times with PBS and diluted in ice cooled PBS at a concentration of 10^6 cells per 150 μ L. One day prior to tumor cell injection the injection side was shaved using a Philishave C486 shaver. One hundred and fifty μ L of the cell suspension were injected subcutaneously at one or both flanks of the mice. Tumor size was measured every second day by caliper and determined as $a*b*c$ (a = length, b = width, c = height). Bioluminescence signal was measured every second day by a CCD camera (IVIS Lumina). Mice were anaesthetized by inhalation of isoflurane in oxygen (2.5% (v/v)) at a flow of 1 liter/min. Thereafter 100 μ L luciferin solution (c = 60 mg/mL) were injected intraperitoneally and allowed to distribute for 10 minutes prior to bioluminescence measurement. Results were evaluated using the Living Image 3.0 software.

2.7.2 siRNA delivery experiments

2.7.2.1 Polyplex mediated siRNA delivery

For these experiments A/J mice, female, 6 – 8 weeks old were used. Subcutaneous Neuro 2a Luc, Neuro 2a Luc+, Neuro 2a Luc2, Neuro 2a eGFP Luc and Neuro 2a ODD Luc tumors

respectively (at one or at both flanks) were set as described in 2.7.1. Two days prior and up to 2 – 4 days after siRNA treatment tumor size and bioluminescence signal were measured every day as described in 2.7.1. When tumors reached a size of about 100 – 200 mm³ siRNA treatment was performed by intravenous or intratumoral injection of polyplexes. For rtQPCR readout tumors were explanted 1 – 4 days after the treatment and rtQPCR was performed as described in 2.5.

For each experiment mice were separated into three groups (n = 5/7 per group): (i) animals treated with target (siLuc or siRAN) siRNA, (ii) animals treated with unspecific scrambled (siContr#3) siRNA and (iii) non-treated animals.

Tf-PLL-DMMA_n-Mel-ss-siRNA was applied in an amount corresponding to 0.625 or 1.250 mg/kg body weight siRNA in 12,5 mL/kg body weight sterile HBG.

OEI-HD/Tf-PEG-OEI/siRNA polyplexes were formed at the OEI-HD/siRNA w/w ratio of 0.5/1 containing 10 % targeting Tf conjugate, and were applied at concentrations of 200 µg/mL siRNA, 90 µg/mL OEI-HD and 10 µg/mL OEI conjugated to Tf-PEG in sterile HBG. The blended carrier in this case contained 43 µg/mL transferrin, i.e. 29 % transferrin by weight of total polymer.

bPEI Succ 10/siRNA polyplexes were formed at the bPEI Succ 10/siRNA w/w ratio of 2/1, and were applied at concentrations of 200 µg/mL siRNA and 400 µg/mL bPEI Succ 10 in sterile HBG.

PEI (22 kDa)/siRNA polyplexes were formed at the PEI (22 kDa)/siRNA w/w ratio of 1/1, and were applied at concentrations of 200 µg/mL siRNA and 200 µg/mL PEI (22 kDa) in sterile HBG.

In case of OEI-HD/Tf-PEG-OEI, bPEI Succ 10 and PEI (22 kDa) polyplexes 2.5 mg/kg body weight siRNA were applied intravenously via the tail vein. Applications were repeated three times, every 24 hours.

PLL50-PEG-DMMA_n-Mel was formed at the PLL50-PEG-DMMA_n-Mel/siRNA w/w ratio of 1/1 and was applied at concentrations of 100 µg/mL siRNA and 100 µg/mL PLL50-PEG-DMMA_n-Mel in sterile HBG. PLL185-PEG-DMMA_n-Mel was formed at the PLL185-PEG-DMMA_n-Mel/siRNA w/w ratio of 0.5/1 and was applied at concentrations of 200 µg/mL siRNA and 100 µg/mL PLL185-PEG-DMMA_n-Mel in sterile HBG.

2.7.2.2 Hydrodynamic siRNA delivery

siRNA delivery to liver tissue was performed in FVB ODD Luc mice (heterozygous/homozygous), female and male, 10 – 16 weeks old, by high pressure tail vein injection (hydrodynamic delivery).

Mice were separated into two groups: (i) animals treated with target (siPHD2) siRNA (n = 4), (ii) animals treated with scrambled (siContr.#3) siRNA (n = 2). Mice were placed into a

restraining device and anesthetized by inhalation of isoflurane in oxygen (2.5% (v/v)) at a flow of 1 liter/min. Intravenous injections were performed by injecting a siRNA solution (12.5 μg /mL in isotonic sodiumchloride solution) in a volume corresponding to 12 % of the total body weight within approx. 5 seconds (this corresponds to 2.4 mL in case of 20 g body weight) using a 30 gauge needle (0.3 x 12 mm). 2 days prior and up to 4 days after hydrodynamic delivery the bioluminescence signal of the liver was measured as described in 2.7.1.

2.7.3 Implantation of tumor fragments

As donor as well as recipient animals A/J mice, female, 6 – 8 weeks old were used. In donor mice Neuro 2a Luc+ tumors were set as described in 2.7.1. When tumors reached a size of approximately 400 mm^3 , donor animals were sacrificed, tumors were explanted, kept in 37 ° C PBS and sliced into 8 mm^3 pieces. Recipient animals (n = 5) were shaved one day prior to implantation. At the day of implantation recipient mice were anaesthetized by intraperitoneal injection of 50 μl of a solution containing 38,5:23:38,5 Ketavet (c = 100 mg / ml): Rompun (2%): isotonic sodium chloride solution. When mice reached anesthesia stage III a dermal incision of 0,5 cm was set at one flank, and a tumor piece was implanted. The incision was closed using EpiGlue. Bioluminescence measurements were performed every day for the first 9 days and additionally on day 13 and 16 as described in 2.7.1.

2.7.4 Transgenic cell injection into wildtype tumor tissue

A/J mice, female, 6 – 8 weeks old were used (n = 5). Neuro 2a wildtype tumors were set as described in 2.7.1. When tumors reached a size of approximately 400 mm^3 , Neuro 2a Luc+ cells were prepared as described in 2.7.1, dissolved in PBS at a concentration of 1×10^6 cells per 50 μL and injected into the wildtype tumors. For injection mice were anaesthetized with isoflurane, which was administered by inhalation of isoflurane in oxygen (2.5% (v/v)) at a flow of 1 liter/min. Bioluminescence measurements were performed every day for 4 days as described in 2.7.1.

2.7.5 Luciferin kinetic studies

A/J mice, female, 6 – 8 weeks old were used. Neuro 2a Luc+ tumors were set as described in 2.7.1.

When tumors reached as size of approximately 100 – 200 mm^3 , bioluminescence imaging was started and performed every day for 5 days. Mice were separated into two groups (n = 5 per group): (i) animals injected intraperitoneally with luciferin solution, (ii) animals treated intravenously with luciferin solution. Animals of both groups received 100 μL luciferin solution (c = 60 mg/mL). Before luciferin injection mice were anaesthetized with isoflurane, which was administered by inhalation of isoflurane in oxygen (2.5% (v/v)) at a flow of 1

liter/min. Directly after luciferin application a sequence bioluminescence measurement was performed for 30 minutes (intravenously applied group) and 60 minutes (intraperitoneally applied group).

3 Results

3.1 Generation of different monoclonal Luc transgenic Neuro 2a cells

3.1.1 Cloning of plasmid GL4.16SV40

The first aim of the present work was the construction of transgenic Neuro 2a cells stably expressing firefly luciferases that differ in expression intensity and half-life of the enzyme and are supposed to serve as a negative readout system for siRNA delivery. Additionally a luciferase based system should be created, that shows signal induction as positive readout for siRNA treatment.

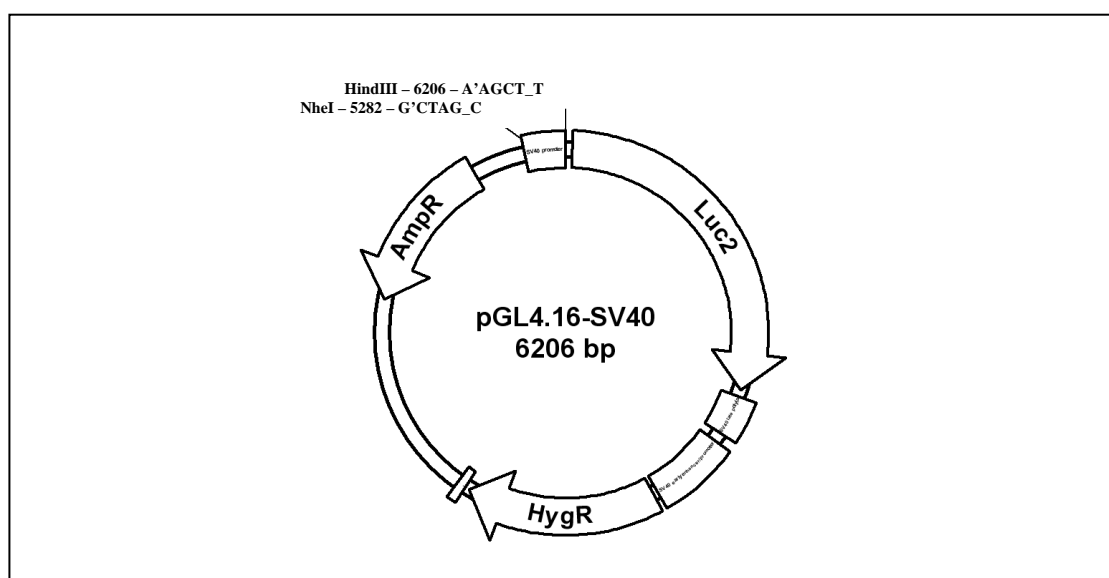


Figure 4: Structure of the newly synthesised pGL4.16SV40.

Luc, Luc⁺ and Luc2 were selected as transgenes for a negative readout system as they have been designed to show increasing expression intensities. To address the aim of decreasing the enzyme half-life Luc2 was equipped with two degradation sequences (CL1-PEST). As transgene for a positive readout bioluminescent system a fusion of a HIF1 α fragment (ODD) and Luc⁺ was chosen (ODD Luc). CMV and SV40 promoter were used, respectively. pC1 (encoding for Luc under CMV promoter), pCDNA3 Luc (encoding for Luc⁺ under CMV promoter) and pCDNA3 ODD Luc (encoding for ODD Luc under CMV promoter) were obtained as stated in 2.1.4.3. To obtain a suitable plasmid encoding for the CL1-PEST modified Luc2, the SV40 promoter sequence was excised from pGL3 control and ligated into pGL4.16 (Figure 4).

3.1.2 Evaluation of expression intensities of luciferase encoding plasmids

The expression intensities of the different plasmids that were chosen for generation of stably transgenic Neuro 2a clones were evaluated by transient transfections prior to stable transfection.

As a transfer vector PEI (22 kDa) was used at different N/P ratios (molar ratio of nitrogen in PEI to phosphate in the nucleic acid). As a positive control pCMV Luc (encoding for firefly luciferase under CMV promoter) was used. Results were evaluated by using the luciferase reporter gene assay (Figure 5).

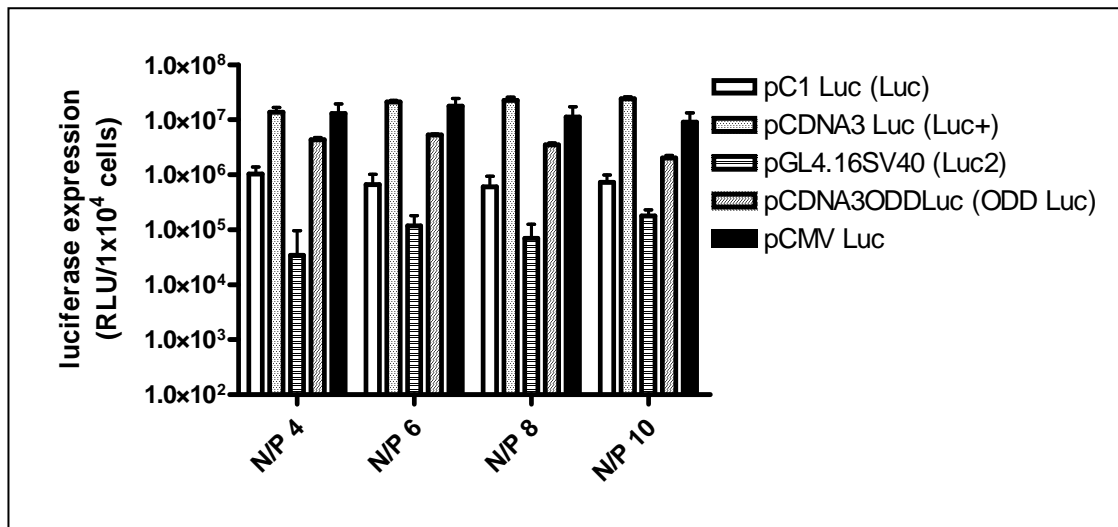


Figure 5: Expression intensities of luciferase encoding plasmids on Neuro 2a cells.

PEI (22 kDa) was complexed with the luciferase encoding plasmids in the indicated N/P ratios. 200 ng pDNA per well were used. Black bars show pCMV Luc as a positive control. Measurements were performed with $n = 8$, mean values from three independent experiments and standard deviations are shown.

As expected, Luc+ exhibited no difference in expression intensity compared to the positive control, which was reported to hold high values (137). Luc, which has not been optimized for high expression intensity, Luc2, which is designed to have a faster kinetic due to its degradation domains, and ODD Luc, which is permanently degraded under normoxic conditions, showed highly significant ($p < 0.001$, One-way-ANOVA) diminished expression intensities in comparison to Luc+. Interestingly ODD Luc exhibited significantly ($p < 0.001$) higher expression activity than Luc and Luc2.

3.1.3 Expression intensities of stably luciferase expressing Neuro 2a cell clones

Stable transfections with the plasmids were performed by using synthetic vectors. After transfection cells were cultured under selection pressure and finally monocloned. The expression intensity of the untreated cell clones was determined by luciferase reporter gene assay (Table 1 –3).

Luc	
Clone number	RLU / 10.000 cells
# 1	46.756
# 2	28.617

Table 1: Luciferase expression intensity of Neuro 2a Luc cell clones.

The clone that was used for further experiments is highlighted in grey. It is thereafter named Neuro 2a Luc.

Luc+	
Clone number	RLU / 10.000 cells
# 1	62.228
# 2	510.535
# 3	758.370

Table 2: Luciferase expression intensity of Neuro 2a Luc+ cell clones.

The clone that was used for further experiments is highlighted in grey. It is thereafter named Neuro 2a Luc+.

Luc2	
Clone number	RLU / 10.000 cells
# 1	82.104
# 2	54.542
# 3	85.794
# 4	53.281
# 5	64.191
# 6	84.466

Table 3: Luciferase expression intensity of Neuro 2a Luc2 cell clones.

The clone that was used for further experiments is highlighted in grey. It is thereafter named Neuro 2a Luc2

To prove the correct connection of luciferase expression to the HIF pathway in ODD Luc cell clones, the expression intensity of untreated cells was compared to the expression intensity of cells treated with 100 mM deferoxamine for 24 hours prior to lysis (Table 4). Deferoxamine treatment leads to an intracellular iron depletion, which subsequently inhibits the activity of the PHD enzymes and thereby causes an inhibition of HIF degradation.

For further experiments the cell clone with the lowest luciferase activity was selected. Those clones should be more sensitive to siRNA treatment due to lower luciferase mRNA levels. In case of the ODD Luc transgene only one clone correctly corresponded to the inhibition of HIF degradation by higher expression intensity of ODD Luc and was therefore selected for further experiments.

ODD Luc		
Clone number	RLU / 10.000 cells	
	untreated	100 mM deferoxamine
# 1	5.733	5.092
# 2	10.498	30.510

Table 4: Luciferase expression intensity of Neuro 2a ODD Luc cell clones before and after induction by deferoxamine.

The clone that was used for further experiments is highlighted in grey. It is thereafter named Neuro 2a ODD Luc.

3.2 Characterization and optimisation of subcutaneous tumor mouse models

3.2.1 Characterization of the different Luc transgenic cell clones

To prove the ability of the selected cell clones to successfully establish subcutaneous tumors in mice, 1×10^6 tumor cells were injected subcutaneously into the flank of A/J mice ($n = 10$). As a positive control Neuro 2a stably expressing eGFP Luc (Neuro 2a eGFP Luc) were used. A subcutaneous tumor mouse model with this cell clone in A/J mice had already been established in our lab (data not shown).

Tumor size was determined by caliper measurements, and luciferase expression intensity by bioluminescence imaging every 2 to 3 days (Figure 6 and 7). Additionally the correlation of bioluminescence intensity to tumor size was calculated (Figure 8).

Independently of the transgene tumors became palpable at around day 7 and measurable at around day 9 after inoculation. Thereafter they showed an exponential increase of the tumor volume until the experiment had to be terminated due to the tumor sizes.

In case of expression intensity Neuro 2a Luc, Luc+ and Luc2 closely resembled the results of the eGFP Luc transgenic cell clone. No significant differences in expression intensity were detected. Bioluminescent signal was distinguishable as early as day 1 after inoculation and increased exponentially until the experiment was terminated. The ODD Luc transgenic cell clone showed a significantly diminished expression level, which remained more or less stable over the time of the experiment. The last measurement revealed a slight decrease of expression.

For Neuro 2a eGFP Luc and Neuro 2a Luc a direct correlation between bioluminescence signal and tumor volume was observed. For Neuro 2a Luc+ and Neuro 2a Luc2 the ratio between bioluminescence signal and tumor size decreased from day 9 to day 11 and thereafter remained stable. In case of Neuro 2a ODD Luc the ratio of bioluminescence signal and tumor volume constantly decreased over the time of the experiment.

For clarity reason the means of the bioluminescent signals are given without standard deviations.

Despite the reliable exponential growth of the bioluminescence signals as indicated by the mean values, there were prominent standard deviations (Figure 9).

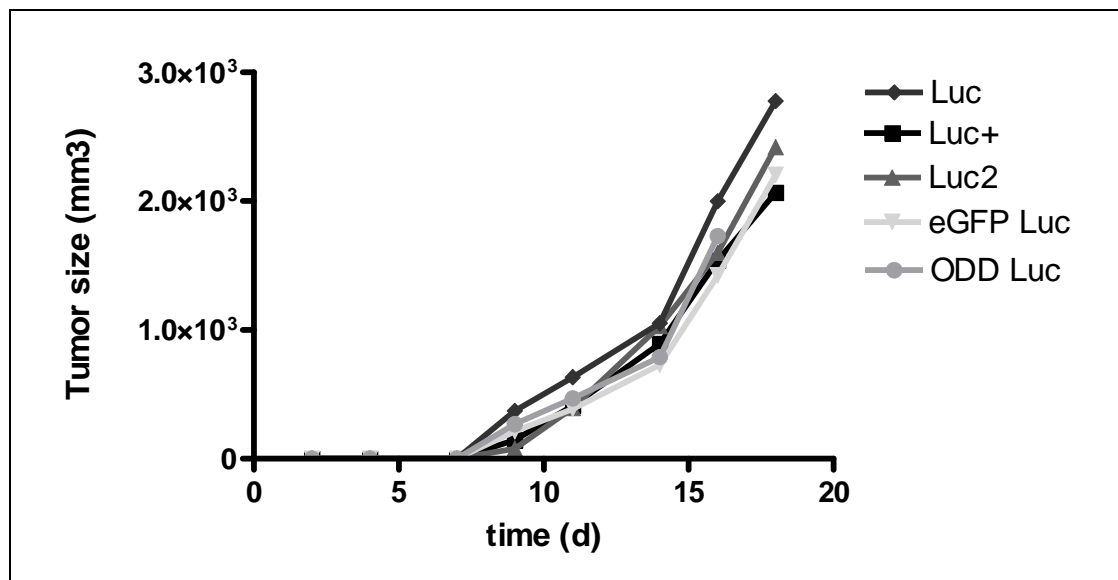


Figure 6: Tumor size development of the different Luc transgenic cell clones.

Neuro 2a Luc, Luc+, Luc2 and ODD Luc respectively were examined. As a positive control Neuro 2a eGFP Luc was used. 1×10^6 tumor cells were injected subcutaneously into the flank of A/J mice ($n = 10$). The tumor size was determined every 2 to 3 days by caliper measurement and calculated as $a*b*c$ (length*height*width). Results are presented as means without standard deviation.

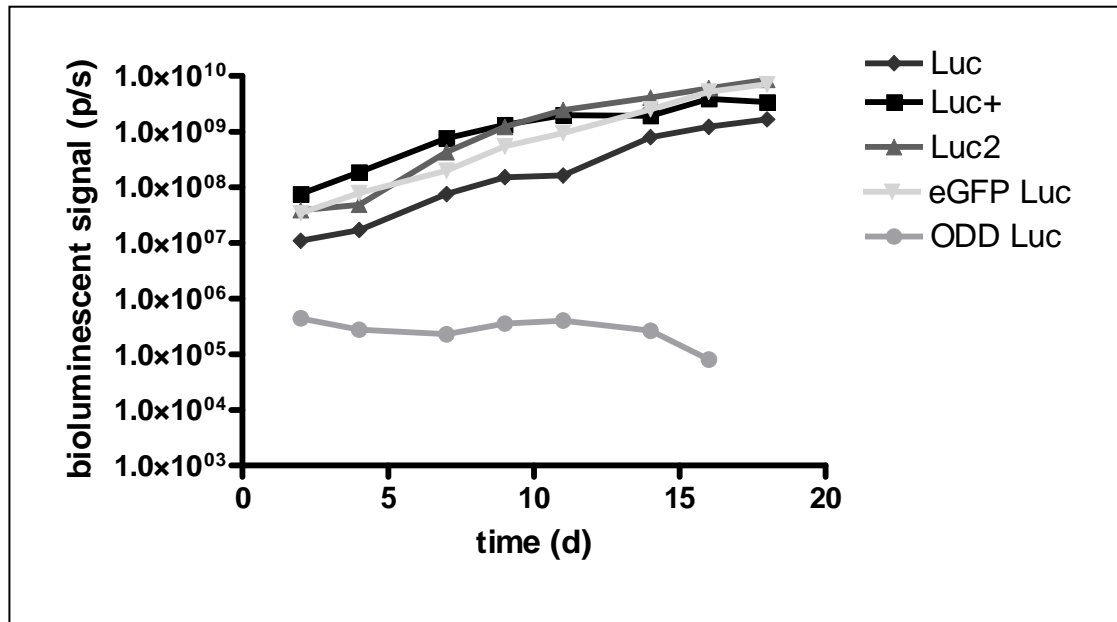


Figure 7: Expression intensity of the different Luc transgenic cell clones.

Neuro 2a Luc, Luc+, Luc2 and ODD Luc respectively were examined. As a positive control Neuro 2a eGFP Luc was used. 1×10^6 tumor cells were injected subcutaneously into the flank of A/J mice ($n = 10$). Expression intensity was determined every 2 to 3 days by bioluminescence imaging.

Results are presented as means without standard deviation.

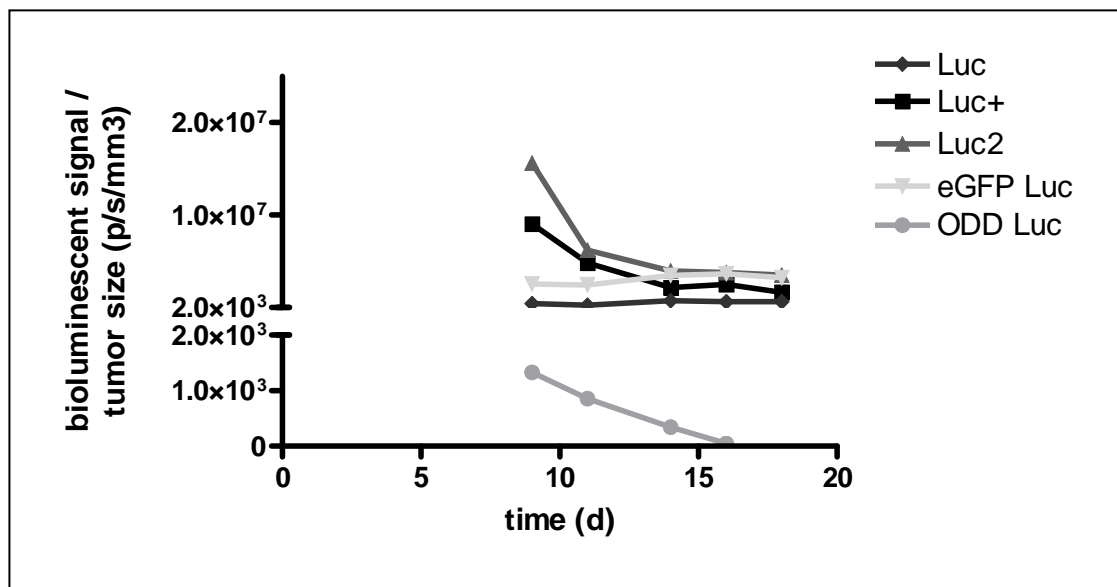


Figure 8: Correlation of bioluminescence signal to tumor size of the different Luc transgenic cell clones.

Neuro 2a Luc, Luc+, Luc2 and ODD Luc respectively were examined. As a positive control Neuro 2a eGFP Luc was used. 1×10^6 tumor cells were injected subcutaneously into the flank of A/J mice ($n = 10$). The correlation was calculated as bioluminescence signal (photons/second)/tumor volume (mm^3). Results are presented as means without standard deviation.

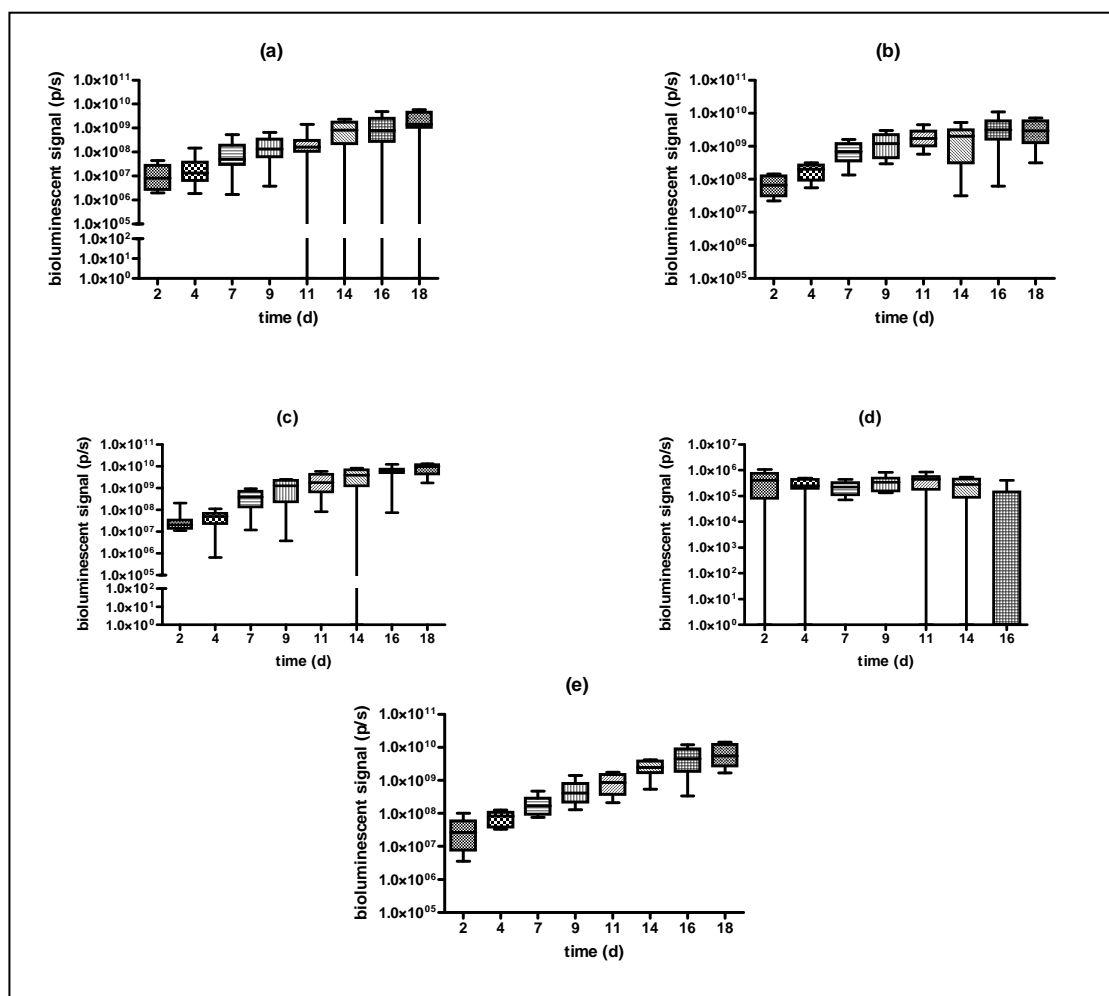


Figure 9: Standard deviations of bioluminescence signals of the different Luc transgenic cell clones.

Data are presented for Neuro 2a Luc (a), Neuro 2a Luc+ (b), Neuro 2a Luc2 (c), Neuro 2a ODD Luc (d) and Neuro 2a eGFP Luc (e). Results are presented as box plots. The boxes show the range of 50% of the values above and beneath the mean. The mark in the box indicates the overall mean. The highest and lowest bioluminescence signals are given by standard deviation signs.

Standard deviations were especially high for the cell clones bearing luciferases with reduced stability, such as Neuro 2a ODD Luc and Neuro 2a Luc2. But even Neuro 2a Luc revealed significant standard deviations. Neuro 2a eGFP Luc and Neuro 2a Luc+ gave more or less robust results with a slight increase in case of Neuro 2a Luc+ after 11 days.

As a robust basic signal has to be one of the main issues due to its impact on significance calculations, Neuro 2a Luc+ was chosen for further optimization.

3.2.2 Influence of luciferin distribution on the bioluminescence signal

Most *in vivo* bioluminescent measurements are carried out 10 minutes after intraperitoneal injection of 150 mg/kg body weight luciferin (119). It was already demonstrated, that this amount of luciferin does not distribute equally and is not able to saturate the enzymatic luciferase reaction in every location of the organism. To exclude possible artifacts, all

bioluminescence measurements of the present thesis are done with 300 mg/kg body weight luciferin according to the findings of Hildebrandt *et al.* (138). In one publication local application was described as more useful than intraperitoneal injection (120). No consent was found concerning the most appropriate time point of measurement after application of luciferin. The exact measurement protocol is discussed as being dependent on the transgenic tissue.

Therefore it was necessary to check the luciferin kinetic after intraperitoneal as well as intravenous injection in the subcutaneous Neuro 2a Luc+ mouse model. Intratumoral injection was not suitable in this case due to its pathological impact on the tumor tissue. In this experiment also the impact of tumor vascularisation status on the luciferin uptake was determined. For this purpose mice bearing two tumors were used. Those mice were injected either intraperitoneally or intravenously with luciferin ($n = 5$). Directly thereafter sequence bioluminescence measurements were performed for 30 minutes in case of the intravenously injected group and for 60 minutes for the intraperitoneally injected group.

Times after injection when maximal bioluminescence signals occurred are given in Figure 10.

Maximal bioluminescence signals for each tumor of selected mice are presented in Figure 11.

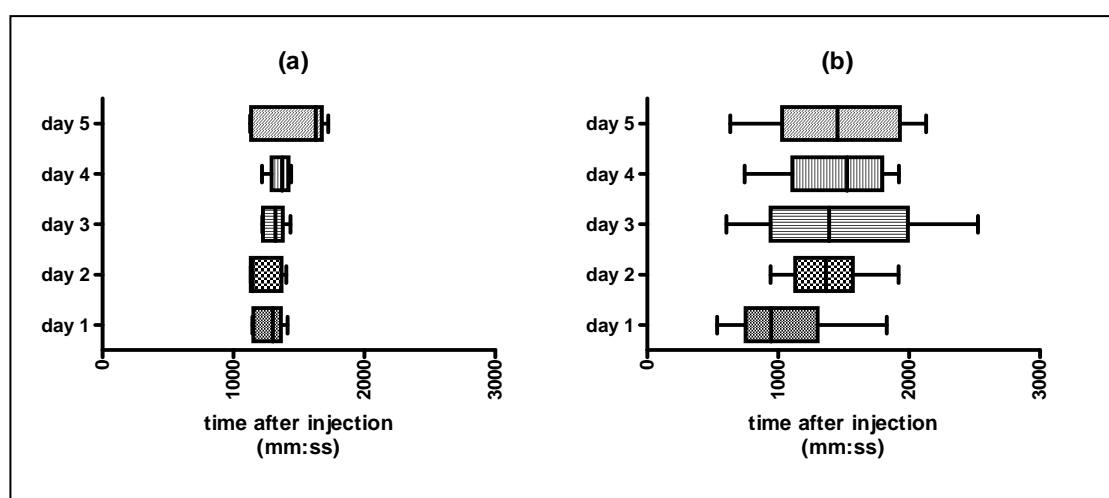


Figure 10: Time point of the maximal bioluminescence signal after intraperitoneal or intravenous injection of luciferin.

A/J mice bearing macroscopically visible ($\sim 100 \text{ mm}^3$) Neuro 2a Luc+ tumors were injected with 300 mg/kg body weight luciferin either intraperitoneally (a) or intravenously (b). Directly after injection sequence bioluminescence measurements were performed in order to determine the time point of the maximal bioluminescent signal. The measurement was performed over 5 consecutive days. The results are given as box plots. The boxes cover the range of 50% of the values above and beneath the mean. The mark in the box indicates the overall mean. The highest and lowest bioluminescence signals are given by standard deviation signs.

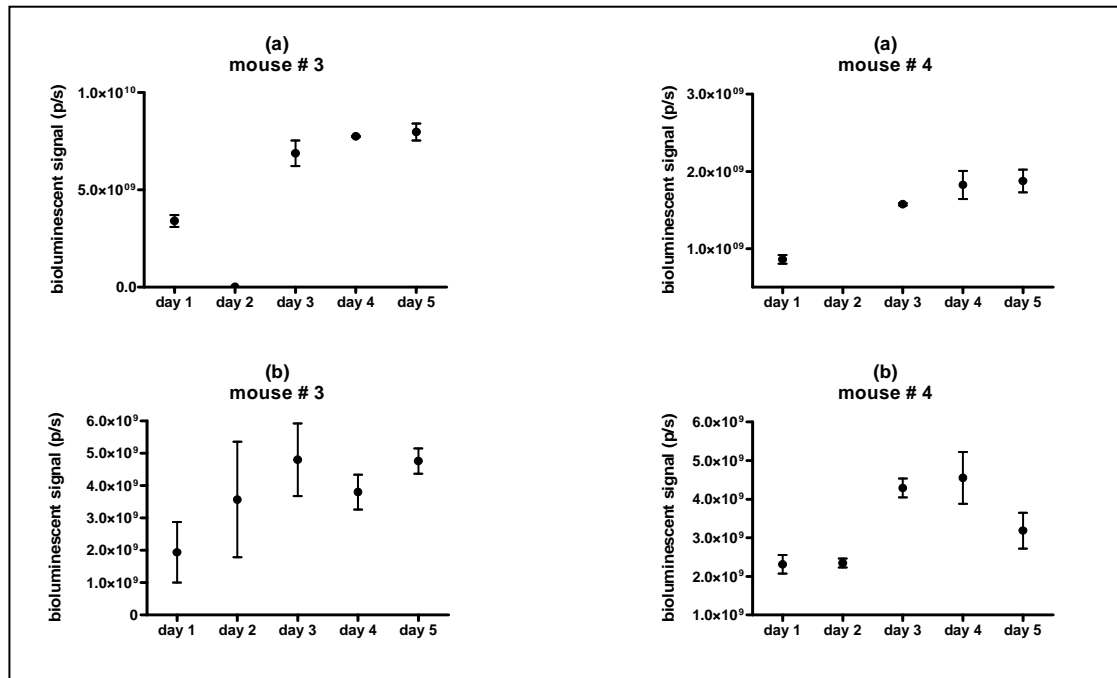


Figure 11: Maximal bioluminescence signals of both tumors of selected mice after intraperitoneal or intravenous injection of luciferin.

A/J mice bearing macroscopically visible ($\sim 100 \text{ mm}^3$) Neuro 2a Luc+ tumors were injected with 300 mg/kg body weight luciferin either intraperitoneally (a) or intravenously (b). Directly after injection sequence bioluminescence measurements were performed in order to determine differences in bioluminescence curves between the tumors within one animal. Measurements were performed over 5 consecutive days.

The results are given as means of both tumor bioluminescence signals. Independent bioluminescence signals are given by the standard deviation.

Interestingly the time-to-peak was almost identical for both groups (intravenous group: 13.4 minutes; intraperitoneal group: 13.3 minutes), but the average delay between the time points when the first and thereafter the second tumor reached maximal levels was much smaller for the intraperitoneal group (< 0.3 minutes) than for the intravenous group (4.2 minutes).

Additionally the variance between maximal bioluminescence signals which existed between the tumors within the same animal remained relatively stable for the intraperitoneal group but differed remarkably for the intravenous group.

3.2.3 Influence of animal positioning on the bioluminescence signal

As bioluminescent light is attenuated by traverse of tissue (107), slight differences in the positioning of the mouse might have an influence on the bioluminescence signal.

To evaluate this possibility nu/nu mice ($n=3$) bearing two Neuro 2a Luc+ tumors were positioned in the IVIS Lumina as shown in Figure 12 and subsequently the bioluminescent signal of both tumors was detected.

The study showed slight changes of signal for positions, in which the tumor was not directly placed under the camera.

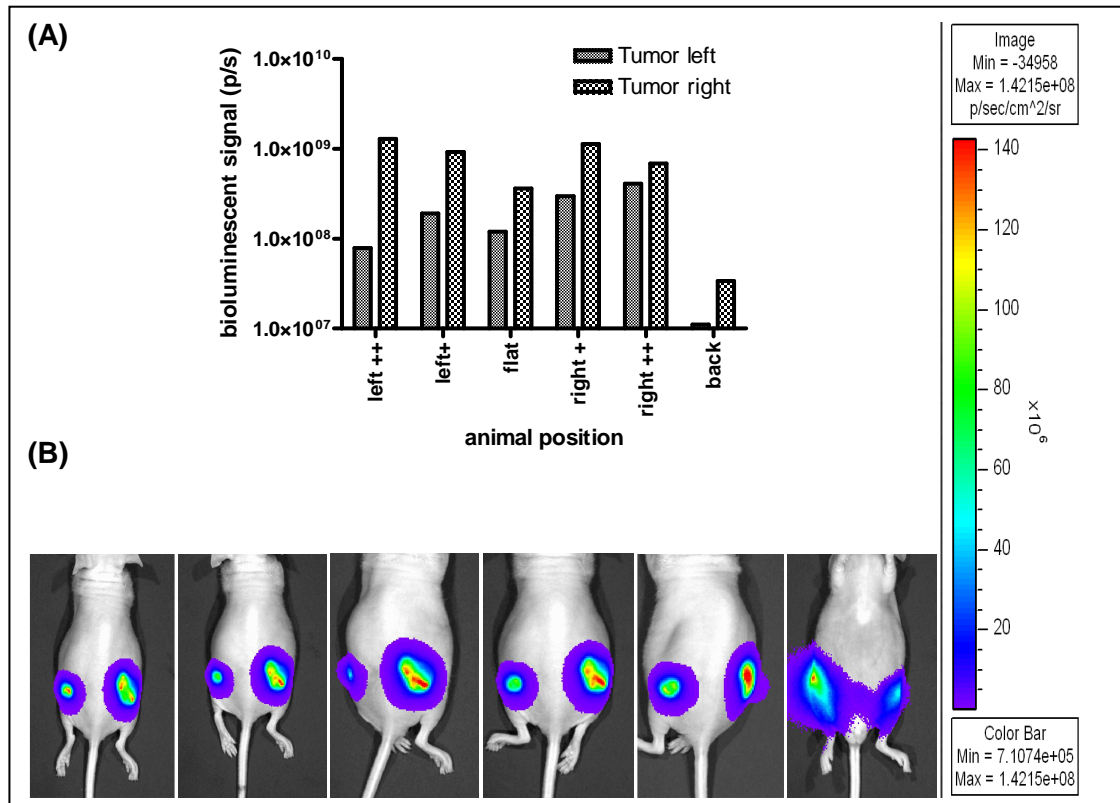


Figure 12: Influence of the positioning on the bioluminescence signal.

Nu/Nu mice bearing two Neuro 2a Luc+ tumors ($\sim 150\text{mm}^3$) were placed in different positions during bioluminescence measurement. (A) Bioluminescence signals of one selected animal in accordance to its position. (B) Animals position given as an overlay of bioluminescent image and photograph.

3.2.4 Influence of transgenic cell number on the bioluminescence signal

As revealed above in case of the Neuro 2a Luc+ model the standard deviation of bioluminescence signals increased during the time course of the study whereas a good correlation between bioluminescence and tumor size developed. This highlights the impact of tumor volume divergence. From this point of view treatment during the first week after inoculation would be preferable, but at that point of time tumors are less than 3 mm in size and do not have a functional vascularisation (135), which hampers the accessibility of tumor tissue for systemically injected polyplexes. For this purpose tumor fragments were implanted to allow for better homogeneity of both, bioluminescence signal and tumor size, within the groups. A small (~ 2 mm) Neuro 2a Luc+ tumor fragment derived from a donor mouse was implanted. The development of the bioluminescence signals was observed until termination of the experiment (Figure 13). Additionally tumor volume of macroscopically visible tumors was determined by caliper measurements.

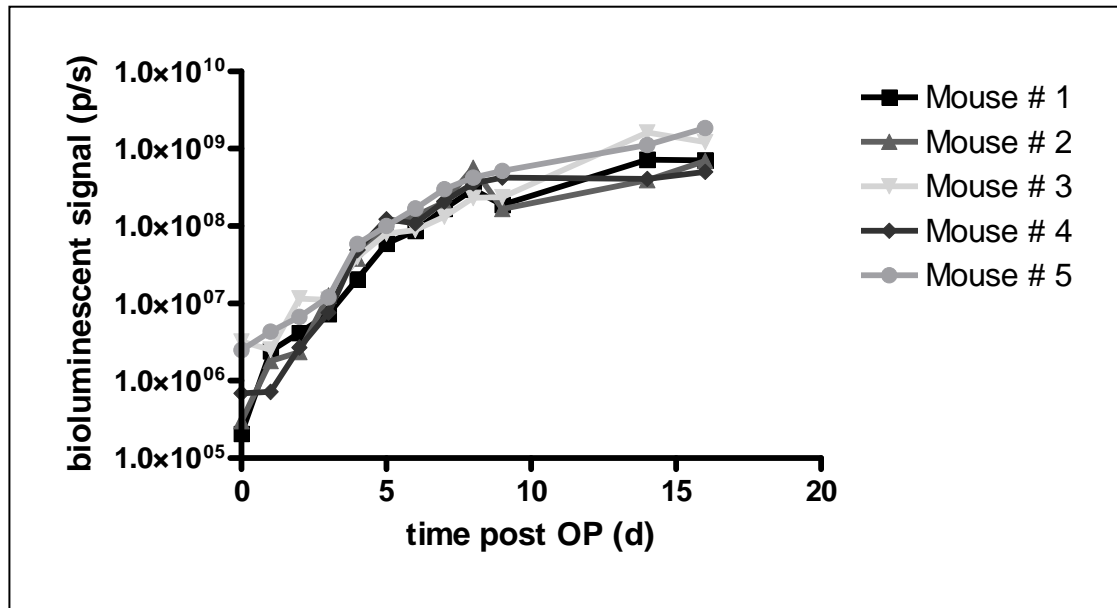


Figure 13: Inoculation of Neuro 2a Luc+ tumor fragments in A/J mice.

A/J mice ($n = 5$) received ~ 2 mm sized Neuro 2a Luc+ tumor fragments, which were derived from a donor mouse. Bioluminescence measurements were performed one hour after inoculation, everyday over the first week and thereafter every two to four days until termination of the experiment.

Bioluminescence signals were detectable as early as one hour after inoculation and increased over time. They showed a low variance over the first week, when tumors were not macroscopically detectable. Thereafter variance increased.

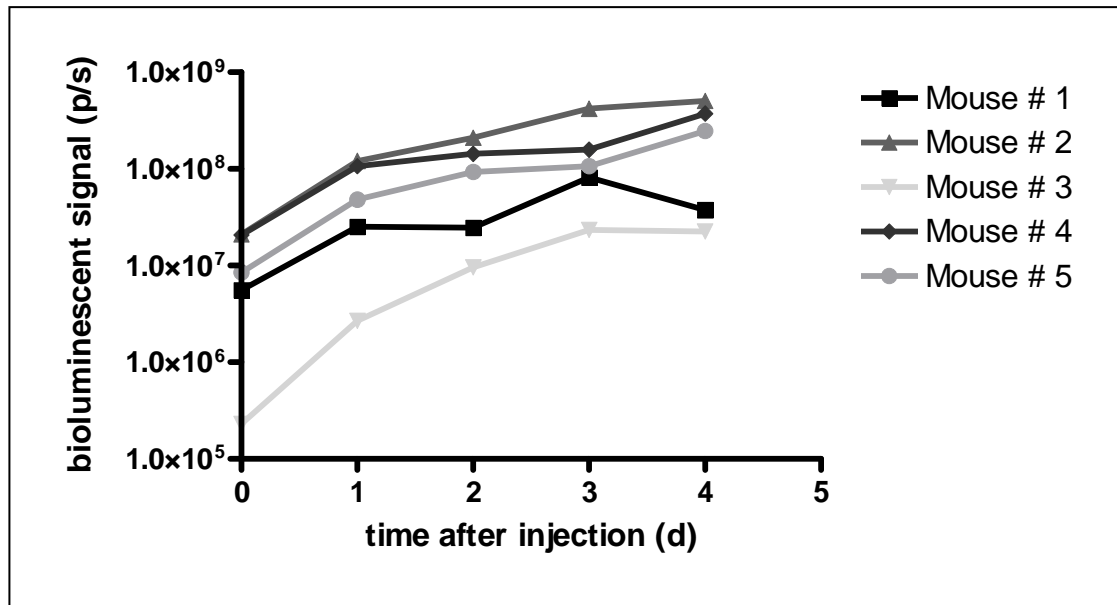


Figure 14: Injection of Neuro 2a Luc+ cells into Neuro 2a wildtype tumors.

A/J mice ($n = 5$) bearing ~ 200 mm³ sized Neuro 2a wildtype tumors were injected intratumorally with 1×10^6 Neuro 2a Luc+. Bioluminescence measurements were performed one hour after injection and thereafter everyday until termination of the experiment.

In a second approach luciferase transgenic cells were injected into already existing subcutaneous wildtype tumors. A/J mice (n = 5) bearing Neuro 2a wildtype tumors (~ 200 mm³) were intratumorally injected with 1 x 10⁶ Neuro 2a Luc+ cells. Thereby a macroscopically visible tumor was created, which contained a defined amount (1 x 10⁶) of luciferase expressing cells. The development of the bioluminescent signals was observed until termination of the experiment. (Figure 14)

Bioluminescence signals were detectable as early as one hour after injection and increased over time. Already directly after injection a considerable variance between the animals could be detected.

3.3 Utilization of mouse models for detection of effective siRNA delivery

Two strategies were pursued to prove successful siRNA delivery by *in vivo* bioluminescence imaging. The first one is direct targeting of luciferase mRNA, which subsequently leads to a reduction of bioluminescence signal (negative readout). The second one is targeting the mRNA of a protein repressing luciferase activity, which thereafter results in an increase of bioluminescence signal (positive readout).

Neuro 2a Luc+ was selected as negative readout system, Neuro 2a ODD Luc was evaluated as positive readout system. Additionally a transgenic mouse strain, expressing ODD Luc in all tissues, was tested. Prior to siRNA delivery studies *in vivo* siRNA transfer was evaluated *in vitro*.

3.3.1 Utilization of the negative readout system (Neuro 2a Luc+)

Different synthetic vector systems were evaluated in the A/J Neuro 2a Luc+ tumor mouse model regarding their siRNA delivery capacity. OEI-HD1 / Tf-OEI-HD1 (90 / 10) had already been proven successful in previous studies for silencing of an endogenous gene (57), the other delivery systems were highly promising regarding their *in vitro* reporter gene silencing capacity.

3.3.1.1 Tf-PLL-DMMA_n-Mel-ss-siRNA

Tf-PLL-DMMA_n-Mel is an analog of the poly-L-lysine (PLL) conjugate described in Meyer *et al.* (58) containing Tf and Mel acylated with DMMA_n. The modification with Tf mediates an effective shielding and a receptor targeting function, and the melittin peptide masked by DMMA_n provides pH-sensitive endosomolytic properties. Extracellular stability is generated by covalent attachment of the siRNA. Therefore this conjugate exhibits high biocompatibility and transfection efficacy *in vitro* (Figure 15). Due to low polymer yields, siRNA delivery was not repeated on Neuro 2a Luc+ *in vitro* but data of siRNA delivery on Neuro 2a eGFP Luc

cells are shown. These data were generated by Christian Dohmen and will be part of his PhD thesis.

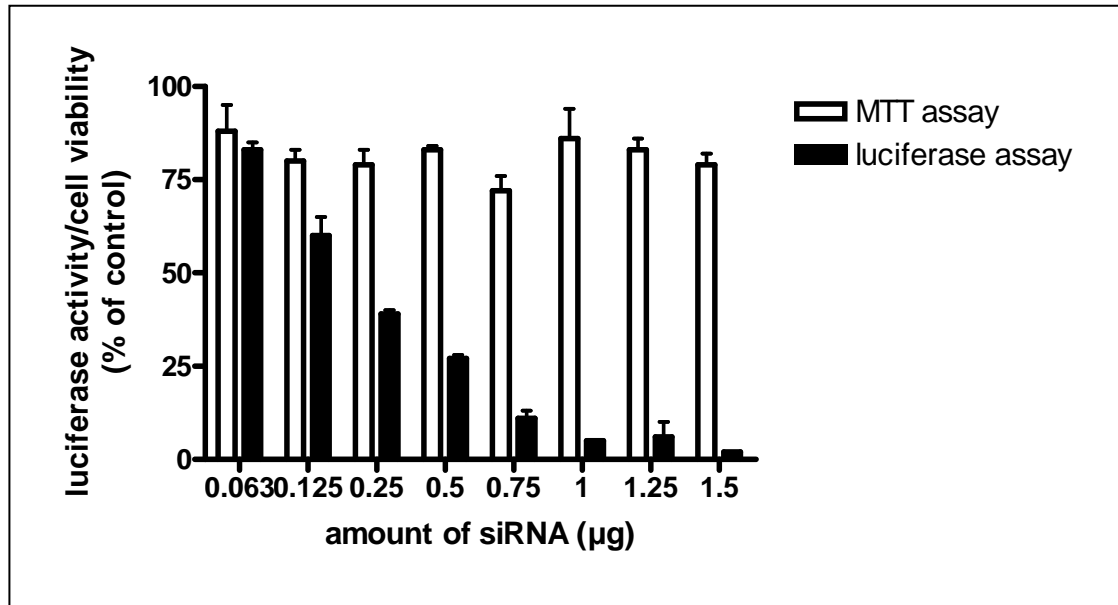


Figure 15: *In vitro* siRNA reporter gene silencing of Tf- PLL-DMMAN-Mel-ss-siRNA on Neuro 2a eGFP Luc.

Five thousand cells per well were treated with the indicated amounts of target siRNA (siLuc) covalently attached to the polymer. Forty-eight hours after transfection cell lysis was performed. Gene silencing was evaluated using the luciferase reporter gene assay and toxicity using the MTT assay. The results are normalized to the values of untreated cells (100%).

Depending on the amount of siRNA an increasing reporter gene silencing effect up to > 90% can be observed. In contrast, the cytotoxic effect remains relatively stable at around 20%.

To evaluate the siRNA gene silencing capability of Tf-PLL-DMMAN-Mel-ss-siRNA *in vivo*, A/J mice bearing Neuro 2a Luc+ tumors of approximately 150 mm³ in size were used (n = 5). The bioluminescent signals were evaluated on two consecutive days prior to siRNA injection. Thereafter mice received a single intravenous treatment with 0.625 mg/kg body weight or 1.25 mg/kg body weight target (siLuc) or scrambled (siControl) siRNA covalently attached to the polymer. The effects of this treatment on the bioluminescent signals of the tumors were measured by daily bioluminescence imaging on day 1, 2 and 4 after treatment (Figure 16). For clarity reasons means are given without standard deviations. Those are presented for each group in Figure 17.

Due to practical reasons according to the polymer synthesis treatment with siLuc and siControl were performed in independent experiments.

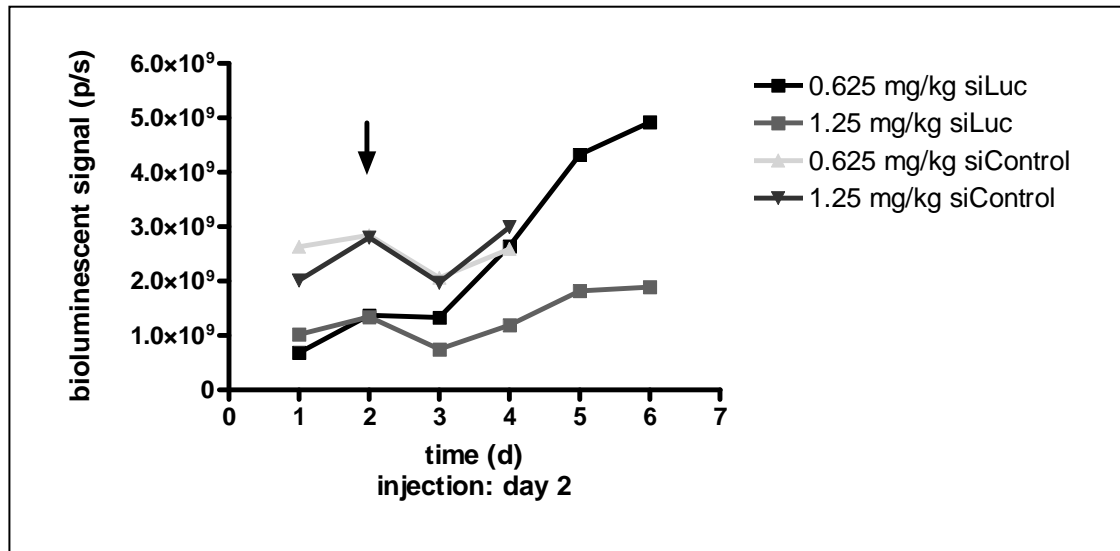


Figure 16: *In vivo* siRNA reporter gene silencing of Tf-PLL-DMMAN-Mel-ss-siRNA on Neuro 2a Luc+ in A/J mice.

A/J mice bearing $\sim 150 \text{ mm}^3$ Neuro 2a Luc+ tumors were measured over two days by bioluminescence imaging. Thereafter treatment was performed by intravenous injection of 0.625 or 1.25 mg/kg body weight target siRNA (siLuc) or scrambled siRNA (siControl) respectively ($n = 5$), and the effects on bioluminescent signals were evaluated for the next two or four days, respectively, by daily bioluminescence imaging. Treatments with target siRNA and scrambled siRNA were performed in independent experiments. The day of injection is marked with an arrow.

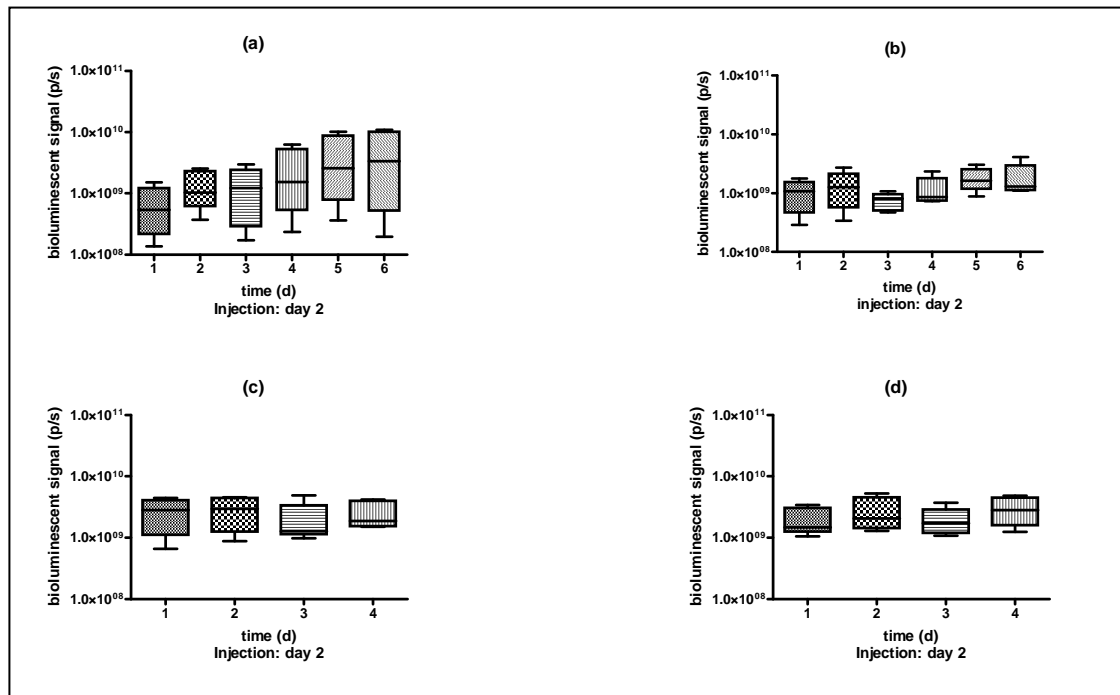


Figure 17: Standard deviations of the *in vivo* siRNA reporter gene silencing of Tf-PLL-DMMAN-Mel-ss-siRNA on Neuro 2a Luc+ in A/J mice.

The data are presented for siLuc treatment with 0.625 mg/kg body weight (a) or 1.25 mg/kg body weight (b) and for siControl treatment with 0.625 $\mu\text{g/kg}$ body weight (c) or 1.25 mg/kg body weight (d). Results are presented as box plots. The boxes cover the range of 50% of the values above and beneath the mean. The mark in the box indicates the overall mean. The highest and lowest bioluminescent signals are given by standard deviation signs.

In all groups a decrease of the bioluminescent signal one day after treatment was detected. This decrease was not statistically significant. Additionally, up from the day after treatment the formation of non-bioluminescent areas within the tumors could be observed, which remained over the time of the study. These observations were made in all groups. An example is shown in Figure 18.

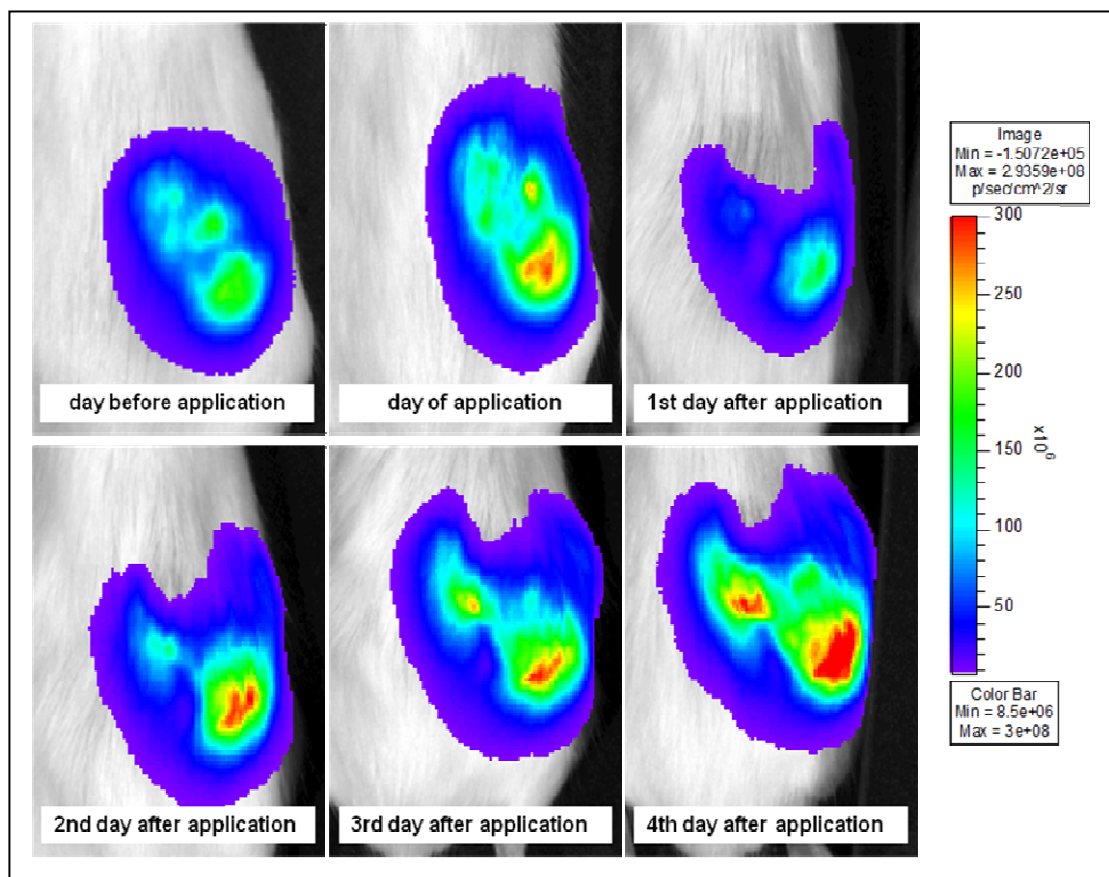


Figure 18: Formation of non-bioluminescent areas within a Neuro 2a Luc⁺ tumor after treatment with Tf-PLL-DMMA-Mel-ss-siRNA.

Bioluminescence images obtained of a tumor treated with 1.25 mg siLuc/kg body weight. Pictures are given as overlays of the bioluminescent signal over a photograph.

3.3.1.2 OEI-HD1/Tf-OEI-HD1 (90/10)

In order to compare the newly derived bioluminescence imaging method with a carrier system already successfully used in the Neuro 2a tumor mouse model, gene silencing experiments were performed on Neuro 2a Luc⁺ cells *in vitro* and *in vivo* using OEI-HD1/Tf-OEI-HD1 (90/10) (Figures 19 and 20).

The polymer is synthesized using OEI 800 Da (OEI) and HD as a linker, resulting in a biodegradable polymer with branched structure (56).

To enhance the specific uptake by tumor cells and provide shielding, OEI-HD1 was further modified adding Tf as a targeting and shielding ligand (Tf-OEI-HD1). It was shown that a

mixture of OEI-HD1 with Tf-OEI-HD1 (w/w: 90/10) is able to promote a specific silencing of the targeted gene in tumor cells *in vitro* and *in vivo* in the absence of unspecific or toxic side effects (57). This formulation is subsequently referred to as OEI-HD1/Tf-OEI-HD1 (90/10). Efficacy of the treatment was shown by tumor growth retardation and tumor cell necrosis, by rtPCR and on the other hand by western blots of the target gene in comparison to a housekeeping gene.

For *in vitro* experiments Neuro 2a Luc+ cells were treated with two different w/w ratios. The lower ratio represents the polyplexes thereafter used in the *in vivo* experiment exhibiting low toxicity, the higher ratio gives an optimal effect *in vitro*.

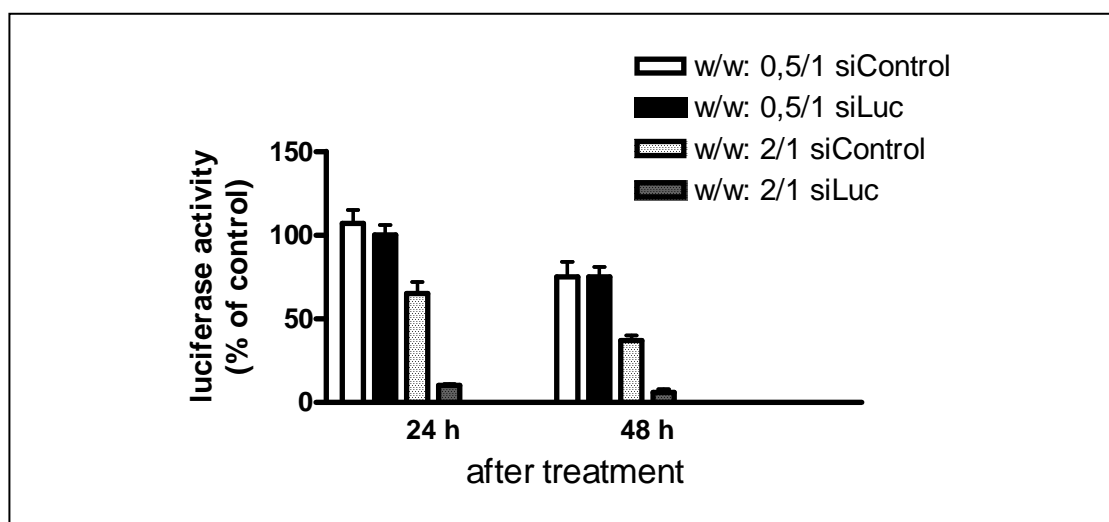


Figure 19: *In vitro* reporter gene silencing of OEI-HD1/Tf-OEI-HD1 (90/10) on Neuro 2a Luc+.

Ten thousand cells were treated with polyplexes containing target (siLuc) or scrambled (siControl) siRNA of the indicated w/w ratios. 24 or 48 hours after transfection cell lysis was performed. The gene silencing was evaluated using the luciferase reporter gene assay. The measurements were performed with $n = 8$, mean values of three independent experiments and standard deviations normalized to untreated cell (100%) are shown.

While the lower w/w ratio proved ineffective after 24 as well as 48 hours, the higher w/w ratio mediated a reporter gene silencing effect of $> 90\%$ after 24 as well as 48 hours. However, a rather high reporter gene silencing in the mock treated group of 35% after 24 hours and 63% after 48 hours was observed indicating an unspecific effect caused by toxicity of the polyplexes.

To evaluate the siRNA gene silencing capability of OEI-HD1/Tf-OEI-HD1 (90/10) *in vivo*, A/J mice bearing Neuro 2a Luc+ tumors of approximately 150 mm^3 in size were used ($n = 7$). The bioluminescent signals were evaluated on two consecutive days prior to siRNA injection. Thereafter mice received three consecutive intravenous treatments every 24 hours with polyplexes containing 2.5 mg/kg body weight target (siLuc) or scrambled (siControl) siRNA (w/w:0.5/1). One group remained untreated. The effects of this treatment on the

bioluminescent signals of the tumors were measured by daily bioluminescence imaging on day 1, 2 and 3 after treatment (Figure 20). For clarity reasons means are given without standard deviations. Those are presented for each group in Figure 21. Bioluminescent signals which had been normalized to the pre-treatment bioluminescent signal are presented in the appendix (7.1).

In contrast to siRNA delivery by bPEI Succ 10, which had been tested in parallel, no significant knockdown could be detected after siRNA delivery by OEI-HD1/Tf-OEI-HD1 (90/10) (One-way-ANOVA).

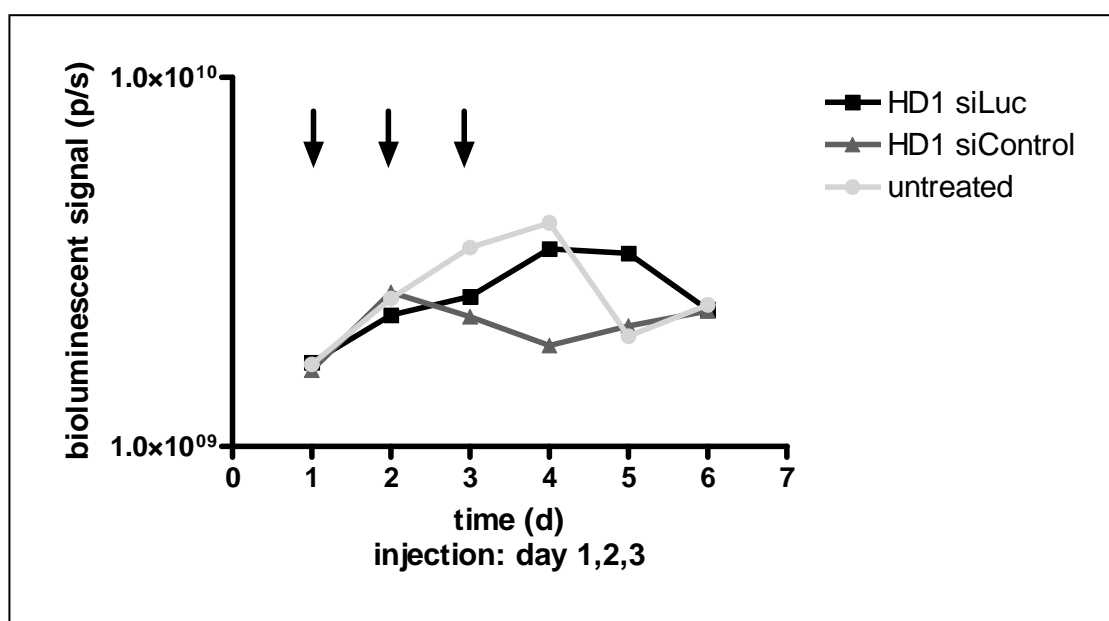


Figure 20: *In vivo* siRNA reporter gene silencing of OEI-HD1/Tf-OEI-HD1 (90/10) on Neuro 2a Luc+ in A/J mice.

A/J mice bearing $\sim 150 \text{ mm}^3$ Neuro 2a Luc+ tumors were measured over two days by bioluminescence imaging. The results of these two measurements are presented as mean on day 1. Thereafter the treatment was performed by three intravenous injections at three consecutive days of 2.5 mg target siRNA (siLuc) or scrambled siRNA (siControl) respectively ($n = 7$) (w/w: 0.5/1) One group remained untreated. The effects on the bioluminescent signals were evaluated for the next three days by daily bioluminescence imaging. Days of injection are marked with arrows.

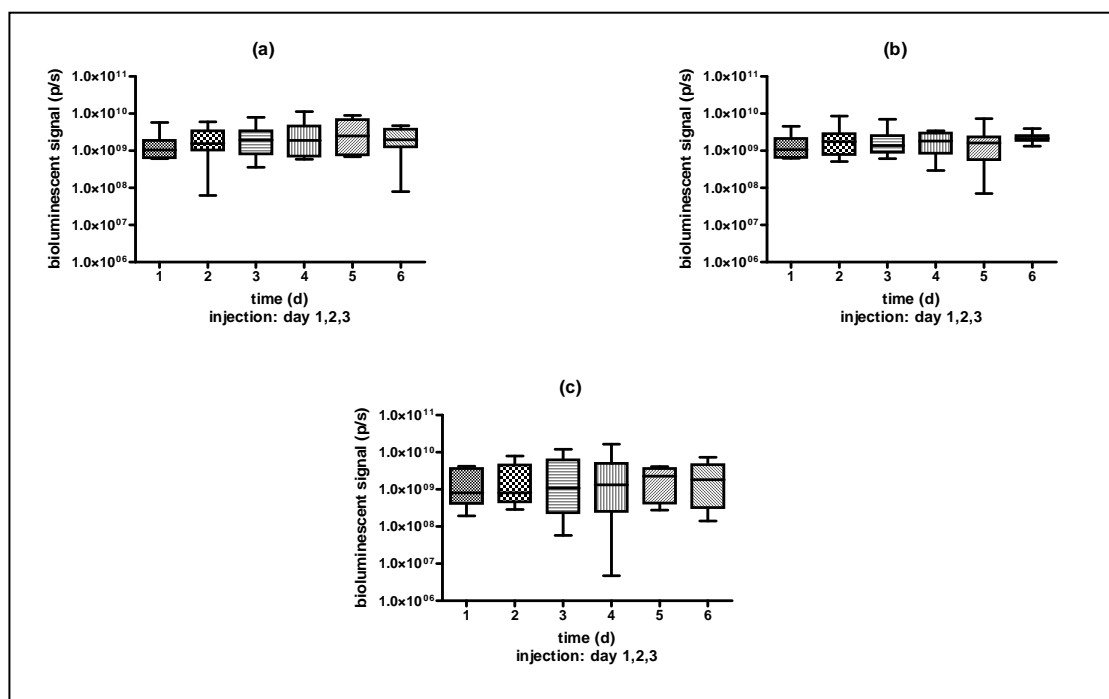


Figure 21: Standard deviations of the *in vivo* siRNA reporter gene silencing of OEI-HD1/Tf-OEI-HD1 (90/10) on Neuro 2a Luc+ in A/J mice.

Data are presented for siLuc treatment (a), for siControl treatment (b) or for an untreated group (c). Results are presented as box plots. The boxes cover the range of 50% of the values above and beneath the mean. The mark in the box indicates the overall mean. The highest and lowest bioluminescent signals are given by standard deviation signs.

3.3.1.3 bPEI Succ 10

Due to its outstanding performance *in vitro* (33), bPEI Succ 10 was considered a potentially active polymer for *in vivo* siRNA gene silencing and therefore tested in parallel to OEI-HD1/Tf-OEI-HD1 (90/10) *in vitro* as well as *in vivo* (Figure 22 and Figure 23).

It is synthesized by succinylation of 10% of the amines of bPEI, which decreases the positive charge of the polymer resulting in high transfection efficacy and less toxicity.

For *in vitro* experiments Neuro 2a Luc+ cells were treated with two different w/w ratios. The lower ratio represents the polyplexes thereafter used in the *in vivo* experiment exhibiting low toxicity, the higher ratio gives an optimal effect *in vitro*.

In contrast to the lower w/w ratio, which was non-toxic but less effective (~20% gene silencing) after 24 as well as 48 hours, the higher w/w ratio showed a specific siLuc mediated reporter gene silencing of ~80% after 24 hours and even > 90% after 48 hours. It did not reveal any unspecific reporter gene silencing within the mock treated group after 24 hours and only a slight decrease after 48 hours (15%).

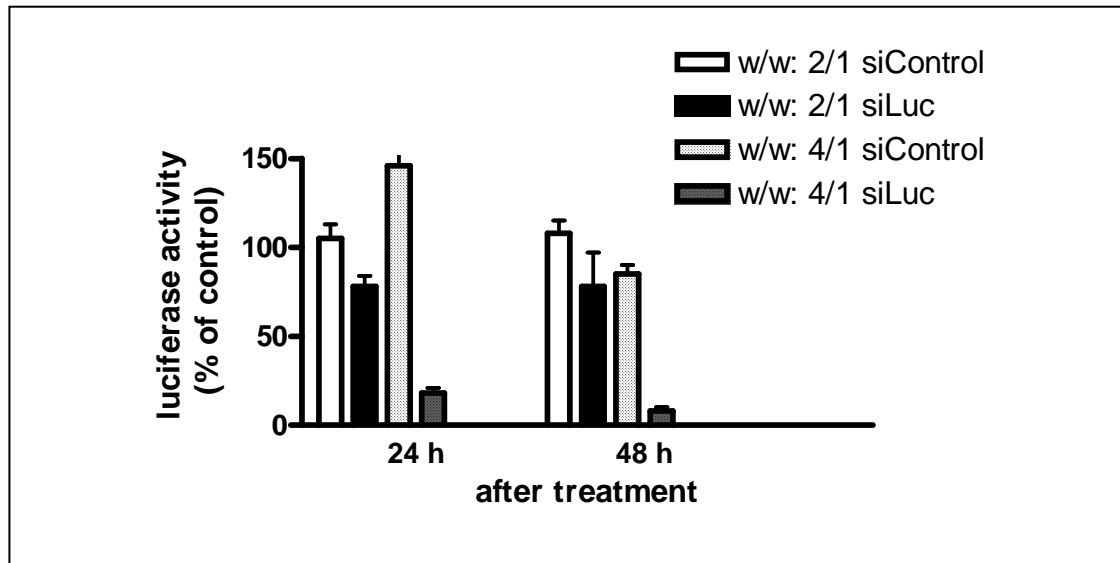


Figure 22: *In vitro* reporter gene silencing of bPEI Succ 10 on Neuro 2a Luc+.

Ten thousand cells were treated with polyplexes formed of polymer and target (siLuc) or scrambled (siControl) siRNA in the indicated w/w ratios. Twentyfour or 48 hours after transfection cell lysis was performed. The gene silencing was evaluated using the Luciferase Reporter Gene Assay. The measurements were performed with $n = 8$, mean values of three independent experiments and standard deviations normalized to untreated cell (100%) are shown.

To evaluate the siRNA gene silencing capability of bPEI Succ 10 *in vivo*, A/J mice bearing Neuro 2a Luc+ tumors of approximately 150 mm^3 in size were used ($n = 7$). The bioluminescent signals were evaluated on two consecutive days prior to siRNA injection. Thereafter mice received three consecutive intravenous treatments every 24 hours with polyplexes containing 2.5 mg/kg body weight target (siLuc) or scrambled (siControl) siRNA (w/w: 2/1). One group remained untreated. The effects of this treatment on the bioluminescent signals of the tumors were measured by daily bioluminescence imaging on day 1, 2 and 3 after treatment (Figure 23). For clarity reasons the means are given without standard deviations. Those are presented for each group in Figure 24. Bioluminescent signals which had been normalized to the pre-treatment bioluminescent signal are presented in the appendix (7.1).

Despite the visible decrease in bioluminescent signal of the siLuc treated group and the unaffected increase in signal of the mock treated and untreated group, the results could not be proven statistically significant on the basis of the total flux data (One-way-ANOVA). However after normalization of the values to the pre-treatment bioluminescent signal (Appendix, 7.1), the siLuc treated group differed significantly from the mock treated and untreated group at day three and day four ($p < 0.01$, One-way-ANOVA). Two days after the last treatment the bioluminescence signal of the siLuc treated group slowly started to increase again.

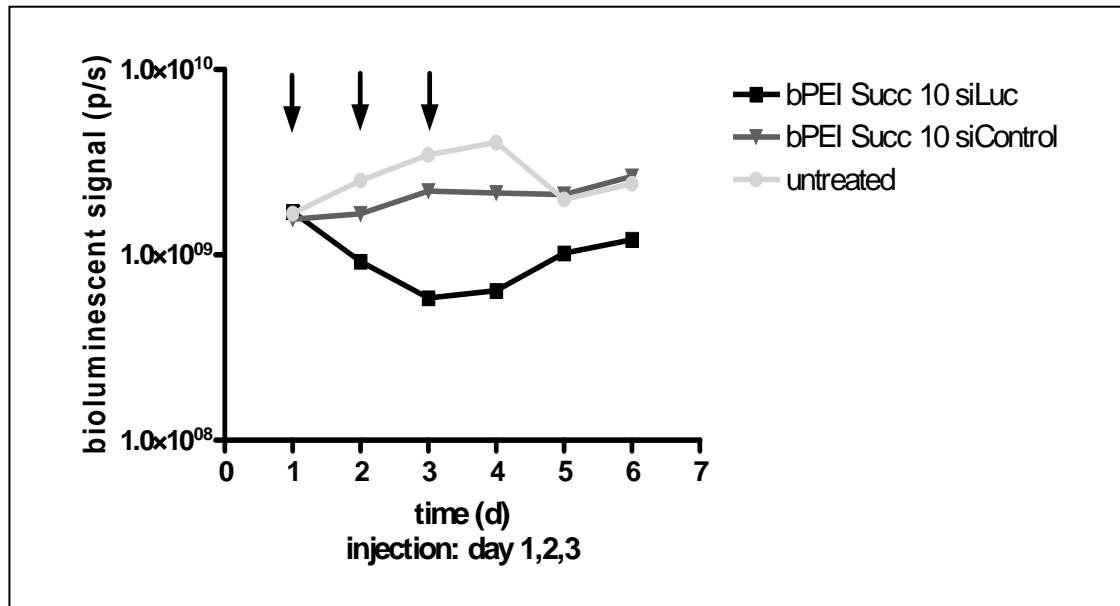


Figure 23: *In vivo* siRNA reporter gene silencing of bPEI Succ 10 on Neuro 2a Luc+ in A/J mice.

A/J mice bearing $\sim 150 \text{ mm}^3$ Neuro 2a Luc+ tumors were measured over two days by bioluminescence imaging. The results of these two measurements are presented as mean on day 1. Thereafter the treatment was performed by three intravenous injections at three consecutive days of 2.5 mg target siRNA (siLuc) or scrambled siRNA (siControl) respectively ($n = 7$) (w/w: 2/1). One group remained untreated. The effects on the bioluminescent signals were evaluated for the next three days by daily bioluminescence imaging. Days of injection are marked with arrows.

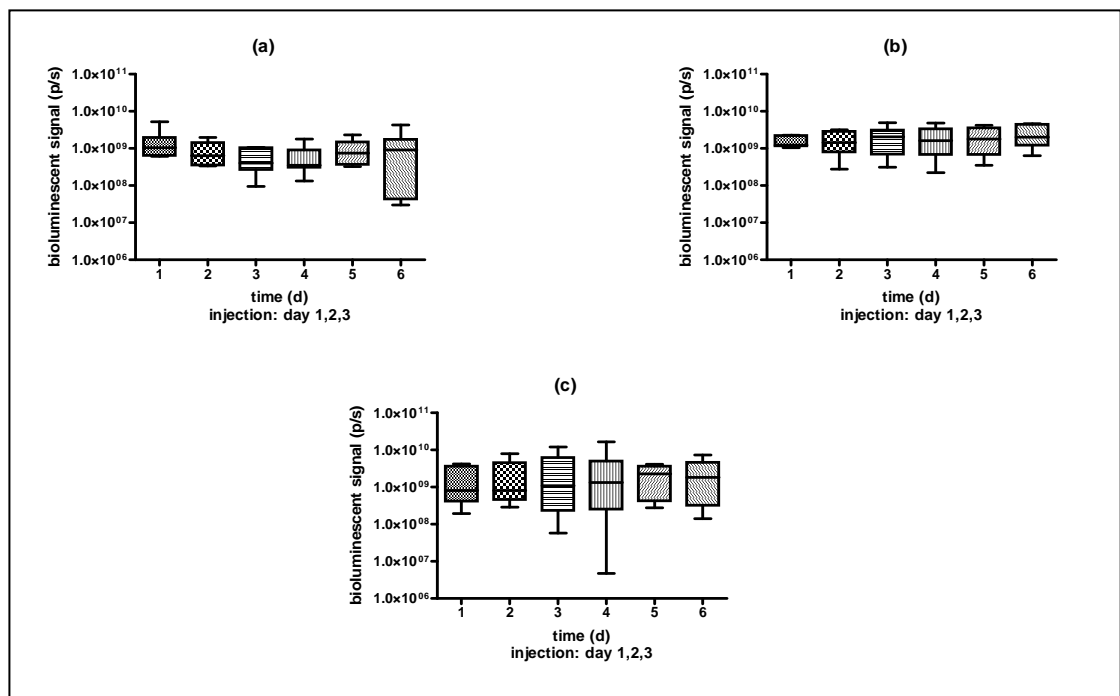


Figure 24: Standard deviations of the *in vivo* siRNA reporter gene silencing of bPEI Succ 10 on Neuro 2a Luc+ in A/J mice.

The data are presented for siLuc treatment (a), for siControl treatment (b) or for an untreated group (c). Results are presented as box plots. The boxes cover the range of 50% of the values above and beneath the mean. The mark in the box indicates the overall mean. The highest and lowest bioluminescence signals are given by standard deviation signs.

To confirm these results the experiment was repeated. This time bPEI Succ 10 was used in parallel to PEI (22 kDa). In order to allow for the collection of tumor samples for rtQPCR measurements, 14 animals were treated per group. Seven animals were euthanized 24 hours after the last treatment and tumors were collected. Seven animals remained for bioluminescence imaging, which was performed daily up to three days after the last treatment (Figure 25). For clarity reasons the means are given without standard deviations. Those are presented for each group in Figure 26. Bioluminescent signals which had been normalized to the pre-treatment bioluminescent signal are presented in the appendix (7.1).

RtQPCR measurement was performed by Alexander Philipp. The data will be part of his PhD thesis. The amount of Luc+ mRNA was calculated in proportion to the mRNA of a housekeeping gene (GAPDH) (Figure 27).

In contrast to the first *in vivo* experiment, in the second study no significant effect of the treatment by bPEI Succ 10/siRNA polyplexes could be detected. RtQPCR revealed relatively stable Luc+ mRNA levels for the untreated group. The ratio between Luc+ mRNA and GAPDH mRNA constantly (despite one exception) ranged from 0.5 to 1. However, in the target as well as the mock treated groups the variance between the Luc+ mRNA levels was very high. The ratio of Luc+ mRNA to GAPDH mRNA varied from 0.1 to 27. No differences could be observed between the target and mock treated groups.

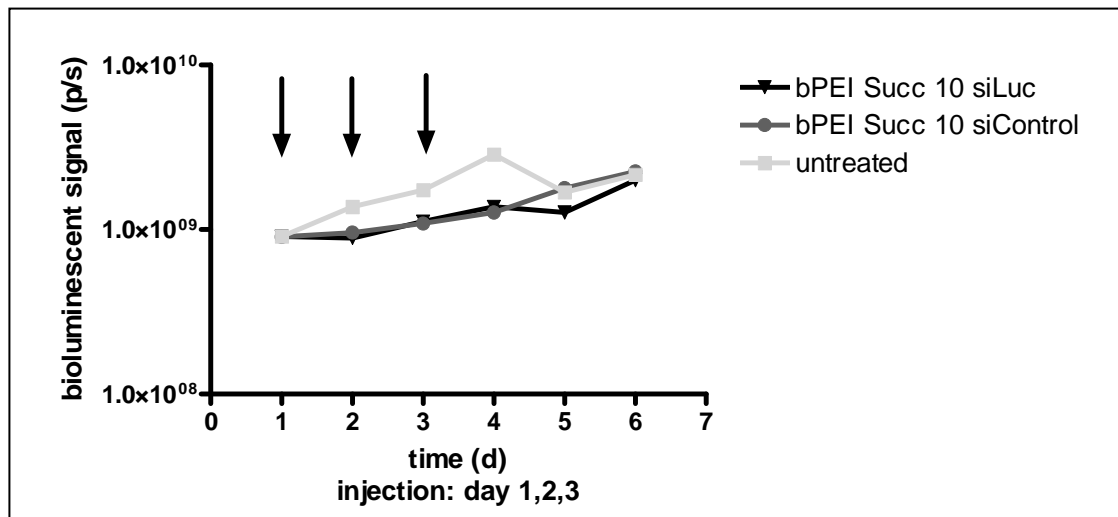


Figure 25: *In vivo* siRNA reporter gene silencing of bPEI Succ 10 on Neuro 2a Luc+ in A/J mice.

A/J mice bearing ~ 150 mm³ Neuro 2a Luc+ tumors were measured over two days by bioluminescence imaging. The results of these two measurements are presented as mean on day 1. Thereafter the treatment was performed by three intravenous injections at three consecutive days of 2.5 mg target siRNA (siLuc) or scrambled siRNA (siControl) respectively (n = 14) (w/w: 2/1). One group remained untreated. The bioluminescent measurement was performed daily up to 24 hours after the last treatment. Thereafter seven animals were euthanized and seven animals remained for bioluminescence imaging up to three days after the last treatment.

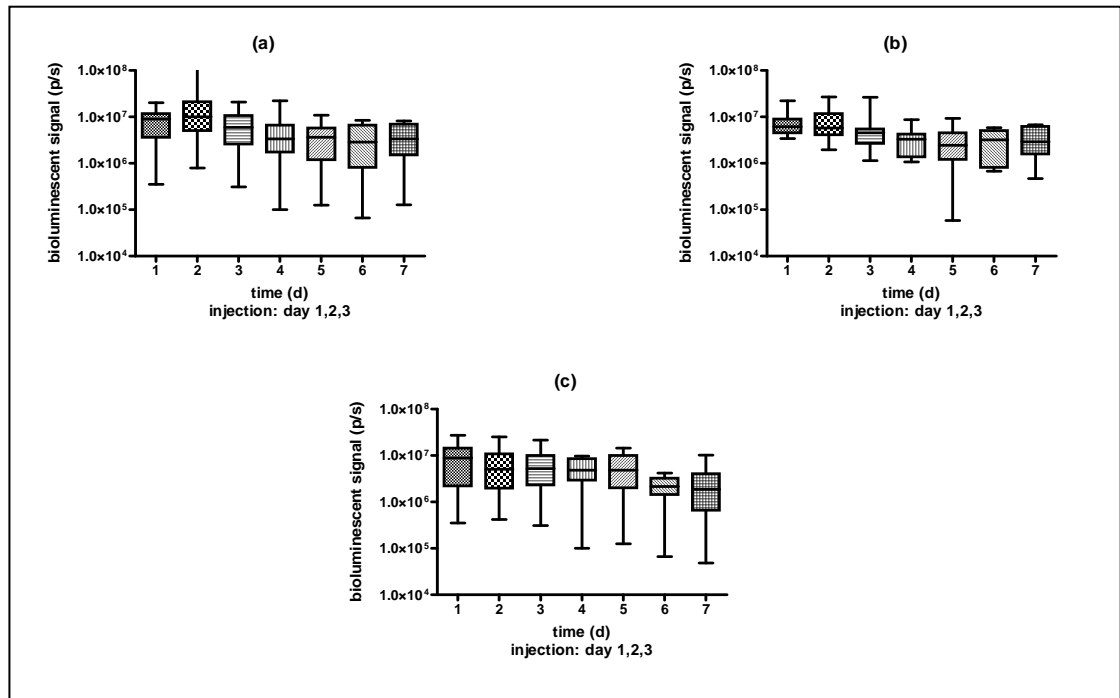


Figure 26: Standard deviations of the *in vivo* siRNA reporter gene silencing of bPEI Succ 10 on Neuro 2a Luc+ in A/J mice.

The data are presented for siLuc treatment (a), for siControl treatment (b) or for an untreated group (c). The results are presented as box plots. The boxes cover the range of 50% of the values above and beneath the mean. The mark in the box indicates the overall mean. The highest and lowest bioluminescence signals are given by standard deviation signs.

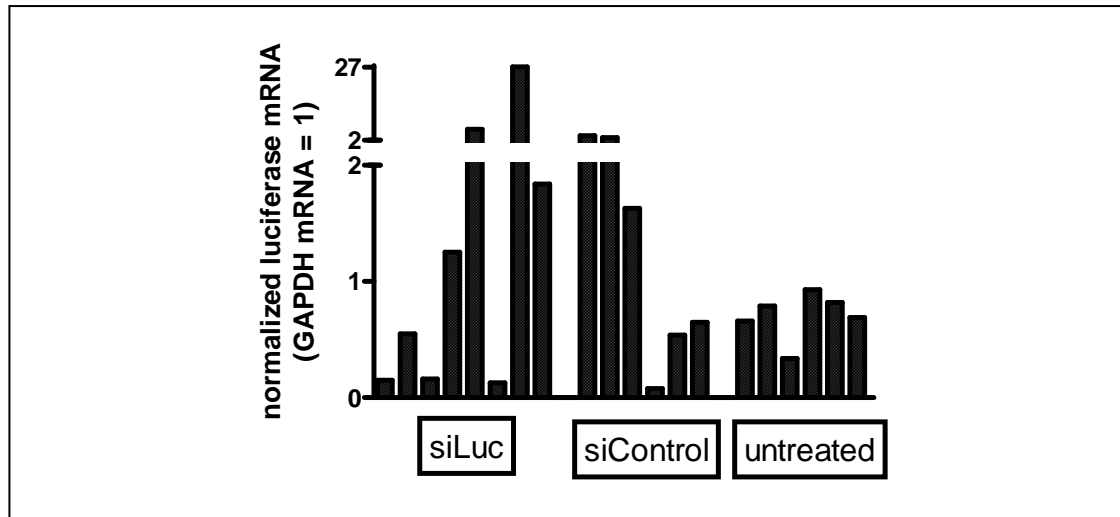


Figure 27: Relative mRNA levels of Luc+ after treatment with bPEI Succ 10 / siRNA polyplexes *in vivo*.

A/J mice bearing $\sim 150 \text{ mm}^3$ Neuro 2a Luc+ tumors were treated by three intravenous injections at three consecutive days of 2.5 mg target siRNA (siLuc) or scrambled siRNA (siControl) respectively ($n = 14$) (w/w: 2/1). One group remained untreated. 24 hours after the last injection mice ($n = 7$) were euthanized and the tumor tissue was collected. After reverse transcription cDNA numbers were evaluated by rtQPCR. The values of the Luc+ mRNA are given in proportion to the values of a housekeeping gene (GAPDH) for every animal of each group.

3.3.1.4 PEI (22 kDa)

Linear PEI (22 kDa) was tested in parallel to bPEI Succ 10, but no samples were collected for rtQPCR. PEI is widely used as a DNA transfer vector due to its high transfection efficacy. In contrast, the siRNA delivery capacity strongly depends on the experimental design. However, its performance is hampered by a high toxicity. Therefore it was also used as a control for unspecific side effects.

For *in vitro* experiments Neuro 2a Luc+ cells were treated with two different w/w ratios. The higher ratio represents the polyplexes thereafter facilitated in the *in vivo* experiment, the lower ratio shows the best performing polyplexes *in vitro*. Both ratios contained either target (siLuc) or scrambled (siControl) siRNA.

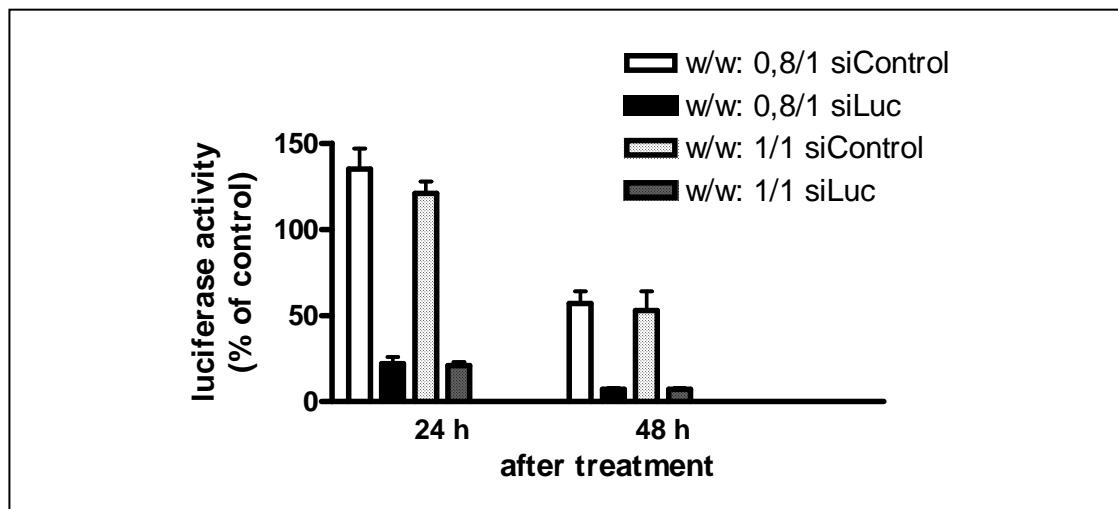


Figure 28: *In vitro* reporter gene silencing of PEI (22kDa) on Neuro 2a Luc+.

Ten thousand cells were treated with polyplexes formed of polymer and target (siLuc) or scrambled (siControl) siRNA in the indicated w/w ratios. 24 or 48 hours after transfection cell lysis was performed. The gene silencing was evaluated using the luciferase reporter gene assay. The measurements were performed with $n = 8$, mean values of three independent experiments and standard deviations normalized to untreated cell (100%) are shown.

Twentyfour hours after treatment both w/w ratios demonstrated no unspecific effect in the mock treated groups but reasonable reporter gene silencing capacity of 80% in the siLuc treated groups. In contrast, 48 hours after treatment the unspecific effect in the mock treated groups simultaneously reached 50% while the specific effect within in the siLuc treated groups was > 90%.

To evaluate the siRNA gene silencing capability of PEI (22 kDa) *in vivo*, A/J mice bearing Neuro 2a Luc+ tumors of approximately 150 mm³ in size were used ($n = 7$). The bioluminescent signals were evaluated on two consecutive days prior to siRNA injection. Thereafter mice received three consecutive intravenous treatments every 24 hours with polyplexes containing 2.5 mg/kg body weight target (siLuc) or scrambled (siControl) siRNA (w/w: 1/1). One group remained untreated. The effects of this treatment on the bioluminescent

signals of the tumors was measured by daily bioluminescence imaging on day 1, 2 and 3 after treatment (Figure 29). For clarity reasons the means are given without standard deviations. Those are presented for each group in Figure 30. The bioluminescent signals which had been normalized to the pre-treatment bioluminescent signals are presented in the appendix (7.1.4). No significant effect of the treatment by PEI (22 kDa)/siRNA polyplexes could be detected *in vivo*.

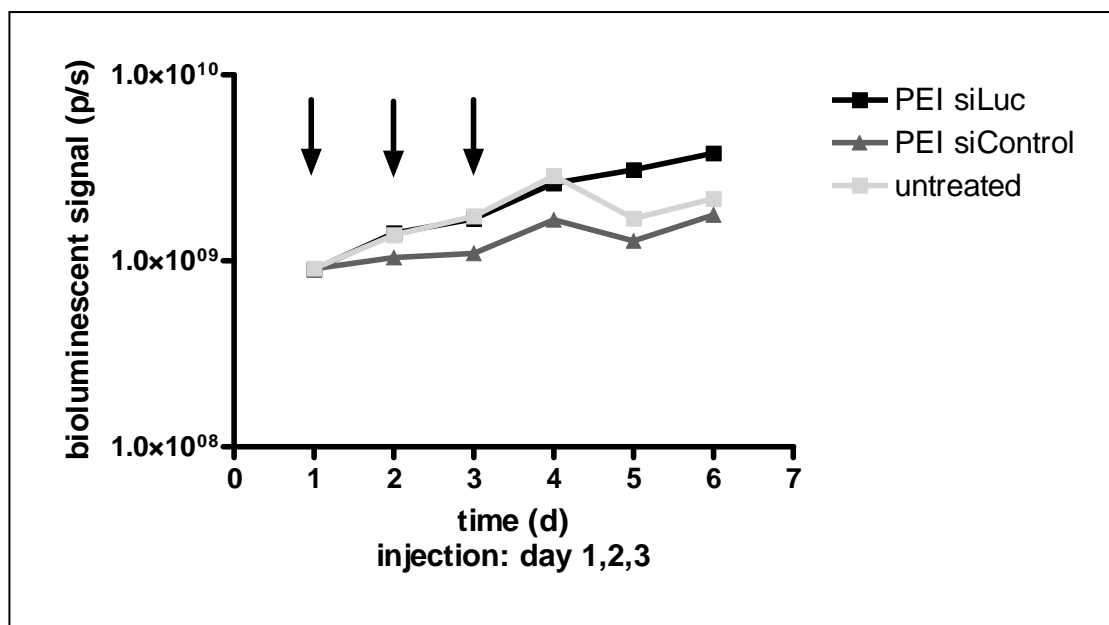


Figure 29: *In vivo* siRNA reporter gene silencing of PEI (22 kDa) on Neuro 2a Luc+ in A/J mice.

A/J mice bearing $\sim 150 \text{ mm}^3$ Neuro 2a Luc+ tumors were measured over two days by bioluminescence imaging. The results of these two measurements are presented as mean on day 1. Thereafter the treatment was performed by three intravenous injections at three consecutive days of 2.5 mg target siRNA (siLuc) or scrambled siRNA (siControl) respectively ($n = 7$) (w/w: 1/1). One group remained untreated. The effects on the bioluminescent signals were evaluated for the next three days by daily bioluminescence imaging. Days of injection are marked with arrows.

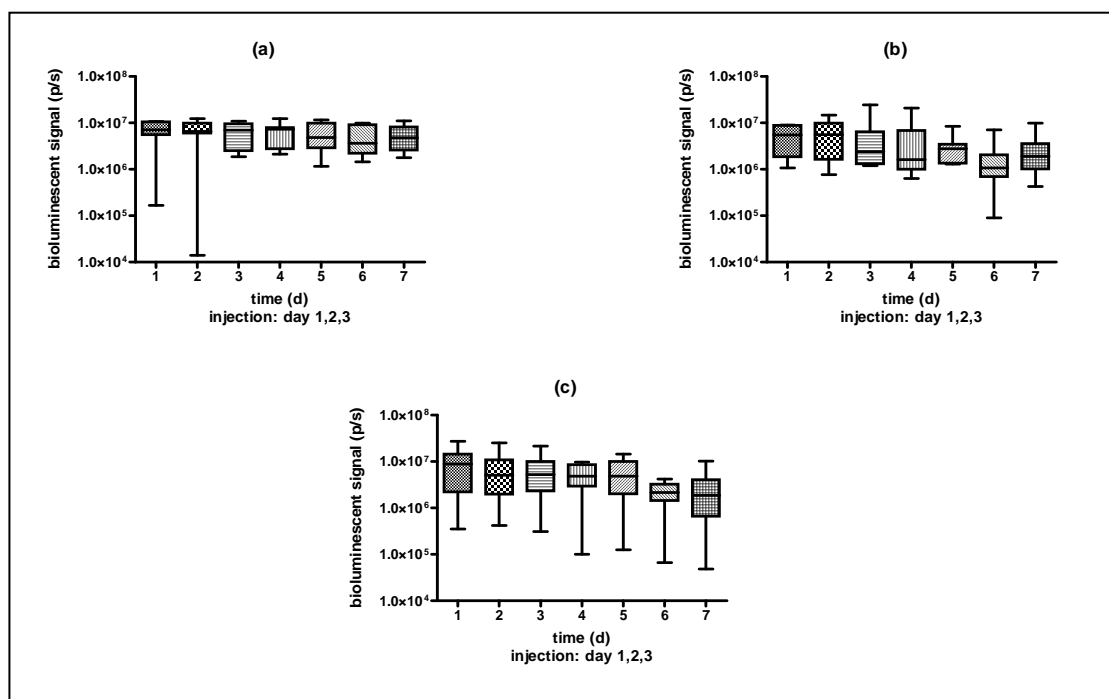


Figure 30: Standard deviations of the *in vivo* siRNA reporter gene silencing of PEI (22 kDa) on Neuro 2a Luc+ in A/J mice.

The data are presented for siLuc treatment (a), for siControl treatment (b) or for an untreated group (c). The results are presented as box plots. The boxes cover the range of 50% of the values above and beneath the mean. The mark in the box indicates the overall mean. The highest and lowest bioluminescence signals are given by standard deviation signs.

3.3.1.5 PLL50- PEG-DMMA_n-Mel / PLL185- PEG-DMMA_n-Mel

Within the *in vivo* results obtained so far, it appeared difficult to show a significant luciferase knockdown. For this purpose intratumoral injection was carried out in animals bearing two tumors in the back, with one tumor serving as internal control to correct for variations in bioluminescence due to substrate distribution and other effects. In addition to bioluminescence imaging rtQPCR measurements were carried out. As a positive control for rtQPCR measurements siRan was used in parallel to siLuc. Ran had already been proven to be targetable *in vivo* in an A/J Neuro 2a wildtype model (57). In addition, the bioluminescence kinetic was measured to exactly determine the bioluminescent signal maximum.

As polymers for intratumoral application of siRNA PLL50-PEG-DMMA_n-Mel or PLL185-PEG-DMMA_n-Mel were chosen. Tf-PLL-DMMA_n-Mel exhibited high efficacy in siRNA delivery together with good biocompatibility *in vitro*. Nevertheless the performance *in vivo* remained unclear as already mentioned above. PLL50 and PLL185 are commercially available PLL analogons. Modification with PLL50 or PLL185, which are PLL molecules of a defined chain length, instead of PLL helps to better define the polymers. Thereby the biocompatibility is enhanced. siRNA delivery was not repeated on Neuro 2a Luc+ *in vitro* but data of siRNA delivery on Neuro 2a eGFP Luc cells are shown. These data were generated by Christian Dohmen and will be part of his PhD thesis. Several w/w ratios were tested. The lower ratio

shown in Figure 31 represents the polyplexes thereafter facilitated in the *in vivo* experiment, the higher ratio shows the best performing polyplexes *in vitro*. Both ratios contained either target (siLuc) or scrambled (siControl) siRNA (Figure 31).

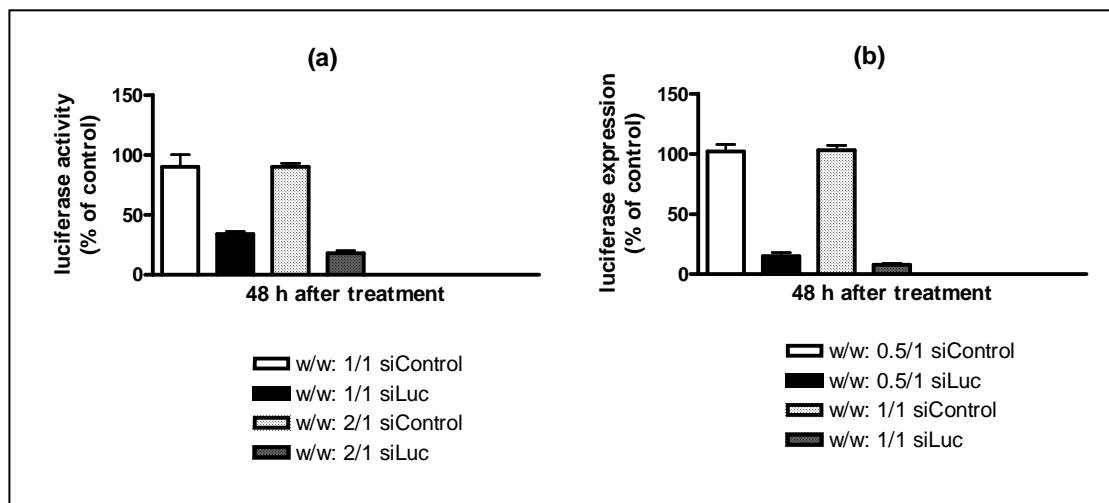


Figure 31: *In vitro* reporter gene silencing of PLL50-PEG-DMMAAn-Mel and PLL185-PEG-DMMAAn-Mel on Neuro 2a eGFPLuc.

Five thousand cells were treated with polyplexes formed of polymer (PLL50-PEG-DMMAAn-Mel (a), PLL185-PEG-DMMAAn-Mel (b)) and target (siLuc) or scrambled (siControl) siRNA in the indicated w/w ratios. 48 hours after transfection cell lysis was performed. The gene silencing was evaluated using the Luciferase Reporter Gene Assay. Results are presented as means and standard deviation and are normalized to the values of untreated cells (100%).

While no unspecific knockdown in the mock treated group was detectable, treatment with the indicated w/w ratios complexed with target siRNA resulted in a knockdown of 70 to 90 %.

To evaluate the siRNA reporter gene silencing capability of PLL50-PEG-DMMAAn-Mel and PLL185-PEG-DMMAAn-Mel *in vivo* A/J mice bearing two Neuro 2a Luc⁺ tumors of around 150 mm³ were used (n = 5). The bioluminescent signals were evaluated over two consecutive days. Thereafter mice received three intravenous treatments at three consecutive days. In every mouse one tumor was treated by intratumoral injection of target siRNA (siLuc), the other one by intratumoral injection of scrambled siRNA (siControl). PLL50-PEG-DMMAAn-Mel polyplexes contained 1.25 mg siRNA/kg body weight in a w/w ratio of 1/1. PLL185-PEG-DMMAAn-Mel polyplexes contained 2.5 mg siRNA/kg body weight in a w/w ratio of 0.5/1. One group remained untreated. The effects of this treatment on the bioluminescent signals of the tumors were followed up to one day after the last treatment by bioluminescence imaging (Figure 32). For clarity reasons the means are given without standard deviations. Those are presented for each group in Figure 33. At the day of the last bioluminescence measurement tumors were explanted for further evaluation of mRNA levels by rtQPCR. (Figure 34) RtQPCR measurement was performed by Alexander Philipp. The data will be part of his PhD thesis.

The treatment of the Ran targeted groups was performed analogously, but without bioluminescent imaging.

No statistically significant knockdown was detected by bioluminescent imaging (One-way-ANOVA). The mRNA measurement showed an unspecific increase of the normalized mRNA levels of Luc as well as Ran of the treated groups compared to the untreated group. Nevertheless the induction as well as the standard deviation were remarkably higher in case of the Luc readout. In case of Ran readout mRNA levels were more stable, but also no knockdown was observed. These results were independent of the housekeeping gene used for normalization.

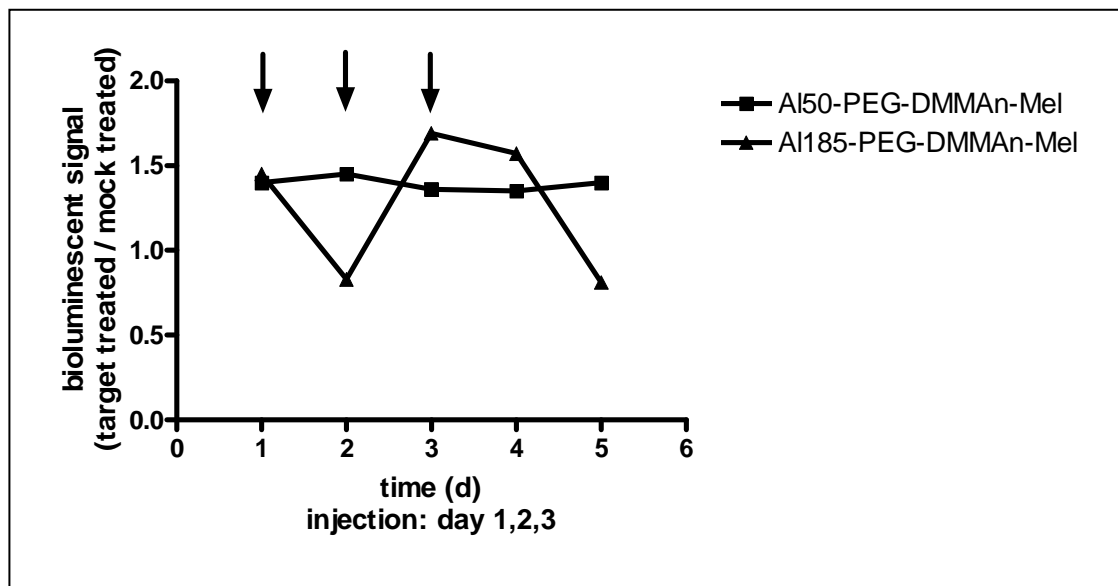


Figure 32: *In vivo* siRNA reporter gene silencing of PLL50-PEG-DMMAn-Mel and PLL185-PEG-DMMAn-Mel on Neuro 2a Luc⁺ in A/J mice normalized to mock treatment.

A/J mice bearing two $\sim 150 \text{ mm}^3$ Neuro 2a Luc⁺ tumors were measured over two days by bioluminescence imaging. The results of these two measurements are presented as mean on day 1. The data is presented as target treated (siLuc) tumor normalized to mock treated (siControl) tumor bioluminescent signals. The treatment was performed by three intratumoral injections at three consecutive days. PLL50-PEG-DMMAn-Mel polyplexes contained 1.25 mg siRNA/kg body weight in a w/w ratio of 1/1. PLL185-PEG-DMMAn-Mel polyplexes contained 2.5 mg siRNA/kg body weight in a w/w ratio of 0.5/1. The control treatment was carried out within the same animal. The effects on the bioluminescent signals were evaluated up to one day after the last treatment by daily bioluminescence imaging. Days of injection are marked with arrows.

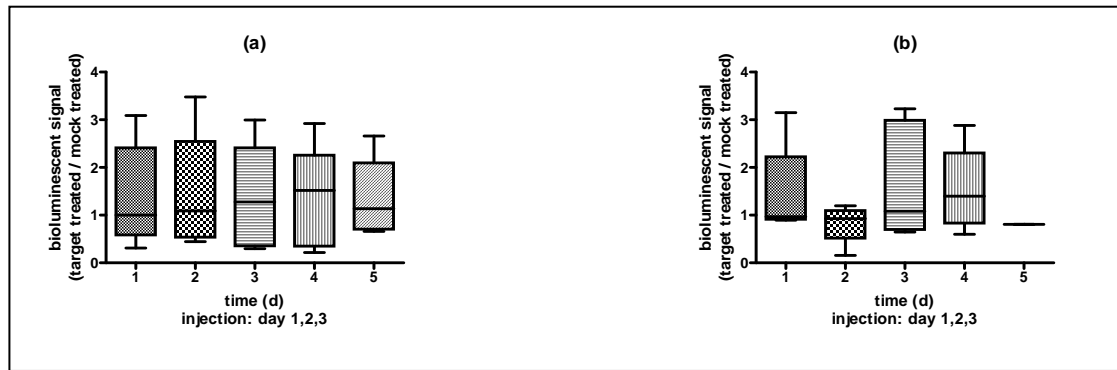


Figure 33: Standard deviations of the *in vivo* siRNA reporter gene silencing of PLL50-PEG-DMMAN-Mel and PLL185-PEG-DMMAN-Mel on Neuro 2a Luc+ in A/J mice.

The data are presented for siLuc treatment (a) and for siControl treatment (b). The results are presented as box plots. The boxes cover the range of 50% of the values above and beneath the mean. The mark in the box indicates the overall mean. The highest and lowest bioluminescence signals are given by standard deviation signs.

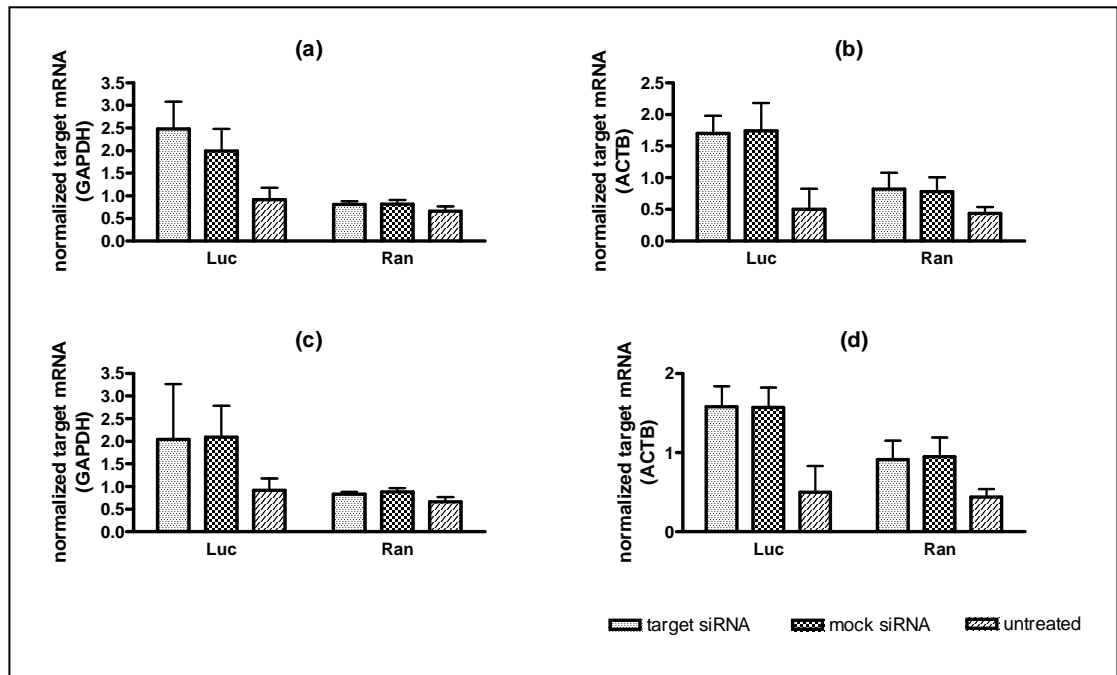


Figure 34: Relative mRNA levels of Luc+ and Ran after treatment with PLL50-PEG-DMMAN-Mel and PLL185-PEG-DMMAN-Mel/siRNA polyplexes *in vivo*.

A/J mice bearing two $\sim 150 \text{ mm}^3$ Neuro 2a Luc+ tumors were treated by three intratumoral injections at three consecutive days. siLuc and siRan were used as target siRNAs, siControl as scrambled siRNA for mock treatment. PLL50-PEG-DMMAN-Mel polyplexes contained 1.25 mg siRNA/kg body weight in a w/w ratio of 1/1. PLL185-PEG-DMMAN-Mel polyplexes contained 2.5 mg siRNA/kg body weight in a w/w ratio of 0.5/1. Control treatment was carried out within the same animal. One group remained untreated. 24 hours after the last injection mice were euthanized and the tumor tissue was collected. After reverse transcription cDNA numbers were evaluated by rtQPCR. Results are presented for the PLL50-PEG-DMMAN-Mel group (a + b) and for the PLL185-PEG-DMMAN-Mel group (c + d), normalized to GAPDH (a + c) and beta-Actin (b + d) as housekeeping genes. The values are given as means with standard deviation.

3.3.2 Utilization of the positive readout system (Neuro 2a ODD Luc)

Two different approaches based on ODD Luc as reporter gene were followed. The first one was the implementation of Neuro 2a ODD Luc cells as subcutaneous tumors in A/J mice. The second one was an ODD Luc transgenic mouse strain expressing the transgene in every tissue. The overall purpose of this concept was to end up with two systems allowing to evaluate efficacy of siRNA delivery into the targeted tissue (ODD Luc tumors), but also in non-targeted tissues, such as liver or lung (ODD Luc transgenic mouse strain).

To gain an induction of the bioluminescent signal the degradation cascade of HIF1 alpha had to be disrupted by siRNA mediated gene silencing. Two proteins hold key positions within this degradation cascade and therefore were potential targets. The first one is prolyl-hydroxylase two (PHD2). Despite being part of an enzyme family, PHD 2 has the highest work load. PHD2 and its family members mediate the hydroxylation of HIF1 alpha in an oxygen and iron depending reaction, thereby initializing the degradation cascade.

The second one is the von-hippel-lindau-factor (VHL). As an essential part of the E3 ubiquitin ligase it is involved in the ubiquitination and degradation of HIF1 alpha.

In order to test the response of the ODD Luc transgenic systems on these siRNA targets, bPEI Succ 10 and lipofectamine were used as delivery systems. As already pointed out in 3.3.1.3, bPEI Succ 10 has an outstanding position due to its high gene silencing capacity in combination with high biocompatibility. Lipofectamine had been proven to work sufficiently for siRNA delivery on fibroblasts *in vitro* (data not shown).

3.3.2.1 A/J Neuro 2a ODD Luc tumor mouse model

The response of Neuro 2a ODD Luc cells on siRNA mediated targeting of PHD2 and VHL was initially tested *in vitro*. (Figure 35) Beside the two target siRNAs, siLuc+ was used as a positive control in order to check for correct siRNA delivery. SiControl was facilitated as a negative control. Additionally one group was treated with deferoxamine. Deferoxamine causes iron depletion, prevents the hydroxylation of HIF1 alpha by the prolyl-hydroxylase family and thereby interrupts the HIF1 alpha degradation cascade.

The data sets obtained after 24, 48 and 72 hours revealed similar results. SiRNA targeting Luc+ caused reporter gene silencing thereby indicating that the siRNA delivery by bPEI Succ 10 was functional. All other siRNA treatments including the scrambled siControl resulted in an unspecific induction of reporter gene signal. In contrast treatment with deferoxamine turned out to be toxic on Neuro 2a ODD Luc cells and therefore did not show the estimated induction in reporter gene signal. In general standard deviations were exceptionally high.

After these results *in vitro* no *in vivo* study was performed with Neuro 2a ODD Luc cells.

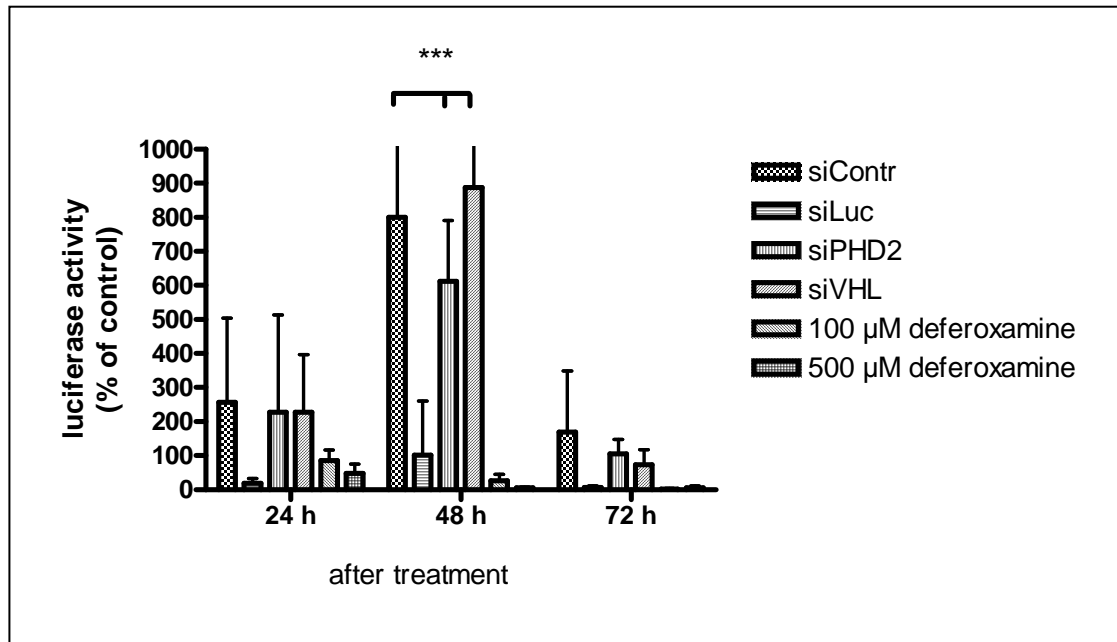


Figure 35: *In vitro* accumulation of ODD Luc fusion protein by siRNA mediated inhibition of HIF1 alpha degradation cascade on Neuro 2a ODD Luc.

Ten thousand cells were treated with polyplexes formed of bPEI Succ 10 and indicated siRNAs. Zero point five μg siRNA/well was used in a w/w ratio of 4/1. Deferoxamine was used as a positive control for the system functionality. Twentyfour, 48 and 72 hours after transfection cell lysis was performed. The gene silencing was evaluated using the luciferase reporter gene assay. The measurements were performed with $n = 8$, mean values of three independent experiments and standard deviations normalized to untreated cell (100%) are shown.

3.3.2.2 ODD Luc transgenic mouse strain

First the response of the system on targeting of PHD2 or VHL was evaluated. Therefore fibroblasts were isolated from a heterozygous ODD Luc transgenic mouse (Figure 36). Treatment was performed as described for Neuro 2a ODD Luc cells with the exception that lipofectamine was used instead of bPEI Succ 10, because lipofectamine had shown higher efficacy in case of siRNA delivery to fibroblasts (data not shown).

The data sets obtained after 24, 48 and 72 hours revealed similar results. Treatment with deferoxamine revealed a significant ($p < 0.001$, One-way-ANOVA) elevated luciferase signal. SiPHD2 treatment as well resulted in an induced signal, which became significant after 48 hours, whereas siVHL and siControl treatment showed no effects. In contrast siLuc+ treatment mediated a significant reduction in reporter signal.

In order to test if these results were as well reproducible *in vivo*, siPHD2 was administered to the liver tissue of ODD Luc transgenic mice by high pressure tail vein injection (Figures 37). This method is approved for delivery of naked siRNA to hepatocytes (139, 140). As a negative control siControl was injected. The basic bioluminescence signal of each transgenic animal was detected before and after siRNA treatment at several time points.

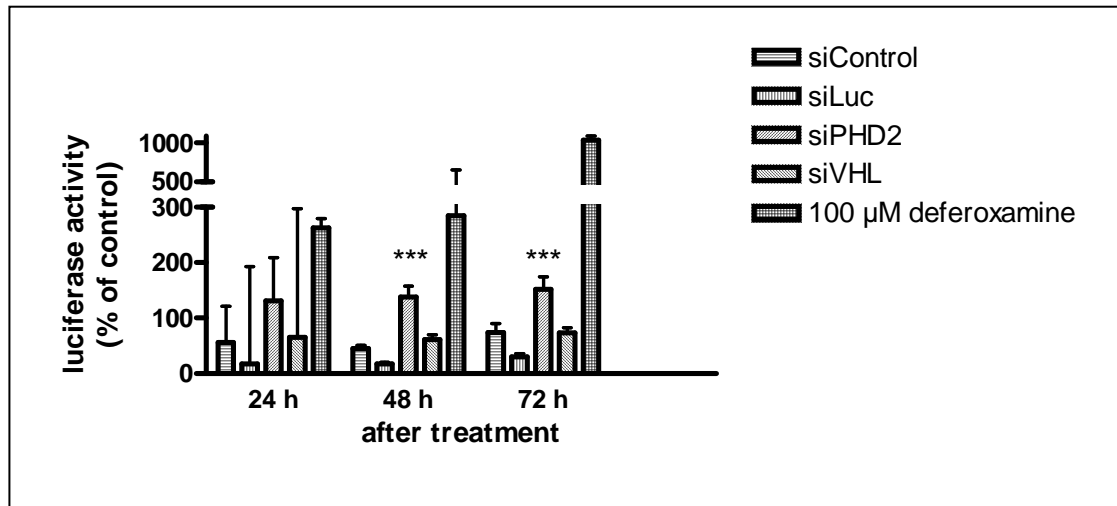


Figure 36: *In vitro* accumulation of ODD Luc fusion protein by siRNA mediated inhibition of HIF1 alpha degradation cascade on primary ODDLuc +/- fibroblasts.

Five thousand cells were treated with polyplexes formed of lipofectamine and indicated siRNAs. Zero point five μg siRNA/well was used in an w/w ratio of 4/1. Twentyfour, 48 and 72 hours after transfection cell lysis was performed. The gene silencing was evaluated using the luciferase reporter gene assay. The measurements were performed with $n = 8$, mean values of three independent experiments and standard deviations normalized to untreated cell (100%) are shown.

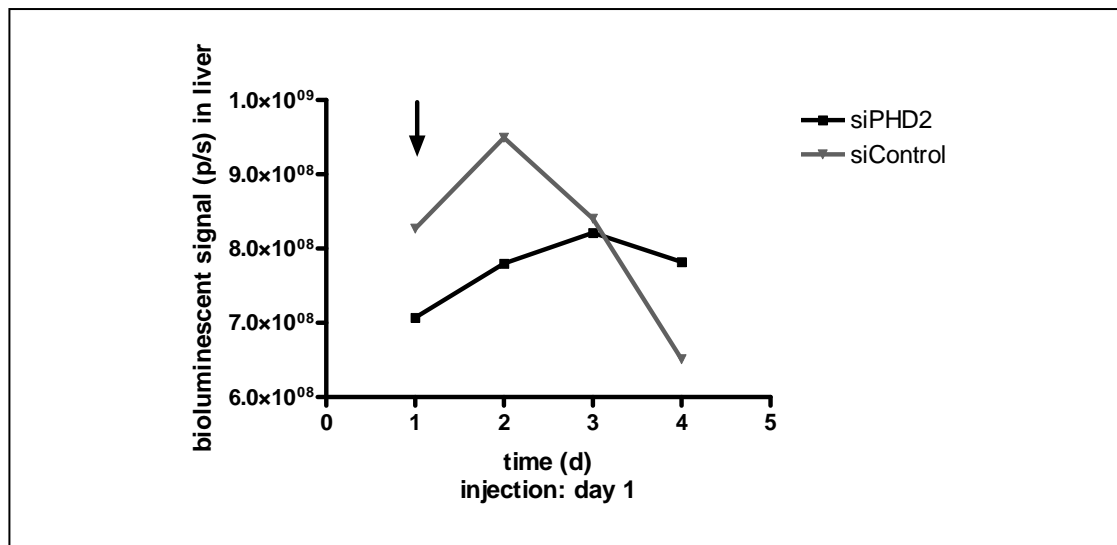


Figure 37: *In vivo* accumulation of ODD Luc fusion protein by siPHD2 mediated inhibition of the HIF1 alpha degradation cascade in ODD Luc transgenic mice.

Basic bioluminescent liver signal of ODD Luc transgenic mice was determined over some days. The results of these measurements are presented as mean on day 1. Thereafter the mice received 2.5 mL ringer-lactat-solution containing either 2.5 μg siPHD2/mL ($n = 5$) or 2.5 μg siControl ($n = 2$). The effects of the treatment on the liver bioluminescent signals were measured daily up to three days after siRNA injection. The values are given as means without standard deviation. The day of injection is marked with an arrow.

No significant difference could be detected between the target and mock treated group. Both groups reacted with an induction of bioluminescent signal at 24 hours after injection. At 48 hours induction of the bioluminescent signal was even more pronounced in the target treated group whereas the signal in the mock treated group had already decreased. 72 hours after injection the bioluminescent signal of the target treated group had as well decreased, but did not reach basic level.

4 Discussion

4.1 Generation of different monoclonal Luc transgenic Neuro 2a cell lines

For the development of efficient synthetic vector systems for siRNA delivery a screening system is needed to test the efficacy of siRNA delivery to target cells *in vivo*. For this purpose *in vivo* bioluminescence imaging appeared to be the most advantageous method (61, 67, 141) and was therefore chosen for the experimental design. Beside the traditional negative readout method the development of a positive readout method was aimed.

Firefly luciferase is known as the most useful enzyme for *in vivo* bioluminescence imaging studies due to the emitted red shifted wavelength, enzyme stability and substrate pharmacology. Nevertheless, different subforms of firefly luciferase vary in terms of activity and other parameters. (142). Therefore in the present work subtypes of firefly luciferase differing in expression intensity and protein stability, namely Luc, Luc+ and Luc2, were evaluated (134).

As positive readout bioluminescent system a fusion construct of one of the oxygen depending domains (ODD) of HIF1alpha and firefly luciferase (ODD Luc) was utilized.

Suitable plasmids were cloned in order to stably transfect tumor cells. The newly derived Luc encoding plasmids were initially tested for luciferase expression intensity after transient transfection with PEI (22 kDa) on Neuro 2a cells. As expected Luc+ exhibited no difference in enzyme activity compared to the positive control, which was previously reported to give high activity levels (137). Luc, which has not been optimized for high expression intensity, Luc2, which is designed to have a faster kinetic due to its degradation domains, and ODD Luc, which is permanently degraded under normoxic conditions, showed highly significant ($p < 0.001$, One-way-ANOVA) diminished enzyme activities in comparison to Luc+. Interestingly ODD Luc exhibited significantly ($p < 0.001$, One-way-ANOVA) higher enzyme activity than Luc and Luc2. This high expression level of the ODD Luc fusion protein 24 hours after transfection with PEI (22 kDa) is most likely caused by the PEI treatment itself. PEI binds unspecifically to negatively charged proteins, thereby hampering their function (143). In case of the ODD Luc fusion protein potential interaction of PEI with one of the essential proteins for the degradation cascade of HIF could result in an accumulation and high activity level of ODD Luc fusion protein. Additionally PEI mediates transcription of immunological response genes and genes of many other cellular processes, such as oxidative stress responses by the redox-system (144). Interference with the redox system is known to have an impact on the activation of the HIF pathway (145, 146). This hypothesis is further supported by the fact, that stably transfected Neuro 2a ODD Luc cells showed basic bioluminescent signals when being

measured several weeks after transfection, but measurements shortly after the transfection revealed that they are unspecifically inducible by the treatment with transfection vectors. This indicates that the event of transfection causes stress and interacts with physiological cellular pathways in a way that activates the HIF pathway and thereby induces ODD Luc levels.

As tumor cell line for generation of transgenic clones the murine neuroblastoma cell line Neuro 2a was chosen. Neuro 2a cells are known to overexpress the Tf-receptor, which allows for proper targeting, and to reliably lead to well vascularized subcutaneous tumors in A/J as well as SCID mice, which is beneficial for systemic delivery (57, 135). Additionally good correlation between *in vitro* and *in vivo* tests was anticipated because these cells have as well been used for *in vitro* experiments. The mean bioluminescent signals of all cell clones of each transgenic cell line again revealed the expected differences in signal intensity with Luc+ showing the highest intensity, followed by the faster degraded Luc2 and the less efficient Luc. As discussed above, several weeks after the transfection Neuro 2a ODD Luc cells had recovered to physiological conditions and therefore showed the anticipated low basic luciferase signal intensity. One of the Neuro 2a ODD Luc clones correctly responded to deferoxamine mediated inactivation of the polyhydroxylases by an induction of the bioluminescent signal.

In general there was a rather high variance in bioluminescent signal and, in case of ODD Luc, in respond to the deferoxamine treatment between the cell clones of each transgenic cell line. This variance can be explained by the random integration of one or multiple copies of linearized DNA into the cells genome during the transfection process. The number of copies as well as the integration side has an impact on the expression level as well as the functionality of the transgene (147-149). These effects become more distinct in monoclonal than in polyclonal cell lines and raise the possibility to select the cell clone which fits best in the experimental protocol.

4.2 Characterization and optimization of subcutaneous tumor mouse models

Subsequently the newly derived transgenic cell clones were characterized *in vivo* by evaluating the growth and the bioluminescent signal in order to assess variances compared to the wildtype cells that might have come along during the selection process of the transgenic clones.

Additionally, the selected tumor mouse model had to be specifically adapted according to the demands of siRNA delivery studies. Therefore the influence of certain protocol parameters on the positive readout of the measurement method was checked and optimized.

Tumor growth was found to be unhampered by the transgene. As previously reported for subcutaneous wildtype Neuro 2a tumors in A/J mice (35, 57), subcutaneous transgenic Neuro

2a clones became palpable around 7 days after inoculation and thereafter showed exponential increase of tumor volume until the termination of the experiment.

Luciferase expression levels developed similarly for Neuro 2a Luc, Luc+, Luc2 and eGFP Luc with Luc showing slightly lower expression levels. These results were anticipated as selection of the clones with the lowest transgene expression already *in vitro* led to similar luciferase expression levels of all clones independently of the transgene.

As it has also been previously reported by Dickson *et al.* (150), bioluminescent signals were distinguishable as early as day 1 after inoculation and increased exponentially according to the tumor growth until the experiment was terminated.

In contrast to the negative readout systems, the positive readout system Neuro 2a ODD Luc revealed the desired and previously *in vitro* assessed low basic luciferase expression level as well *in vivo*, which remained stable over the time of the experiment. Due to the enhanced number of tumor cells and additionally due to the formation of hypoxic zones within the tumor we expected an exponential and hypoxia induced increase of expression level over the time. On the other hand there have been several reports on lower bioluminescent signals in larger tumors that could be caused by poor penetration of substrate into the tumor tissue, attenuation of the signal within the tumor or alteration of the transgenic status (151-153). This effect apparently has a higher impact on the already low basic signal of Neuro 2a ODD Luc than on very high bioluminescent signals such as the signals of Neuro 2a Luc+ or Neuro 2a eGFP Luc. However, the high variance of the data obtained by the Neuro 2a ODD Luc mouse model required additional *in vitro* experiments before utilization of this mouse model for tests of siRNA delivery (discussed in 4.3).

In general standard deviations were significant and especially high for the cell clones bearing luciferases with reduced stability, such as Neuro 2a ODD Luc and Neuro 2a Luc2. This is not surprising given the fact that in these cases physiological pathways are involved in the degradation process of luciferase. Those are likely to be influenced interindividually over time thereby causing the assessed deviations. But even Neuro 2a Luc revealed notable standard deviations presumably due to the non optimized transcription pattern of this transgene, which causes an overall lower luciferase activity (134). Slight changes become more distinct in case of low than in case of abundant luciferase activity. Neuro 2a eGFP Luc and Neuro 2a Luc+ gave the most robust results. As a stable basic signal is a crucial factor for *in vivo* delivery studies further effort was done to optimize the Neuro 2a Luc+ tumor mouse model regarding the standard deviation.

One critical point of bioluminescent imaging that is diversely discussed is the application procedure of the luciferin substrate, including amount, time point and application site (151). Typically, an amount of 150 mg/kg body weight luciferin is injected intraperitoneally 10 minutes prior to bioluminescent imaging. Paroo *et al.* have already shown that this procedure

is not sufficient to evoke maximized bioluminescent signals depending on the transgenic tissue (119). They were able to prove that either a higher amount of substrate or local application into the transgenic tissue dramatically increased bioluminescent signal compared to the standard procedure. Therefore 300 mg/kg body weight luciferin was used in the present studies according to the findings of Hildebrandt *et al.* (138). Kayearts *et al.* examined the effect of intravenous compared to intraperitoneal substrate injection (151). They showed a shorter time-to-peak, a lower variance and a higher maximum bioluminescent level for intravenous injection offering a better reproducibility and sensitivity compared to the standard procedure. These results are further supported by Wang *et al.* (154). Nevertheless no consent has been found so far regarding the best time point of measurement after injection (151, 155). In the present study we used A/J mice bearing two subcutaneous Neuro 2a Luc+ tumors. Time-to-peak was almost identical after intraperitoneal and intravenous application of substrate, but the interindividual variation of time-to-peak in the tumors was far lower for the intraperitoneally injected group than for the intravenously injected group. Additionally the variance between intraindividual peak signals remained relatively stable for the intraperitoneal group but differed remarkably for the intravenous group.

Taken together these data indicate that in case of subcutaneous Neuro 2a tumors on the animals flank the substrate, which is a small molecule, reaches the tumor size over the blood stream and equally *per diffusionem*. Both distribution patterns appear to be equally fast and sufficient to provide the luciferase enzyme with the needed amount of substrate. Similar results were observed by Paroo *et al.*, in luciferin distribution studies (119). The higher intraindividual delay and variance between the tumors in the intravenously treated group reveals a lower reproducibility compared to the intraperitoneal treated group, which stands in contrast to the findings presented by Kayaerts *et al.* (151). A possible explanation lies within the exclusively vascular distribution of luciferin after intravenous injection. In this case time-to-peak depends to a higher extent onto the vascularisation level of the transgenic tumor tissue than in the case of distribution *per diffusionem*. Tumor blood vessel density as well as their dilatation status will consecutively have a higher influence on the time-to-peak and the peak level and cause higher variance between individual tumors.

Another parameter that can influence the outcome of bioluminescent measurements is the position of the transgenic tissue and camera to each other. In concordance with the accepted assumption it could be shown in the present work that slight changes in the position can alter the outcome of the measurement.

A major challenge for bioluminescent imaging of transgenic tumor tissue is the fact that tumor growth develops differently in each individual, which over time causes increasing interindividual variances. Therefore it is generally recommended to use tumors as small as possible. On the other hand successful systemic siRNA treatment relies on accessibility via the

tumor vascularisation, which is dependent on the tumor size. This conflict is solved by some working groups by calculation of a correction factor (105).

In the present study a tumor mouse model with low interindividual variance in transgenic cell number in combination with well vascularisation was aimed at. Therefore different modifications of the tumor mouse model were tested. It had been shown in the literature that cells being injected into tumor tissue remain intact and functional (156, 157). To standardize all animals on a certain number of transgenic cells we therefore performed injection of a defined amount of transgenic cells into wildtype Neuro 2a tumors. This did not lead to less variance in bioluminescent signals. As the variance occurred already at the first measurement and persisted even over the exponential growth curve of the transgenic cells in the wildtype tissue, this effect is most likely caused by variances in the wildtype tumors regarding for example vascularisation, tissue density or necrosis, which would give rise to different implantation, growth and bioluminescence of the injected transgenic tumor cells.

Another effort was made to standardize the tumor size and hence the bioluminescence signal by insertion of small tumor fragments. By this method the variance in bioluminescent signal could be significantly decreased. On the other hand it has to be taken into account that insertion of tumor fragments is more elaborate than injection of transgenic tumor cells - especially for larger groups of animals – and thus not suitable for a screening protocol. Therefore the standard method was used for further experiments. But the newly assessed method remains as a good option to standardize on tumor size and bioluminescent signal if needed.

A final aspect that has to be considered in *in vivo* bioluminescent measurements is the anaesthesia stage. Anaesthesia in imaging studies is mostly done by isoflurane inhalation, which comes along with distribution of isoflurane throughout the whole body, diminished oxygen levels and lower body temperatures. Those parameters have been shown to influence the distribution of marker molecules (158). A standardised method of animal preparation and imaging was applied to limit the effects from these factors. (as described in 2.7.2.1)

In conclusion, in the present work it has been shown that in case of the A/J Neuro 2a Luc+ subcutaneous tumor mouse model the optimized working protocol includes

- intraperitoneal injection of 300 mg/kg body weight luciferin
- time-to-measurement of 13.30 minutes or preferable sequence measurements from 10 to 15 minutes
- carefully positioning of the transgenic tumor tissue in relation to the camera
- standardised anaesthesia methods

Additionally insertion of transgenic tumor fragments came out to be a time consuming but highly reliable protocol to prepare tumor bearing mice for bioluminescent imaging studies.

4.3 Utilization of mouse models for detection of effective siRNA delivery

There are only a few reports on successful siRNA delivery to tumor tissue by systemic injection so far. (see 1.4) This is not exceptional taken into consideration the obstacle of siRNA delivery itself combined with the complexity of successful proof *in vivo*. Hence, beside the development of effective synthetic vector systems, major effort is made establishing an appropriate screening method. In the present study the Neuro 2a Luc⁺ subcutaneous tumor mouse model was evaluated as a very promising model for further implementation for detection of effective siRNA delivery as a negative readout system, as good vascularisation and overexpression of the Tf-receptor makes Neuro 2a cells well targetable by systemic siRNA delivery and Luc⁺ provides a stable enzyme activity.

Additionally the Neuro 2a ODD Luc subcutaneous tumor mouse model was evaluated for the same purpose as a potential positive readout system.

4.3.1 Utilization of the negative readout system (Luc⁺)

Reduction of bioluminescent signal in transgenic tumor tissue by direct targeting of luciferase using *in vivo* bioluminescent imaging as the readout technique has so far successfully been proven only by Bartlett *et al.* (105, 106) However, the main focus of this working group lies on the development of calculation factors to correctly predict the influence of certain parameters such as cell doubling rate or application protocol on the mediated knockdown effect. Therefore they predominantly show a correlation of the predicted outcome with the data of single individuals, which are often corrected by calculation factors. However, significance tests are needed to assess the potential of new siRNA delivery vectors to induce a specific protein knockdown in the target tissue. In the present siRNA knockdown studies presumable specific as well as unspecific effects of the treatments on the bioluminescent readout could be shown. Treatment with Tf- PLL-DMMAn-Mel-ss-siRNA showed a clearly unspecific knockdown of the bioluminescent signal. Characteristic non-bioluminescent areas were detectable after treatment with this vector complexed with targeting as well as scrambled siRNA that persisted until the termination of the study. This effect might be evoked either by blockage of blood vessels resulting in a depletion of oxygen and luciferin within the vascularized tumor area or by local toxic effects of the polyplexes leading to necrosis. However, this phenomenon was not analyzed any further as the aim of this study was mainly the implementation of the mouse model and not predominantly the evaluation of the siRNA delivery systems. Significance could be proven for the specific knockdown of the bioluminescent signal following the treatment with bPEI Succ 10 delivering siLuc. However, these results could not be confirmed when repeating the experiment, neither by bioluminescent imaging nor by rtQPCR.

Treatment with OEI-HD1/Tf-OEI-HD1 (90/10) and PEI (22 kDa) did not reveal any visible knockdown effects, nor did PLL50-PEG-DMMA_n-Mel or PLL185-PEG-DMMA_n-Mel.

This data highlights that verifying significance is one of the most important aspects and on the other hand one of the biggest hurdles.

In significance testing a high confidence always depends on the signal-to-noise ratio and on the number of individuals tested. The signal-to-noise ratio thereby stands for the treatment mediated effect in comparison to the inherent signal variation of the readout (159).

In order to enhance the confidence either the signal-to-noise ratio has to be improved or the number of animals treated per group has to be increased. As increasing the animal numbers cannot be an infinite option due to many – most importantly ethical – reasons optimizing the efficacy of the siRNA transfer vectors and eliminating the random effects on the readout parameter (variance of the readout parameter) has to be the major goal.

4.3.1.1 Impact of the transfer vector

Tf-PLL-DMMA_n-Mel-ss-siRNA came out of the physicochemical and *in vitro* tests as a very promising candidate for *in vivo* testing. Physicochemical and *in vitro* data of the very similar PEG-PLL-DMMA_n-Mel-ss-siRNA have recently been published by our working group (58). Nevertheless, the already published polymer still showed remarkable toxicity *in vivo* disqualifying it for further *in vivo* tests. Modification of the polymer with transferrin as targeting ligand and shielding moiety greatly enhanced biocompatibility without hampering its performance in physicochemical as well as *in vitro* tests. Hence there should be no reason for inefficacy in siRNA delivery *in vivo*. Nevertheless efficacy *in vivo* has not been proven using another method yet.

OEI-HD1/Tf-OEI-HD1 (90/10) was previously shown to promote a specific knockdown of the target mRNA (Ran) in tumor cells *in vitro* and *in vivo* without unspecific toxicity (57). *In vivo* knockdown was therein confirmed by the therapeutic effect (tumor growth reduction and induction of apoptosis due to Ran knockdown), on the protein level by Western Blot and on the mRNA level by rtPCR. These findings could not be confirmed in the present work.

Slight changes within the studies protocol could have an impact on the results. Tietze *et al.* carried out three siRNA applications every 72 hours, starting with wildtype Neuro 2a tumors approximately 3 mm in size. In the present study three siRNA applications every 24 hours were performed, and the Neuro 2a Luc⁺ tumors were approximately 7 mm in size. While Tietze *et al.* targeted an endogeneous gene, a transgene was targeted in the present work. Another aspect, that has to be taken into consideration, is the tolerated w/w ratio *in vivo*. This ratio comes out to be nearly non effective *in vitro*, despite the siRNA is fully complexed by the polymer. It has been shown in our working group recently, that free polymer is essential for sufficient endosomal escape of the polyplexes and consequently for siRNA delivery.

(Alexander Philipp; data not published) It could be argued that there is less free polymer in *in vivo* tests and therefore polyplexes got stuck within the endosomes. On the other hand free polymer and polyplexes in the blood stream do not necessarily end up in the same cells (34). Given the fact that the same ratio has already been proven successful *in vivo*, this parameter seems to be negligible.

bPEI Succ 10 showed an outstanding performance *in vitro* regarding efficacy and biocompatibility (33). The two independent but equally performed *in vivo* experiments showed differing results. In the first series a significant and specific knockdown effect was detectable, whereas in the second experiment no specific knockdown was observed.

The reason might be that this polymer does not include any targeting moiety. While being of less impact regarding *in vitro* efficacy, targeting is known to be of extreme importance when it comes to *in vivo* performance, especially after systemic injection such as performed in the present study (160). This and the fact of a suboptimal w/w ratio (as discussed above in case of OEI-HD1/Tf-OEI-HD1 (90/10)) might hamper the effectivity of bPEI Succ 10 *in vivo* when compared to *in vitro* data resulting in a very low effect near the detection limit.

For the second experiments rtQPCR data support the results that were obtained by the bioluminescent study, for the first experiments unfortunately no rtQPCR readout was performed.

PEI (22 kDa) exhibits rather high unspecific toxic effects in proportion to the specific knockdown *in vitro*. Its effectivity for siRNA delivery has recently been investigated *in vitro* as well as *in vivo* (38, 161, 162). Nevertheless its performance might be hampered, because it does not have a targeting moiety and additionally sticks to the reticuloendothelial organs such as lung and liver.

PLL50-PEG-DMMA_n-Mel and PLL185-PEG-DMMA_n-Mel are very similar to PLL-PEG-DMMA_n-Mel, but are - due to the exchange of undefined PLL to PLL with a certain chain length (PLL50, PLL185) - better defined and hence supposed to be better biocompatible. As intratumoral injection in a mouse model bearing two Neuro 2a Luc⁺ tumors was planned and the polyplexes were not assumed to end up in circulation, modification of these polymers with a targeting ligand as well as conjugation of the siRNA to the polymer were skipped. But it could be proven by Meyer *et al.* (58) that intratumoral injection of PLL- PEG-DMMA_n-Mel-ss-siRNA in Neuro 2a tumors due to the distinguished vascularization consecutively leads to systemic distribution. Hence PLL50-PEG-DMMA_n-Mel and PLL185-PEG-DMMA_n-Mel could as well have been distributed throughout the body. On the one hand they could – without a targeting moiety - not specifically attach to the tumor tissue on the other hand these polyplexes might be subject to fast dissociation in the blood stream. Therefore without targeting and conjugated siRNA payload, no specific effects can be presumed after entrance into the circulation. Additionally both tumors within one mouse had been treated, the first one

with target siRNA, the second one with scrambled siRNA. Given the event of systemic distribution of target as well as scrambled polyplexes the effects could possibly have been neutralized.

Beside the individual aspects, that have to be considered, in general the higher dilution of the polyplexes within the bloodstream compared to the situation in the cell culture medium can have an impact on the performance. In principle, *in vitro* data and *in vivo* data are hardly comparable. Therefore an evaluated *in vivo* screening method would be needed to precisely assess the performance of the newly developed tumor mouse models.

4.3.1.2 Impact of the measurement method

As described above inherent signal variations of the readout parameter can influence the reliability of the resulting data. The A/J Neuro 2a Luc+ tumor mouse model reveals such inherent variances in the bioluminescent readout caused for example by intrinsic inhomogeneities in the group due to tumor size or vascularisation level or by minor changes within the measurement protocol. Despite the effort that was made in order to precisely optimize and thereafter perform the measurement protocol as discussed in 4.2, variances could not be diminished in the utilization studies.

They seemed to be randomly affected by mock as well as targeted treatments. This assumption was further supported by the rtQPCR data, which revealed an unspecific effect – both inductive and reductive – on the Luc+ mRNA levels after treatment with bPEI Succ 10, whereas the mRNA levels of untreated animals were stable. After treatment with PLL50-PEG-DMMAAn-Mel and PLL185-PEG-DMMAAn-Mel Luc+ mRNA levels were induced unspecifically in comparison to the untreated group. This effect was detectable to a far less extent for the Ran mRNA levels. This difference between unspecific effects on the expression of a transgene or of an endogenous gene could be explained as follows.

Transfection efficacy with synthetic vectors is relatively low when compared to the viral transfection and stably integration of the transgene occurs only in rare cases. Even stably transgenic cells very likely lose their transgene if not constantly kept under selection pressure. While this is not a major concern *in vitro* maintenance of selection pressure is not easily possible *in vivo*. Therefore there is a reasonable chance that some of the tumor cells will lose their transgene during the phase of the exponential growth of the tumor. Depending on the number of cells and the time-point of this event, those “wildtype” cells will distort the readout. A mixed tissue of “wildtype” and transgenic tumor cells could explain the higher variance of luciferase to housekeeper ratio in comparison to Ran to housekeeper ratio in rtQPCR. However, the unspecific perturbation of the bioluminescent signals as well as the Luc+ mRNA levels after any treatment is not explainable by a mixed culture.

A reason for this could be the influence of the promoter. In Neuro 2a Luc+ the transgene is controlled by the CMV promoter. This promoter is known to be highly susceptible to silencing *in vivo* (163-165). The enhancement of CMV promoter activity was shown to be - amongst others - mediated by NFκB (166-168). NFκB is connected to the immune system and known to be activated by certain growth factors, cytokines (for example TNF alpha, IL-1beta) and antigens, such as double-stranded RNA (169-171) By those stimuli a strong activation or even reactivation of the CMV promoter after silencing is mediated by intervention of NFκB (172). Consequently every treatment that is able to induce the immune system might induce NFκB and therefore activate or reactivate the CMV promoter.

Given the fact that the luciferase transgene itself causes antibody formation, which means immune stimulation, the CMV promoter is subject to constant inactivation, reactivation and hyperactivation. Taken the several other transcription factors into account that are involved in mediation of the promoter activity such as CREB/ATF, NF-1 (173), AP-1 (167), SP 1 (174) and MDBP (175, 176) the influence of the polyplex treatment on these transcription factors cannot be predicted. Therefore every transgene expression which is driven by the CMV promoter will be subject to unpredictable changes *in vivo*, especially after interference with the immune system or cellular signalling pathways, for example by polyplex treatment. This consequently disqualifies CMV promoter driven luciferase as a tool for proof of successful siRNA delivery.

Summarizing the implementation studies of the negative readout tumor mouse model, it became apparent that it was mostly not possible to significantly prove the efficacy of the tested synthetic siRNA delivery vectors. Significant results could either be obtained by optimization of the transfer vectors performance or by eradication of the random variance of the models basic signal.

As the performance of the transfer vectors naturally is not predictable and even lower efficacy should be detected, suppression of the basic signal variance had to be aimed at.

This goal cannot be reached using the A/J Neuro 2a Luc+ model, because the CMV promoter is influenced by a variety of physiological pathways and drives luciferase expression in a random pattern.

Even if the Luciferase transgene construct provided a stable signal without variance, the evaluation of knockout after systemic *in vivo* delivery would be difficult. Established tumor-targeted transfection systems usually reach only a small fraction of the target tumor (2, 177). While in case of DNA delivery studies the introduction of luciferase genes into few (e.g. 10%) of the wildtype tumor cells would result in a very strong luciferase signal, a similar (e.g. 10%) reduction of luciferase in a transgenic tumor would hardly be measurable. Therefore positive readout systems, where silencing induces (not reduces) luciferase, are required (see next section).

4.3.2 Utilization of the positive readout system (ODD Luc)

Induction of bioluminescent signal in transgenic tumor tissue by siRNA mediated targeting of a repressor protein of luciferase using *in vivo* bioluminescent imaging as the readout technique has not been proven so far. In the present studies two different approaches based on ODD Luc as reporter gene were followed. The first was the implementation of Neuro 2a ODD Luc cells as subcutaneous tumors in A/J mice. The second was the evaluation of an existing ODD Luc transgenic mouse strain expressing the transgene in every tissue.

4.3.2.1 A/J Neuro 2a ODD Luc tumor mouse model

SiRNA delivery tests *in vitro* using bPEI Succ 10 as a transfer vector were conducted to assess the inducibility of the Neuro 2a ODD Luc cells by the specific knockdown of certain essential proteins of the HIF1alpha degradation cascade. They revealed an unspecific inducibility of the system independently of the siRNA sequence. This effect was covered by a pronounced knockdown effect when the luciferase was directly targeted by siLuc+. In contrary, targeting essential proteins of the degradation cascade could not mediate a further induction compared to the treatment with scrambled siRNA.

As discussed above treatment with PEI (22 kDa) had already shown inducibility of the Neuro 2a ODD Luc system by the treatment itself. In the present study this effect was as well observed for the treatment with bPEI Succ 10, which is a modification of bPEI. Hence it is very likely that the same mechanisms – namely interaction with essential proteins, mediation of gene transcription and activation of oxidative stress responses – are responsible for the unspecific signal induction.

Additionally treatment with deferoxamine should assess the correct inductive response of the ODD Luc system to interruption of the degradation cascade. Deferoxamine causes a depletion of iron (178). Because iron is an essential cofactor of the prolylhydroxylases, they are inactivated, and the degradation cascade is stopped. This effect could not be proven as deferoxamine turned out to be toxic on Neuro 2a ODD Luc cells. Lee *et al.* as well observed toxicity of deferoxamine on neuronal cell lines and found it to be independent of the iron depletion but due to the production of hydroxyl radicals and intracellular Ca²⁺ release (179).

Taken together the unspecific inducibility *in vitro* and the random signal variances within the untreated A/J Neuro 2a ODD Luc tumor mouse model *in vivo*, this model was not used for further implementation in siRNA delivery studies.

4.3.2.2 ODD Luc transgenic mouse strain

Primary fibroblasts derived from a heterozygous ODD Luc transgenic mouse were used for first *in vitro* siRNA delivery tests.

In contrast to the Neuro 2a ODD Luc cells, in ODD Luc fibroblasts treatment with deferoxamine was well tolerated, and the cells responded with a pronounced induction of

bioluminescent signal as it had been described by Safran *et al.* (133). In accordance with the effects observed on Neuro 2a ODD Luc, treatment with siLuc+ resulted in a clear reduction of the bioluminescent signal, whereas scrambled siRNA did not mediate any effect.

Most importantly the ODD Luc fibroblasts could be shown to be inducible by knockdown of PHD2, but not by knockdown of VHL. Wu *et al.* already discussed that specific silencing of PHD2 is sufficient for stabilizing HIF1alpha and increasing its transcriptional activity (131). In the present study this could as well be proven for the ODD Luc fusion protein.

In contrary it was surprising, that treatment with siRNA targeting VHL should not interrupt the HIF 1alpha degradation cascade and cause a signal induction.

It is well known, that knockout of VHL in different cell lines leads to accumulation of HIF 1alpha comparable to hypoxic conditions (180). Meanwhile it is frequently discussed, that VHL additionally plays its role within many physiological pathways. VHL has been implicated in extracellular-matrix formation as well as in stabilisation of the cellular microtubules (181, 182). Particularly in case of murine fibroblasts VHL depletion has been shown to impair growth (183), initialize a senescence program (184) and cause spindle misorientation and chromosomal instability (185). Those results indicate that beside accumulation of HIF 1alpha versatile effects can be mediated by VHL depletion which seem to have variable impacts on different cell lines. With respect to murine fibroblasts – as have been used in the present study – VHL depletion resulted in severe intervention with cell growth and viability. Such a condition – despite sublethal – could definitely have an impact on expression and accumulation of the ODD Luc fusion protein.

In summary, PHD2 came out to be a promising target for further investigation *in vivo*.

siRNA delivery *in vivo* was performed by hydrodynamic delivery of the naked siRNA into the animals. This technique resulted in an unspecific induction of bioluminescent signal, as had been observed similarly in Neuro 2a ODD Luc cells.

Hydrodynamic delivery is known to be a highly efficient method for delivery of naked siRNA predominantly to the liver (139, 140, 186). On the other hand damage of liver cells has been reported that naturally comes with the large volume injected. Increase of ALT serum levels indicating the cellular damage became apparent 20 minutes after injection and dropped significantly 24 hours after injection (187-189). Coming along with this cellular damage an immunogenic reaction occurs, which on the one hand can interfere with the cellular redox-system and on the other hand with the CMV promoter of the transgene. Intervention with the redox-system could mediate an induction of the bioluminescent signal by activation of the HIF 1alpha pathway, whereas dysregulation of the CMV promoter due to immunogenic stimuli would lead to diverse transgene expression. A connection of the cellular damage to the unspecific induction of the bioluminescent signal is further supported by the fact, that the induction of the mock treated group lasted for 24 hours after injection, whereas the induction

of the target treated group was even increased after 48 hours. This indicates that there is a specific signal induction which is partly covered by an unspecific induction coming along with the liver damage.

This in general proves the positive readout system functional. However, overall it has to be stated, that the high sensitivity of this system to physiological parameters such as oxygen saturation, immunogenic responses and cellular pathways hampers its utility for siRNA delivery studies.

5 Summary

Nucleic acid-based therapy holds tremendous promise in the treatment of many genetic and acquired diseases by delivering therapeutic nucleic acids into patients. Within nucleic acid-based therapy a tool that has newly emerged but has already gained high importance is siRNA mediated therapy.

As siRNA is subject to fast degradation in the blood stream when being injected unprotected, the employment of the siRNA technology for therapeutic settings requires the development of effective siRNA delivery vector systems. In order to optimize the delivery vectors an *in vivo* screening method for the proof of efficacy of the newly modified vector system is urgently needed.

Bioluminescence imaging using firefly luciferase as the light emitting enzyme is considered the most advantageous technique for this purpose. Nevertheless the measurement protocol as well as the employment of firefly luciferase faces many problems, especially in transgenic tumor models. The accurate selection of the appropriate transgene and the careful adaptation of the tumor mouse model to the specific demands of siRNA delivery studies are crucial steps within the developmental process towards an appropriate *in vivo* screening method.

This thesis aimed at the establishment of tumor mouse models based on firefly luciferase expressing murine neuroblastoma cells where siRNA triggered silencing should either reduce (negative readout system) or induce (positive readout system) the luciferase signal in the tumor. For the negative readout system, firefly luciferase enzymes that differ regarding expression intensity and half-life (Luc, Luc+, Luc2) were evaluated. A fusion product of an oxygen-sensitive HIF1 alpha fragment and firefly luciferase (ODD Luc) was tested as positive readout system. For this purpose also an available transgenic mouse strain (FVB ODD Luc) was tested expressing this hypoxia-inducible firefly luciferase system in every tissue.

The plasmids encoding for the appropriate transgenes under the control of the CMV or SV40 promoter were at first tested on expression intensity and thereafter stably transfected on Neuro 2a cells. Subsequently the newly derived transgenic cell clones were characterized in A/J mice regarding tumor growth capacity and development of the bioluminescent signal. The A/J Neuro 2a Luc+ subcutaneous tumor mouse model which came out as the most reliable system was chosen for further optimization and implementation for siRNA delivery studies. Additionally the A/J Neuro 2a ODD Luc subcutaneous tumor mouse model was utilized. Effort was made to discover proper siRNA target genes (PHD2, VHL) for specific induction of this system in case of successful siRNA delivery.

Optimization studies revealed the importance of a standardized anaesthesia protocol and animal positioning. For the generation of reproducible data also the timing of the

intraperitoneal application of the substrate with an appropriate distribution time of 13 minutes was important.

In vivo studies using the negative readout system revealed, that despite the optimized measurement protocol the performance of the system is still hampered by a high random variance of the basic bioluminescent signal. This variance could to a high extent be caused by a dysregulation of the CMV promoter towards various experimental treatments, thereby unspecifically modulating the *in vivo* transcription of the transgene.

Implementation studies using the positive readout system demonstrated a too high extent of RNAi-independent, unspecific induction of the hypoxia-responsive Neuro 2a ODD Luc tumor system in respond to various treatments.

For the ODD Luc transgenic mouse strain inducibility of the system in case of siRNA mediated knockdown of PHD2 (but not in case of VHL knockdown) could be shown on primary ODD Luc fibroblasts *in vitro*. *In vivo* this effect was partly hampered by an unspecific induction of the bioluminescent signal. This result was mainly due to the rather rough technique of hydrodynamic delivery of siRNA to the liver. In summary, the positive readout system was functional but too sensitive to disturbances of physiological parameters to be successfully employed for siRNA delivery studies.

6 Zusammenfassung

Durch die Anwendung von nukleinsäurebasierten Therapieformen verspricht sich die biomedizinische Forschung gewaltige Fortschritte bei der Behandlung von angeborenen sowie erworbenen Krankheitsbildern. Die Anwendung von siRNA ist ein in diesem Gebiet neu entwickelter jedoch bereits sehr wichtiger Ansatz.

Da ungeschützt in den Blutstrom eingebrachte siRNA sehr schnell degradiert wird, kommt der Entwicklung von Transfervektoren für den Transport von siRNA eine große Bedeutung bei der Implementierung dieser Technik für Therapieansätze zu. Um die Effektivität der neu entwickelten oder modifizierten Transfervektoren im Organismus testen zu können, wird dringend eine *in vivo* Screeningmethode benötigt.

Hinsichtlich dieses Ziels hat sich die biolumineszente Bildgebung auf Basis der Lichtemission der Firefly Luciferase als am ehesten zielführend erwiesen. Trotzdem ist selbst diese Technik bezüglich des genauen Messprotokolls und des verwendeten Luciferaseenzym problembehaftet – insbesondere bei der Anwendung in Tumor-Maus-Modellen. Deshalb sind sowohl die sorgfältige Auswahl des geeigneten Transgenes als auch die exakte Anpassung des Messprotokolls an die Ansprüche beim Nachweis von siRNA Transfer äußerst wichtige Schritte innerhalb des Entwicklungsprozesses eines *in vivo* Screeningverfahrens.

In der vorliegenden Arbeit wurde parallel die Entwicklung eines Systems mit reduziertem biolumineszenten Signal nach erfolgreichem siRNA Transfer sowie eines Systems mit induziertem biolumineszenten Signal vorangetrieben. Beide Systeme wurden in Form von subkutanen Tumor-Maus-Modellen etabliert. Im Fall des induzierbaren Systems wurde zusätzlich ein transgener Mäusestamm getestet.

Als reduzierbares System wurden verschiedene Formen der Firefly Luciferase, die sich hinsichtlich ihrer Expressionsaktivität sowie der Halbwertszeit unterscheiden, herangezogen. Das induzierbare System basierte auf einem Fusionsprodukt des sauerstoffabhängigen Fragments von HIF1 alpha mit der Firefly Luciferase.

Entsprechende für diese Transgene kodierende Plasmide wurden zunächst hinsichtlich ihrer Expressionsaktivität überprüft und dann stabil in das Genom von murinen Neuroblastomzellen integriert.

Im Folgenden wurden die neu gewonnenen transgenen Zellklone als subkutane Tumoren in A/J Mäusen etabliert und auf Wachstumsrate sowie Entwicklung des biolumineszenten Signals überprüft.

In diesen Versuchen stellte sich das subkutane A/J Neuro 2a Luc+ Model als am zuverlässigsten hinsichtlich des biolumineszenten Basissignals heraus und wurde daher für die weitere Optimierung sowie erste Anwendungsversuche für siRNA Transferstudien herangezogen. Zusätzlich wurde auch die Anwendung des subkutanen A/J Neuro 2a ODD Luc

Modells weiter vorangetrieben. In diesem Zusammenhang wurde besonderer Augenmerk auf die Evaluierung geeigneter Zielgene (PHD2, VHL) zur Induktion des biolumineszenten Signals nach erfolgreichem siRNA-basiertem Knockdown gelegt.

In den Optimierungsstudien konnte gezeigt werden, dass der strengen Einhaltung eines gleichbleibenden Narkoseprotokoll sowie einheitlicher Lagerung der Tiere eine große Rolle bei der Auswertbarkeit der Ergebnisse zukommt. Intraperitoneale Injektion eines Überschusses an Substrat und entsprechend lange Distributionszeit von 13 Minuten erwiesen sich als wichtig für die Generierung maximaler Biolumineszenzsignale.

Erste Anwendungsstudien mit dem reduzierbaren System legten offen, dass die Aussagefähigkeit dieses Systems trotz sorgfältiger Anpassung des Messprotokolls noch immer durch die hohe Schwankungsbreite des Grundsignals beeinträchtigt wird. Da diese Schwankungsbreite höchstwahrscheinlich durch eine Dysregulation des CMV Promotors, der die Ablesung des Transgenes steuert, ausgelöst wird, ist eine weitere Verbesserung des Modells ausgeschlossen.

Bei den ersten Anwendungsstudien des induzierbaren Modells *in vitro* wurde für die Neuro 2a ODD Luc Zellen eine unspezifische Induzierbarkeit des biolumineszenten Signals durch die Behandlung festgestellt.

Auf den primären ODD Luc transgenen Fibroblasten, die wir für erste *in vitro* Versuche aus der transgenen Mauslinie gewonnen hatten, konnte eine Signalinduktion durch siRNA-basierten Knockdown der PHD2 (nicht aber durch Knockdown von VHL) erreicht werden. Dieser Effekt wurde jedoch bei der nachfolgenden Anwendung *in vivo* zum Teil von unspezifisch induktiven Effekten überlagert. Zwar war die gewählte Behandlungsmethode des Einbringens von siRNA mittels Hochdruckinjektion sehr invasiv; das induzierbare System erwies sich aber, obgleich vom Grundsatz funktionell, auch insgesamt als zu anfällig gegenüber physiologischen Veränderungen, um als Nachweismethode für siRNA Transfer angewendet werden zu können.

7 Appendix

7.1 Supplements

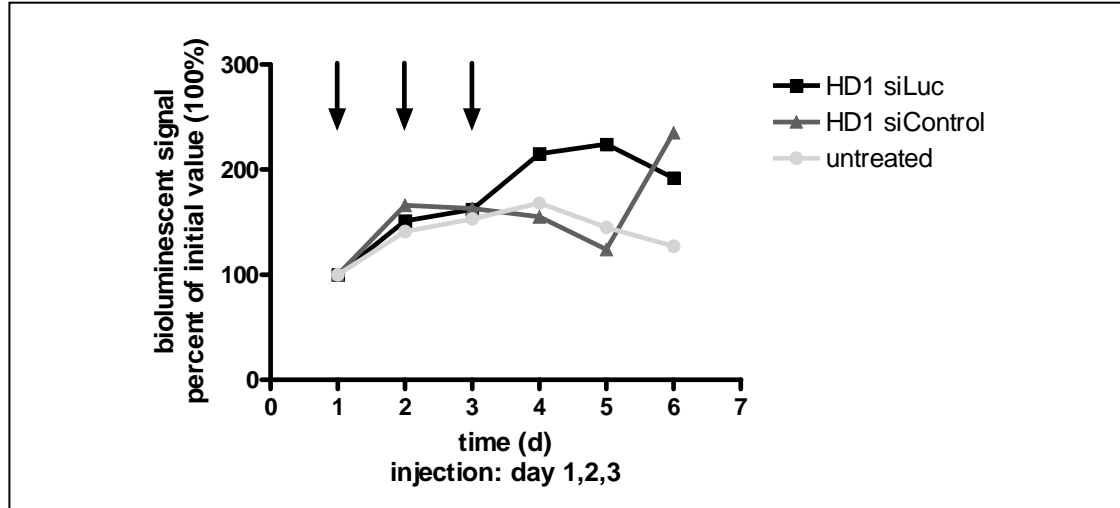


Figure 7.1.1 *In vivo* siRNA reporter gene silencing of OEI-HD1/Tf-OEI-HD1 (90/10) on Neuro 2a Luc+ in A/J mice normalized to the basic value.

A/J mice bearing $\sim 150 \text{ mm}^3$ Neuro 2a Luc+ tumors were measured over two days by bioluminescence imaging. The mean of the results of these two measurements was set as 100% and presented on day 1. Thereafter the treatment was performed by three intravenous injections at three consecutive days of 2.5 mg target siRNA (siLuc) or scrambled siRNA (siControl) respectively ($n = 7$) (w/w: 0,5/1). One group remained untreated. The effects on the bioluminescent signals were evaluated for the next three days by daily bioluminescence imaging and normalized to the basic value before treatment.

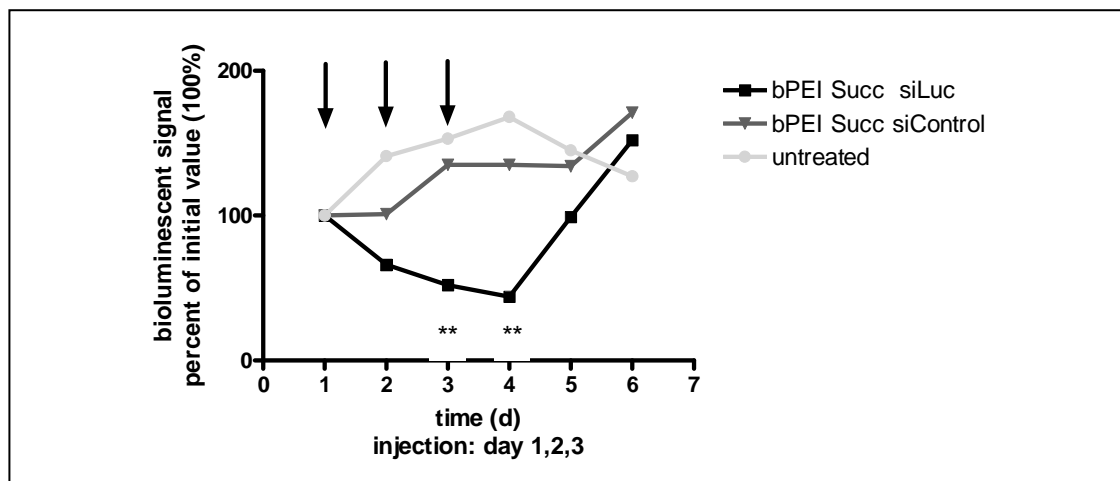


Figure 7.1.2 *In vivo* siRNA reporter gene silencing of bPEI Succ 10 on Neuro 2a Luc+ in A/J mice normalized to the basic value.

A/J mice bearing $\sim 150 \text{ mm}^3$ Neuro 2a Luc+ tumors were measured over two days by bioluminescence imaging. The mean of the results of these two measurements was set as 100% and presented on day 1. Thereafter the treatment was performed by three intravenous injections at three consecutive days of 2.5 mg target siRNA (siLuc) or scrambled siRNA (siControl) respectively ($n = 7$) (w/w: 2/1). One group remained untreated. The effects on the bioluminescent signals were evaluated for the next three days by daily bioluminescence imaging and normalized to the basic value before treatment.

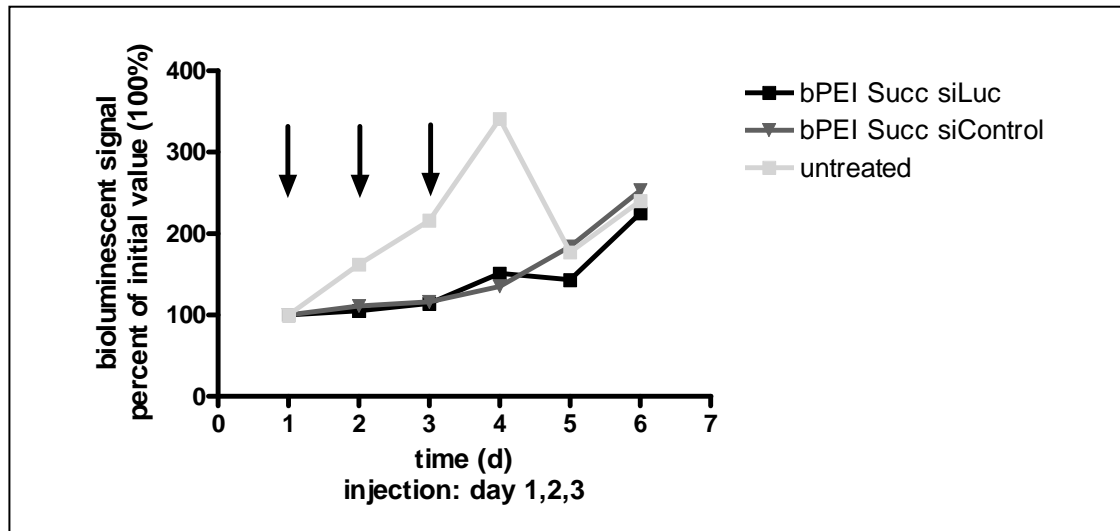


Figure 7.1.3 *In vivo* siRNA reporter gene silencing of bPEI Succ 10 on Neuro 2a Luc+ in A/J mice normalized to the basic value.

A/J mice bearing $\sim 150 \text{ mm}^3$ Neuro 2a Luc+ tumors were measured over two days by bioluminescence imaging. The mean of the results of these two measurements was set as 100% and presented on day 1. Thereafter the treatment was performed by three intravenous injections at three consecutive days of 2.5 mg target siRNA (siLuc) or scrambled siRNA (siControl) respectively ($n = 14$) (w/w: 2/1). One group remained untreated. The bioluminescent measurement was performed daily up to 24 hours after the last treatment and the signals were normalized to the basic value before treatment. Thereafter seven animals were euthanized and seven animals remained for bioluminescence imaging up to three days after the last treatment.

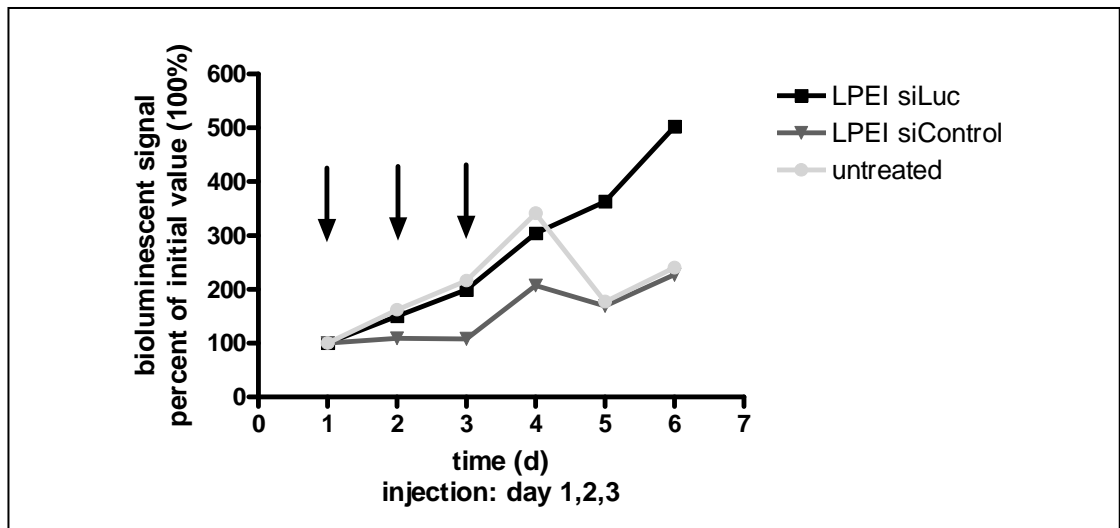


Figure 7.1.4 *In vivo* siRNA reporter gene silencing of PEI (22 kDa) on Neuro 2a Luc+ in A/J mice normalized to the basic value.

A/J mice bearing $\sim 150 \text{ mm}^3$ Neuro 2a Luc+ tumors were measured over two days by bioluminescence imaging. The mean of the results of these two measurements was set as 100% and presented on day 1. Thereafter the treatment was performed by three intravenous injections at three consecutive days of 2.5 mg target siRNA (siLuc) or scrambled siRNA (siControl) respectively ($n = 7$) (w/w: 1/1). One group remained untreated. The effects on the bioluminescent signals were evaluated for the next three days by daily bioluminescence imaging and normalized to the basic value before treatment.

7.2 Abbreviations

ALT	alanine aminotransferase
AST	aspartate aminotransferase
bPEI	branched polyethylenimine
BSA	bovine serum albumine
CCD	charge-coupled device
cDNA	complementary desoxyribonucleic acid
CMV	cytomegalovirus
CT	computer tomography
DMMA _n	2,3-dimethylmaleicanhydride
DNA	desoxyribonucleic acid
EGF	epidermal growth factor
eGFP	enhanced green fluorescent protein
EPO	erythropoietin
FIH	factor inhibiting hypoxia inducible factor
GFP	green fluorescent protein
GTP	guanosine triphosphate
HIF	hypoxia inducible factor
HSV	herpes simplex virus
iNOS	inducible nitric oxide synthase
LDH	lactatdehydrogenase
Mel	melittin peptide
min	minute
MRI	magnetic resonance imaging
mRNA	messenger ribonucleic acid
NIR	near infrared
nu/nu	NMRI nude
ODD	oxygen depending domain
OEI	oligoethylenimine
pDNA	plasmid desoxyribonucleic acid
PCR	polymerase chain reaction
PEG	polyethylenglycol
PEI	polyethylenimine
PET	positron emission tomography
PHD	prolyl hydroxylase domains
PLL	poly-L-lysine
PLL50	poly-L-lysine with 50 lysine monomer units

PLL185	poly-L-lysine with 185 lysine monomer units
RFP	red fluorescent protein
RISC	ribonucleic acid induced silencing complex
RNA	ribonucleic acid
rtQPCR	real time quantitative polymerase chain reaction
SCID	severe combined immunodeficiency
sec	second
siRNA	short interfering ribonucleic acid
shRNA	short hairpin ribonucleic acid
SPECT	single photon emission computed tomography
SPIO	super-paramagnetic iron oxide
SV	simian virus
Tf	transferrin
TNF alpha	tumor necrosis factor alpha
QD	quantum dot
VEGF	vascular endothelial growth factor
VHL	von Hippel-Lindau factor

7.3 Publications

Navarro G, Maiwald G, Haase R, Rogach A, Wagner E, Tros de Ilarduya C, Ogris M. **Low generation PAMAM dendrimers and CpG free plasmids for systemic tumor gene targeting and extended tumor transgene expression.** In Revision

Meyer M, Dohmen C, Philipp A, Kiener D, Maiwald G, Scheu C, Ogris M, Wagner E., **Synthesis and biological evaluation of a bioresponsive and endosomolytic siRNA - polymer conjugate.** Mol.Pharm.2009, 6:752-762.

8 References

1. <http://www.wiley.co.uk/genmed/clinical/>.
2. Kircheis, R., Ostermann, E., Wolschek, M. F., Lichtenberger, C., Magin-Lachmann, C., Wightman, L., Kursa, M., and Wagner, E. (2002) Tumor-targeted gene delivery of tumor necrosis factor-alpha induces tumor necrosis and tumor regression without systemic toxicity, *Cancer Gene Ther* 9, 673-680.
3. Raty, J. K., Pikkarainen, J. T., Wirth, T., and Yla-Herttuala, S. (2008) Gene therapy: the first approved gene-based medicines, molecular mechanisms and clinical indications, *Curr Mol Pharmacol* 1, 13-23.
4. Elbashir, S. M., Harborth, J., Lendeckel, W., Yalcin, A., Weber, K., and Tuschl, T. (2001) Duplexes of 21-nucleotide RNAs mediate RNA interference in cultured mammalian cells 1, *Nature* 411, 494-498.
5. Zamore, P. D., Tuschl, T., Sharp, P. A., and Bartel, D. P. (2000) RNAi: double-stranded RNA directs the ATP-dependent cleavage of mRNA at 21 to 23 nucleotide intervals, *Cell* 101, 25-33.
6. Bumcrot, D., Manoharan, M., Kotliansky, V., and Sah, D. W. (2006) RNAi therapeutics: a potential new class of pharmaceutical drugs, *Nat.Chem Biol* 2, 711-719.
7. Fire, A., Xu, S., Montgomery, M. K., Kostas, S. A., Driver, S. E., and Mello, C. C. (1998) Potent and specific genetic interference by double-stranded RNA in *Caenorhabditis elegans* 2, *Nature* 391, 806-811.
8. Mahato, R. I., Kawabata, K., Takakura, Y., and Hashida, M. (1995) In vivo disposition characteristics of plasmid DNA complexed with cationic liposomes, *J Drug Target* 3, 149-157.
9. Kawabata, K., Takakura, Y., and Hashida, M. (1995) The fate of plasmid DNA after intravenous injection in mice: involvement of scavenger receptors in its hepatic uptake, *Pharm.Res* 12, 825-830.
10. Houk, B. E., Martin, R., Hochhaus, G., and Hughes, J. A. (2001) Pharmacokinetics of plasmid DNA in the rat, *Pharm.Res* 18, 67-74.
11. Gao, S., Dagnaes-Hansen, F., Nielsen, E. J., Wengel, J., Besenbacher, F., Howard, K. A., and Kjems, J. (2009) The effect of chemical modification and nanoparticle formulation on stability and biodistribution of siRNA in mice, *Mol Ther* 17, 1225-1233.
12. Isaka, Y., and Imai, E. (2007) Electroporation-mediated gene therapy, *Expert.Opin.Drug Deliv.* 4, 561-571.
13. Nishitani, M., Sakai, T., Kanayama, H., Himeno, K., and Kagawa, S. (2000) Cytokine gene therapy for cancer with naked DNA, *Mol.Urol.* 4, 47-50.
14. Hagstrom, J. E. (2003) Plasmid-based gene delivery to target tissues in vivo: the intravascular approach, *Curr Opin Mol Ther* 5, 338-344.
15. Wolff, J. A., and Budker, V. (2005) The mechanism of naked DNA uptake and expression, *Adv Genet* 54, 3-20.
16. Reich, S. J., Fosnot, J., Kuroki, A., Tang, W., Yang, X., Maguire, A. M., Bennett, J., and Tolentino, M. J. (2003) Small interfering RNA (siRNA) targeting VEGF effectively inhibits ocular neovascularization in a mouse model, *Mol Vis* 9, 210-216.
17. <http://clinicaltrials.gov>.
18. Nair, V. (2008) Retrovirus-induced oncogenesis and safety of retroviral vectors, *Curr Opin Mol Ther* 10, 431-438.
19. Yi, Y., Hahm, S. H., and Lee, K. H. (2005) Retroviral gene therapy: safety issues and possible solutions, *Curr Gene Ther* 5, 25-35.
20. Duzgunes, N., De Ilarduya, C. T., Simoes, S., Zhdanov, R. I., Konopka, K., and Pedroso de Lima, M. C. (2003) Cationic liposomes for gene delivery: novel cationic lipids and enhancement by proteins and peptides, *Curr.Med.Chem.* 10, 1213-1220.

21. Liu, D., Ren, T., and Gao, X. (2003) Cationic transfection lipids, *Curr.Med Chem.* 10, 1307-1315.
22. Mahato, R. I. (2005) Water insoluble and soluble lipids for gene delivery, *Adv.Drug Deliv.Rev.* 57, 699-712.
23. Godbey, W. T., Wu, K. K., and Mikos, A. G. (1999) Poly(ethylenimine) and its role in gene delivery 988, *J.Control Release* 60, 149-160.
24. Lungwitz, U., Breunig, M., Blunk, T., and Gopferich, A. (2005) Polyethylenimine-based non-viral gene delivery systems, *Eur.J.Pharm.Biopharm.* 60, 247-266.
25. Shir, A., Ogris, M., Wagner, E., and Levitzki, A. (2006) EGF receptor-targeted synthetic double-stranded RNA eliminates glioblastoma, breast cancer, and adenocarcinoma tumors in mice, *PLoS Med* 3, e6.
26. Ogris, M., Brunner, S., Schuller, S., Kircheis, R., and Wagner, E. (1999) PEGylated DNA/transferrin-PEI complexes: reduced interaction with blood components, extended circulation in blood and potential for systemic gene delivery, *Gene Ther* 6, 595-605.
27. Brownlie, A., Uchegbu, I. F., and Schatzlein, A. G. (2004) PEI-based vesicle-polymer hybrid gene delivery system with improved biocompatibility, *Int.J Pharm.* 274, 41-52.
28. Plank, C., Mechtler, K., Szoka, F. C., Jr., and Wagner, E. (1996) Activation of the complement system by synthetic DNA complexes: a potential barrier for intravenous gene delivery, *Hum.Gene Ther* 7, 1437-1446.
29. Kircheis, R., and Wagner, E. (2000) Polycation/ DNA complexes for in vivo gene delivery *Gene Therapy and Regulation* 1, 95-114.
30. Chollet, P., Favrot, M. C., Hurbin, A., and Coll, J. L. (2002) Side-effects of a systemic injection of linear polyethylenimine-DNA complexes, *J Gene Med.* 4, 84-91.
31. Ogris, M., Walker, G., Blessing, T., Kircheis, R., Wolschek, M., and Wagner, E. (2003) Tumor-targeted gene therapy: strategies for the preparation of ligand-polyethylene glycol-polyethylenimine/DNA complexes, *J.Control Release* 91, 173-181.
32. Zhang, X., Pan, S. R., Hu, H. M., Wu, G. F., Feng, M., Zhang, W., and Luo, X. (2008) Poly(ethylene glycol)-block-polyethylenimine copolymers as carriers for gene delivery: effects of PEG molecular weight and PEGylation degree, *J Biomed Mater Res A* 84, 795-804.
33. Zintchenko, A., Philipp, A., Dehshahri, A., and Wagner, E. (2008) Simple Modifications of Branched PEI Lead to Highly Efficient siRNA Carriers with Low Toxicity, *Bioconjug Chem* 19, 1448-1455.
34. Ogris, M., Kotha, A. K., Tietze, N., Wagner, E., Palumbo, F. S., Giammona, G., and Cavallaro, G. (2007) Novel biocompatible cationic copolymers based on polyaspartylhydrazide being potent as gene vector on tumor cells, *Pharm.Res.* 24, 2213-2222.
35. Russ, V., Elfberg, H., Thoma, C., Kloeckner, J., Ogris, M., and Wagner, E. (2008) Novel degradable oligoethylenimine acrylate ester-based pseudodendrimers for in vitro and in vivo gene transfer, *Gene Ther* 15, 18-29.
36. Russ, V., Gunther, M., Halama, A., Ogris, M., and Wagner, E. (2008) Oligoethylenimine-grafted polypropylenimine dendrimers as degradable and biocompatible synthetic vectors for gene delivery, *J Control Release* 132, 131-140.
37. Buyens, K., Lucas, B., Raemdonck, K., Braeckmans, K., Vercammen, J., Hendrix, J., Engelborghs, Y., De Smedt, S. C., and Sanders, N. N. (2008) A fast and sensitive method for measuring the integrity of siRNA-carrier complexes in full human serum, *J Control Release* 126, 67-76.
38. Merkel, O. M., Librizzi, D., Pfestroff, A., Schurrat, T., Buyens, K., Sanders, N. N., De Smedt, S. C., Behe, M., and Kissel, T. (2009) Stability of siRNA polyplexes from poly(ethylenimine) and poly(ethylenimine)-g-poly(ethylene glycol) under in vivo conditions: effects on pharmacokinetics and biodistribution measured by Fluorescence Fluctuation Spectroscopy and Single Photon Emission Computed Tomography (SPECT) imaging, *J Control Release* 138, 148-159.

39. Philipp, A., Meyer, M., and Wagner, E. (2008) Extracellular targeting of synthetic therapeutic nucleic Acid formulations, *Curr Gene Ther* 8, 324-334.
40. Jeong, J. H., Lee, M., Kim, W. J., Yockman, J. W., Park, T. G., Kim, Y. H., and Kim, S. W. (2005) Anti-GAD antibody targeted non-viral gene delivery to islet beta cells, *J.Control Release* 107, 562-570.
41. Kunath, K., Merdan, T., Hegener, O., Haberlein, H., and Kissel, T. (2003) Integrin targeting using RGD-PEI conjugates for in vitro gene transfer, *J.Gene Med.* 5, 588-599.
42. Kircheis, R., Kichler, A., Wallner, G., Kursa, M., Ogris, M., Felzmann, T., Buchberger, M., and Wagner, E. (1997) Coupling of cell-binding ligands to polyethylenimine for targeted gene delivery, *Gene Ther.* 4, 409-418.
43. Zanta, M. A., Boussif, O., Adib, A., and Behr, J. P. (1997) In vitro gene delivery to hepatocytes with galactosylated polyethylenimine, *Bioconjug.Chem.* 8, 839-844.
44. Weiss, S. I., Sieverling, N., Niclasen, M., Maucksch, C., Thunemann, A. F., Mohwald, H., Reinhardt, D., Rosenecker, J., and Rudolph, C. (2006) Uronic acids functionalized polyethyleneimine (PEI)-polyethyleneglycol (PEG)-graft-copolymers as novel synthetic gene carriers, *Biomaterials* 27, 2302-2312.
45. Chul, C. K., Hoon, J. J., Jung, C. H., Joe, C. O., Wan, K. S., and Gwan, P. T. (2005) Folate receptor-mediated intracellular delivery of recombinant caspase-3 for inducing apoptosis, *J.Control Release* 108, 121-131.
46. Blessing, T., Kursa, M., Holzhauser, R., Kircheis, R., and Wagner, E. (2001) Different strategies for formation of pegylated EGF-conjugated PEI/DNA complexes for targeted gene delivery, *Bioconjug Chem* 12, 529-537.
47. Sonawane, N. D., Szoka, F. C., Jr., and Verkman, A. S. (2003) Chloride Accumulation and Swelling in Endosomes Enhances DNA Transfer by Polyamine-DNA Polyplexes, *J.Biol.Chem.* 278, 44826-44831.
48. Akinc, A., Thomas, M., Klibanov, A. M., and Langer, R. (2005) Exploring polyethylenimine-mediated DNA transfection and the proton sponge hypothesis, *J Gene Med* 7, 657-663.
49. Plank, C., Oberhauser, B., Mechtler, K., Koch, C., and Wagner, E. (1994) The influence of endosome-disruptive peptides on gene transfer using synthetic virus-like gene transfer systems, *J Biol.Chem.* 269, 12918-12924.
50. Mechtler, K., and Wagner, E. (1997) Gene transfer mediated by influenza virus peptides: the role of peptide sequence, *New J Chem* 21, 105-111.
51. Ogris, M., Carlisle, R. C., Bettinger, T., and Seymour, L. W. (2001) Melittin enables efficient vesicular escape and enhanced nuclear access of nonviral gene delivery vectors, *J Biol Chem* 276, 47550-47555.
52. Chen, C. P., Kim, J. S., Steenblock, E., Liu, D., and Rice, K. G. (2006) Gene transfer with poly-melittin peptides, *Bioconjug Chem* 17, 1057-1062.
53. Li, W., Nicol, F., and Szoka, F. C., Jr. (2004) GALA: a designed synthetic pH-responsive amphipathic peptide with applications in drug and gene delivery, *Adv.Drug Deliv.Rev.* 56, 967-985.
54. Schaffert, D., and Wagner, E. (2008) Gene therapy progress and prospects: synthetic polymer-based systems, *Gene Ther* 15, 1131-1138.
55. Meyer, M., and Wagner, E. (2006) Recent developments in the application of plasmid DNA-based vectors and small interfering RNA therapeutics for cancer, *Hum.Gene Ther* 17, 1062-1076.
56. Kloeckner, J., Wagner, E., and Ogris, M. (2006) Degradable gene carriers based on oligomerized polyamines, *Eur.J.Pharm.Sci.* 29, 414-425.
57. Tietze, N., Pelisek, J., Philipp, A., Roedl, W., Merdan, T., Tarcha, P., Ogris, M., and Wagner, E. (2008) Induction of apoptosis in murine neuroblastoma by systemic delivery of transferrin-shielded siRNA polyplexes for downregulation of Ran, *Oligonucleotides* 18, 161-174.
58. Meyer, M., Dohmen, C., Philipp, A., Kiener, D., Maiwald, G., Scheu, C., Ogris, M., and Wagner, E. (2009) Synthesis and Biological Evaluation of a Bioresponsive and Endosomolytic siRNA-Polymer Conjugate, *Mol Pharm* 6, 752-762.

59. Alves Rodrigues, M. T., and Moro, A. M. (2007) Preclinical Studies, in *Animal Cell Technology: From Biopharmaceuticals to Gene Therapy* (Castilho, L. R., Moraes, A. M., and Augusto, E. F. P., Eds.), pp 363-364, Taylor & Francis, London.
60. Bogdanov, A., Jr., and Weissleder, R. (1998) The development of in vivo imaging systems to study gene expression, *Trends Biotechnol* 16, 5-10.
61. Bogdanov, A. J., and Weissleder, R. (2002) In vivo imaging of gene delivery and expression, *Trends Biotechnol* 20, 11S-18S.
62. Bartlett, D. W., Su, H., Hildebrandt, I. J., Weber, W. A., and Davis, M. E. (2007) Impact of tumor-specific targeting on the biodistribution and efficacy of siRNA nanoparticles measured by multimodality in vivo imaging, *Proc.Natl.Acad.Sci U.S.A* 104, 15549-15554.
63. Mackay, I. M., Arden, K. E., and Nitsche, A. (2002) Real-time PCR in virology, *Nucleic Acids Res* 30, 1292-1305.
64. Morgan-Lappe, S. E., Tucker, L. A., Huang, X., Zhang, Q., Sarthy, A. V., Zakula, D., Verneti, L., Schurdak, M., Wang, J., and Fesik, S. W. (2007) Identification of Ras-Related Nuclear Protein, Targeting Protein for Xenopus Kinesin-like Protein 2, and Stearoyl-CoA Desaturase 1 as Promising Cancer Targets from an RNAi-Based Screen, *Cancer Res.* 67, 4390-4398.
65. Sazer, S., and Dasso, M. (2000) The ran decathlon: multiple roles of Ran, *J Cell Sci* 113 (Pt 7), 1111-1118.
66. Gruss, O. J., and Vernos, I. (2004) The mechanism of spindle assembly: functions of Ran and its target TPX2, *J Cell Biol* 166, 949-955.
67. Koo, V., Hamilton, P. W., and Williamson, K. (2006) Non-invasive in vivo imaging in small animal research, *Cell Oncol* 28, 127-139.
68. Bogdanov, A. A., Jr. (2008) Merging molecular imaging and RNA interference: early experience in live animals, *J Cell Biochem* 104, 1113-1123.
69. Berger, F., Lee, Y. P., Loening, A. M., Chatziioannou, A., Freedland, S. J., Leahy, R., Lieberman, J. R., Belldegrun, A. S., Sawyers, C. L., and Gambhir, S. S. (2002) Whole-body skeletal imaging in mice utilizing microPET: optimization of reproducibility and applications in animal models of bone disease, *Eur J Nucl Med Mol Imaging* 29, 1225-1236.
70. Paulus, M. J., Gleason, S. S., Easterly, M. E., and Foltz, C. J. (2001) A review of high-resolution X-ray computed tomography and other imaging modalities for small animal research, *Lab Anim (NY)* 30, 36-45.
71. Pickhardt, P. J., Halberg, R. B., Taylor, A. J., Durkee, B. Y., Fine, J., Lee, F. T., Jr., and Weichert, J. P. (2005) Microcomputed tomography colonography for polyp detection in an in vivo mouse tumor model, *Proc Natl Acad Sci U S A* 102, 3419-3422.
72. Weber, S. M., Peterson, K. A., Durkee, B., Qi, C., Longino, M., Warner, T., Lee, F. T., Jr., and Weichert, J. P. (2004) Imaging of murine liver tumor using microCT with a hepatocyte-selective contrast agent: accuracy is dependent on adequate contrast enhancement, *J Surg Res* 119, 41-45.
73. Massoud, T. F., and Gambhir, S. S. (2003) Molecular imaging in living subjects: seeing fundamental biological processes in a new light, *Genes Dev* 17, 545-580.
74. Kauppinen, R. A. (2002) Monitoring cytotoxic tumour treatment response by diffusion magnetic resonance imaging and proton spectroscopy, *NMR Biomed* 15, 6-17.
75. Crich, S. G., Lanzardo, S., Barge, A., Esposito, G., Tei, L., Forni, G., and Aime, S. (2005) Visualization through magnetic resonance imaging of DNA internalized following "in vivo" electroporation, *Mol Imaging* 4, 7-17.
76. Louie, A. Y., Huber, M. M., Ahrens, E. T., Rothbacher, U., Moats, R., Jacobs, R. E., Fraser, S. E., and Meade, T. J. (2000) In vivo visualization of gene expression using magnetic resonance imaging, *Nat Biotechnol* 18, 321-325.
77. Ichikawa, T., Hogemann, D., Saeki, Y., Tyminski, E., Terada, K., Weissleder, R., Chiocca, E. A., and Basilion, J. P. (2002) MRI of transgene expression: correlation to therapeutic gene expression, *Neoplasia* 4, 523-530.

78. Delikatny, E. J., and Poptani, H. (2005) MR techniques for in vivo molecular and cellular imaging, *Radiol Clin North Am* 43, 205-220.
79. Genove, G., DeMarco, U., Xu, H., Goins, W. F., and Ahrens, E. T. (2005) A new transgene reporter for in vivo magnetic resonance imaging, *Nat Med* 11, 450-454.
80. Tjuvajev, J. G., Avril, N., Oku, T., Sasajima, T., Miyagawa, T., Joshi, R., Safer, M., Beattie, B., DiResta, G., Daghighian, F., Augensen, F., Koutcher, J., Zweit, J., Humm, J., Larson, S. M., Finn, R., and Blasberg, R. (1998) Imaging herpes virus thymidine kinase gene transfer and expression by positron emission tomography, *Cancer Res* 58, 4333-4341.
81. Gambhir, S. S., Bauer, E., Black, M. E., Liang, Q., Kokoris, M. S., Barrio, J. R., Iyer, M., Namavari, M., Phelps, M. E., and Herschman, H. R. (2000) A mutant herpes simplex virus type 1 thymidine kinase reporter gene shows improved sensitivity for imaging reporter gene expression with positron emission tomography, *Proc Natl Acad Sci U S A* 97, 2785-2790.
82. Tarantal, A. F., Lee, C. C., Jimenez, D. F., and Cherry, S. R. (2006) Fetal gene transfer using lentiviral vectors: in vivo detection of gene expression by microPET and optical imaging in fetal and infant monkeys, *Hum Gene Ther* 17, 1254-1261.
83. Auricchio, A., Acton, P. D., Hildinger, M., Louboutin, J. P., Plossl, K., O'Connor, E., Kung, H. F., and Wilson, J. M. (2003) In vivo quantitative noninvasive imaging of gene transfer by single-photon emission computerized tomography, *Hum Gene Ther* 14, 255-261.
84. Haberkorn, U., Oberdorfer, F., Gebert, J., Morr, I., Haack, K., Weber, K., Lindauer, M., van Kaick, G., and Schackert, H. K. (1996) Monitoring gene therapy with cytosine deaminase: in vitro studies using tritiated-5-fluorocytosine, *J Nucl Med* 37, 87-94.
85. Stegman, L. D., Rehemtulla, A., Beattie, B., Kievit, E., Lawrence, T. S., Blasberg, R. G., Tjuvajev, J. G., and Ross, B. D. (1999) Noninvasive quantitation of cytosine deaminase transgene expression in human tumor xenografts with in vivo magnetic resonance spectroscopy, *Proc Natl Acad Sci U S A* 96, 9821-9826.
86. Buursma, A. R., Beerens, A. M., de Vries, E. F., van Waarde, A., Rots, M. G., Hospers, G. A., Vaalburg, W., and Haisma, H. J. (2005) The human norepinephrine transporter in combination with ¹¹C-m-hydroxyephedrine as a reporter gene/reporter probe for PET of gene therapy, *J Nucl Med* 46, 2068-2075.
87. Dwyer, R. M., Bergert, E. R., O'Connor, M. K., Gendler, S. J., and Morris, J. C. (2006) Sodium iodide symporter-mediated radioiodide imaging and therapy of ovarian tumor xenografts in mice, *Gene Ther* 13, 60-66.
88. Miyagawa, M., Anton, M., Wagner, B., Haubner, R., Souvatzoglou, M., Gansbacher, B., Schwaiger, M., and Bengel, F. M. (2005) Non-invasive imaging of cardiac transgene expression with PET: comparison of the human sodium/iodide symporter gene and HSV1-tk as the reporter gene, *Eur J Nucl Med Mol Imaging* 32, 1108-1114.
89. Kaneko, K., Yano, M., Yamano, T., Tsujinaka, T., Miki, H., Akiyama, Y., Taniguchi, M., Fujiwara, Y., Doki, Y., Inoue, M., Shiozaki, H., Kaneda, Y., and Monden, M. (2001) Detection of peritoneal micrometastases of gastric carcinoma with green fluorescent protein and carcinoembryonic antigen promoter, *Cancer Res* 61, 5570-5574.
90. Chudakov, D. M., Lukyanov, S., and Lukyanov, K. A. (2005) Fluorescent proteins as a toolkit for in vivo imaging, *Trends Biotechnol* 23, 605-613.
91. Shaner, N. C., Steinbach, P. A., and Tsien, R. Y. (2005) A guide to choosing fluorescent proteins, *Nat Methods* 2, 905-909.
92. Giepmans, B. N., Adams, S. R., Ellisman, M. H., and Tsien, R. Y. (2006) The fluorescent toolbox for assessing protein location and function, *Science* 312, 217-224.
93. Ke, S., Wen, X., Gurfinkel, M., Charnsangavej, C., Wallace, S., Sevcik-Muraca, E. M., and Li, C. (2003) Near-infrared optical imaging of epidermal growth factor receptor in breast cancer xenografts, *Cancer Res* 63, 7870-7875.

94. Mook, O. R., Baas, F., de Wissel, M. B., and Fluiter, K. (2007) Evaluation of locked nucleic acid-modified small interfering RNA in vitro and in vivo, *Mol Cancer Ther* 6, 833-843.
95. Golzio, M., Mazzolini, L., Ledoux, A., Paganin, A., Izard, M., Hellaudais, L., Bieth, A., Pillaire, M. J., Cazaux, C., Hoffmann, J. S., Couderc, B., and Teissie, J. (2007) In vivo gene silencing in solid tumors by targeted electrically mediated siRNA delivery, *Gene Ther* 14, 752-759.
96. Townsend, D. W. (2001) A combined PET/CT scanner: the choices, *J Nucl Med* 42, 533-534.
97. Weissleder, R. (2002) Scaling down imaging: molecular mapping of cancer in mice, *Nat Rev Cancer* 2, 11-18.
98. Lin, Y., Weissleder, R., and Tung, C. H. (2002) Novel near-infrared cyanine fluorochromes: synthesis, properties, and bioconjugation, *Bioconjug Chem* 13, 605-610.
99. Michalet, X., Pinaud, F. F., Bentolila, L. A., Tsay, J. M., Doose, S., Li, J. J., Sundaresan, G., Wu, A. M., Gambhir, S. S., and Weiss, S. (2005) Quantum dots for live cells, in vivo imaging, and diagnostics, *Science* 307, 538-544.
100. Hardman, R. (2006) A toxicologic review of quantum dots: toxicity depends on physicochemical and environmental factors, *Environ Health Perspect* 114, 165-172.
101. Heidel, J. D., Liu, J. Y., Yen, Y., Zhou, B., Heale, B. S., Rossi, J. J., Bartlett, D. W., and Davis, M. E. (2007) Potent siRNA inhibitors of ribonucleotide reductase subunit RRM2 reduce cell proliferation in vitro and in vivo, *Clin Cancer Res* 13, 2207-2215.
102. McAnuff, M. A., Rettig, G. R., and Rice, K. G. (2007) Potency of siRNA versus shRNA mediated knockdown in vivo, *J Pharm Sci* 96, 2922-2930.
103. Wang, Q., Ilves, H., Chu, P., Contag, C. H., Leake, D., Johnston, B. H., and Kaspar, R. L. (2007) Delivery and inhibition of reporter genes by small interfering RNAs in a mouse skin model, *J Invest Dermatol* 127, 2577-2584.
104. Bisanz, K., Yu, J., Edlund, M., Spohn, B., Hung, M. C., Chung, L. W., and Hsieh, C. L. (2005) Targeting ECM-integrin interaction with liposome-encapsulated small interfering RNAs inhibits the growth of human prostate cancer in a bone xenograft imaging model, *Mol Ther* 12, 634-643.
105. Bartlett, D. W., and Davis, M. E. (2006) Insights into the kinetics of siRNA-mediated gene silencing from live-cell and live-animal bioluminescent imaging, *Nucleic Acids Res* 34, 322-333.
106. Bartlett, D. W., and Davis, M. E. (2008) Impact of tumor-specific targeting and dosing schedule on tumor growth inhibition after intravenous administration of siRNA-containing nanoparticles, *Biotechnol. Bioeng.* 99, 975-985.
107. Contag, C. H., Contag, P. R., Mullins, J. I., Spilman, S. D., Stevenson, D. K., and Benaron, D. A. (1995) Photonic detection of bacterial pathogens in living hosts, *Mol Microbiol* 18, 593-603.
108. Zhao, H., Doyle, T. C., Coquoz, O., Kalish, F., Rice, B. W., and Contag, C. H. (2005) Emission spectra of bioluminescent reporters and interaction with mammalian tissue determine the sensitivity of detection in vivo, *J Biomed Opt* 10, 41210.
109. Miloud, T., Henrich, C., and Hammerling, G. J. (2007) Quantitative comparison of click beetle and firefly luciferases for in vivo bioluminescence imaging, *J Biomed Opt* 12, 054018.
110. Bhaumik, S., and Gambhir, S. S. (2002) Optical imaging of Renilla luciferase reporter gene expression in living mice, *Proc Natl Acad Sci U S A* 99, 377-382.
111. Tannous, B. A., Kim, D. E., Fernandez, J. L., Weissleder, R., and Breakefield, X. O. (2005) Codon-optimized Gaussia luciferase cDNA for mammalian gene expression in culture and in vivo, *Mol Ther* 11, 435-443.
112. Venisnik, K. M., Olafsen, T., Gambhir, S. S., and Wu, A. M. (2007) Fusion of Gaussia luciferase to an engineered anti-carcinoembryonic antigen (CEA) antibody for in vivo optical imaging, *Mol Imaging Biol* 9, 267-277.
113. Loening, A. M., Wu, A. M., and Gambhir, S. S. (2007) Red-shifted Renilla reniformis luciferase variants for imaging in living subjects, *Nat Methods* 4, 641-643.

114. Leclerc, G. M., Boockfor, F. R., Faught, W. J., and Frawley, L. S. (2000) Development of a destabilized firefly luciferase enzyme for measurement of gene expression, *Biotechniques* 29, 590-591, 594-596, 598 passim.
115. Luker, G. D., Pica, C. M., Song, J., Luker, K. E., and Piwnica-Worms, D. (2003) Imaging 26S proteasome activity and inhibition in living mice, *Nat Med* 9, 969-973.
116. White, P. J., Squirrell, D. J., Arnaud, P., Lowe, C. R., and Murray, J. A. (1996) Improved thermostability of the North American firefly luciferase: saturation mutagenesis at position 354, *Biochem J* 319 (Pt 2), 343-350.
117. Baggett, B., Roy, R., Momen, S., Morgan, S., Tisi, L., Morse, D., and Gillies, R. J. (2004) Thermostability of firefly luciferases affects efficiency of detection by in vivo bioluminescence, *Mol Imaging* 3, 324-332.
118. Loening, A. M., Fenn, T. D., Wu, A. M., and Gambhir, S. S. (2006) Consensus guided mutagenesis of Renilla luciferase yields enhanced stability and light output, *Protein Eng Des Sel* 19, 391-400.
119. Paroo, Z., Bollinger, R. A., Braasch, D. A., Richer, E., Corey, D. R., Antich, P. P., and Mason, R. P. (2004) Validating bioluminescence imaging as a high-throughput, quantitative modality for assessing tumor burden, *Mol Imaging* 3, 117-124.
120. Lee, K. H., Byun, S. S., Paik, J. Y., Lee, S. Y., Song, S. H., Choe, Y. S., and Kim, B. T. (2003) Cell uptake and tissue distribution of radioiodine labelled D-luciferin: implications for luciferase based gene imaging, *Nucl Med Commun* 24, 1003-1009.
121. Pichler, A., Prior, J. L., and Piwnica-Worms, D. (2004) Imaging reversal of multidrug resistance in living mice with bioluminescence: MDR1 P-glycoprotein transports coelenterazine, *Proc Natl Acad Sci U S A* 101, 1702-1707.
122. Zhao, H., Doyle, T. C., Wong, R. J., Cao, Y., Stevenson, D. K., Piwnica-Worms, D., and Contag, C. H. (2004) Characterization of coelenterazine analogs for measurements of Renilla luciferase activity in live cells and living animals, *Mol Imaging* 3, 43-54.
123. Semenza, G. L. (1998) Hypoxia-inducible factor 1: master regulator of O₂ homeostasis, *Curr Opin Genet Dev* 8, 588-594.
124. Ivan, M., Kondo, K., Yang, H., Kim, W., Valiando, J., Ohh, M., Salic, A., Asara, J. M., Lane, W. S., and Kaelin, W. G., Jr. (2001) HIF α targeted for VHL-mediated destruction by proline hydroxylation: implications for O₂ sensing, *Science* 292, 464-468.
125. Jaakkola, P., Mole, D. R., Tian, Y. M., Wilson, M. I., Gielbert, J., Gaskell, S. J., Kriegsheim, A., Hebestreit, H. F., Mukherji, M., Schofield, C. J., Maxwell, P. H., Pugh, C. W., and Ratcliffe, P. J. (2001) Targeting of HIF- α to the von Hippel-Lindau ubiquitylation complex by O₂-regulated prolyl hydroxylation, *Science* 292, 468-472.
126. Maxwell, P. H., Wiesener, M. S., Chang, G. W., Clifford, S. C., Vaux, E. C., Cockman, M. E., Wykoff, C. C., Pugh, C. W., Maher, E. R., and Ratcliffe, P. J. (1999) The tumour suppressor protein VHL targets hypoxia-inducible factors for oxygen-dependent proteolysis, *Nature* 399, 271-275.
127. Lando, D., Peet, D. J., Gorman, J. J., Whelan, D. A., Whitelaw, M. L., and Bruick, R. K. (2002) FIH-1 is an asparaginyl hydroxylase enzyme that regulates the transcriptional activity of hypoxia-inducible factor, *Genes Dev* 16, 1466-1471.
128. Berra, E., Ginouves, A., and Pouyssegur, J. (2006) The hypoxia-inducible-factor hydroxylases bring fresh air into hypoxia signalling, *EMBO Rep* 7, 41-45.
129. Appelhoff, R. J., Tian, Y. M., Raval, R. R., Turley, H., Harris, A. L., Pugh, C. W., Ratcliffe, P. J., and Gleadle, J. M. (2004) Differential function of the prolyl hydroxylases PHD1, PHD2, and PHD3 in the regulation of hypoxia-inducible factor, *J Biol Chem* 279, 38458-38465.
130. Berra, E., Benizri, E., Ginouves, A., Volmat, V., Roux, D., and Pouyssegur, J. (2003) HIF prolyl-hydroxylase 2 is the key oxygen sensor setting low steady-state levels of HIF-1 α in normoxia, *EMBO J* 22, 4082-4090.
131. Wu, S., Nishiyama, N., Kano, M. R., Morishita, Y., Miyazono, K., Itaka, K., Chung, U. I., and Kataoka, K. (2008) Enhancement of angiogenesis through stabilization of

- hypoxia-inducible factor-1 by silencing prolyl hydroxylase domain-2 gene, *Mol Ther* 16, 1227-1234.
132. Gillespie, D. L., Whang, K., Ragel, B. T., Flynn, J. R., Kelly, D. A., and Jensen, R. L. (2007) Silencing of hypoxia inducible factor-1alpha by RNA interference attenuates human glioma cell growth in vivo, *Clin Cancer Res* 13, 2441-2448.
133. Safran, M., Kim, W. Y., O'Connell, F., Flippin, L., Gunzler, V., Horner, J. W., Depinho, R. A., and Kaelin, W. G., Jr. (2006) Mouse model for noninvasive imaging of HIF prolyl hydroxylase activity: assessment of an oral agent that stimulates erythropoietin production, *Proc Natl Acad Sci U S A* 103, 105-110.
134. www.promega.com.
135. Smrekar, B., Wightman, L., Wolschek, M. F., Lichtenberger, C., Ruzicka, R., Ogris, M., Rodl, W., Kursa, M., Wagner, E., and Kircheis, R. (2003) Tissue-dependent factors affect gene delivery to tumors in vivo, *Gene Ther.* 10, 1079-1088.
136. Brissault, B., Kichler, A., Guis, C., Leborgne, C., Danos, O., and Cheradame, H. (2003) Synthesis of linear polyethylenimine derivatives for DNA transfection, *Bioconjug.Chem.* 14, 581-587.
137. Plank, C., Zatloukal, K., Cotten, M., Mechtler, K., and Wagner, E. (1992) Gene transfer into hepatocytes using asialoglycoprotein receptor mediated endocytosis of DNA complexed with an artificial tetra-antennary galactose ligand, *Bioconjug.Chem.* 3, 533-539.
138. Hildebrandt, I. J., Iyer, M., Wagner, E., and Gambhir, S. S. (2003) Optical imaging of transferrin targeted PEI/DNA complexes in living subjects, *Gene Ther.* 10, 758-764.
139. McCaffrey, A. P., Meuse, L., Pham, T. T., Conklin, D. S., Hannon, G. J., and Kay, M. A. (2002) RNA interference in adult mice, *Nature* 418, 38-39.
140. Lewis, D. L., Hagstrom, J. E., Loomis, A. G., Wolff, J. A., and Herweijer, H. (2002) Efficient delivery of siRNA for inhibition of gene expression in postnatal mice, *Nat Genet* 32, 107-108.
141. Raty, J. K., Liimatainen, T., Unelma Kaikkonen, M., Grohn, O., Airene, K. J., and Yla-Herttuala, S. (2007) Non-invasive Imaging in Gene Therapy, *Mol Ther* 15, 1579-1586.
142. Luker, K. E., and Luker, G. D. (2008) Applications of bioluminescence imaging to antiviral research and therapy: multiple luciferase enzymes and quantitation, *Antiviral Res* 78, 179-187.
143. Iida, T., Mori, T., Katayama, Y., and Niidome, T. (2007) Overall interaction of cytosolic proteins with the PEI/DNA complex, *J Control Release* 118, 364-369.
144. Regnstrom, K., Ragnarsson, E. G., Koping-Hoggard, M., Torstensson, E., Nyblom, H., and Artursson, P. (2003) PEI - a potent, but not harmless, mucosal immunostimulator of mixed T-helper cell response and FasL-mediated cell death in mice, *Gene Ther* 10, 1575-1583.
145. Bel Aiba, R. S., and Gorch, A. (2003) Regulation of the hypoxia-inducible transcription factor HIF-1 by reactive oxygen species in smooth muscle cells, *Adv Exp Med Biol* 536, 171-178.
146. Li, F., Sonveaux, P., Rabbani, Z. N., Liu, S., Yan, B., Huang, Q., Vujaskovic, Z., Dewhirst, M. W., and Li, C. Y. (2007) Regulation of HIF-1alpha stability through S-nitrosylation, *Mol Cell* 26, 63-74.
147. Wang, A. B., Liu, D. P., and Liang, C. C. (2003) Regulation of human apolipoprotein B gene expression at multiple levels, *Exp Cell Res* 290, 1-12.
148. Horn, P. J., and Peterson, C. L. (2002) Molecular biology. Chromatin higher order folding--wrapping up transcription, *Science* 297, 1824-1827.
149. Wolffe, A. P., and Guschin, D. (2000) Review: chromatin structural features and targets that regulate transcription, *J Struct Biol* 129, 102-122.
150. Dickson, P. V., Hamner, B., Ng, C. Y., Hall, M. M., Zhou, J., Hargrove, P. W., McCarville, M. B., and Davidoff, A. M. (2007) In vivo bioluminescence imaging for early detection and monitoring of disease progression in a murine model of neuroblastoma, *J Pediatr Surg* 42, 1172-1179.

151. Keyaerts, M., Verschuere, J., Bos, T. J., Tchouate-Gainkam, L. O., Peleman, C., Breckpot, K., Vanhove, C., Caveliers, V., Bossuyt, A., and Lahoutte, T. (2008) Dynamic bioluminescence imaging for quantitative tumour burden assessment using IV or IP administration of D: -luciferin: effect on intensity, time kinetics and repeatability of photon emission, *Eur J Nucl Med Mol Imaging* 35, 999-1007.
152. Sarraf-Yazdi, S., Mi, J., Dewhirst, M. W., and Clary, B. M. (2004) Use of in vivo bioluminescence imaging to predict hepatic tumor burden in mice, *J Surg Res* 120, 249-255.
153. Scatena, C. D., Hepner, M. A., Oei, Y. A., Dusich, J. M., Yu, S. F., Purchio, T., Contag, P. R., and Jenkins, D. E. (2004) Imaging of bioluminescent LNCaP-luc-M6 tumors: a new animal model for the study of metastatic human prostate cancer, *Prostate* 59, 292-303.
154. Wang, W., and El-Deiry, W. S. (2003) Bioluminescent molecular imaging of endogenous and exogenous p53-mediated transcription in vitro and in vivo using an HCT116 human colon carcinoma xenograft model, *Cancer Biol Ther* 2, 196-202.
155. Baba, S., Cho, S. Y., Ye, Z., Cheng, L., Engles, J. M., and Wahl, R. L. (2007) How reproducible is bioluminescent imaging of tumor cell growth? Single time point versus the dynamic measurement approach, *Mol Imaging* 6, 315-322.
156. Tanaka, F., Yamaguchi, H., Ohta, M., Mashino, K., Sonoda, H., Sadanaga, N., Inoue, H., and Mori, M. (2002) Intratumoral injection of dendritic cells after treatment of anticancer drugs induces tumor-specific antitumor effect in vivo, *Int J Cancer* 101, 265-269.
157. Tong, Y., Song, W., and Crystal, R. G. (2001) Combined intratumoral injection of bone marrow-derived dendritic cells and systemic chemotherapy to treat pre-existing murine tumors, *Cancer Res* 61, 7530-7535.
158. Avram, M. J., Krejcie, T. C., Niemann, C. U., Enders-Klein, C., Shanks, C. A., and Henthorn, T. K. (2000) Isoflurane alters the recirculatory pharmacokinetics of physiologic markers, *Anesthesiology* 92, 1757-1768.
159. Sackett, D. L. (2001) Why randomized controlled trials fail but needn't: 2. Failure to employ physiological statistics, or the only formula a clinician-trialist is ever likely to need (or understand!), *CMAJ* 165, 1226-1237.
160. Wu, G. Y., and Wu, C. H. (1988) Receptor-mediated gene delivery and expression in vivo 738, *J Biol Chem* 262, 14621-14624.
161. Boe, S., Longva, A. S., and Hovig, E. (2008) Evaluation of various polyethylenimine formulations for light-controlled gene silencing using small interfering RNA molecules, *Oligonucleotides* 18, 123-132.
162. Grzelinski, M., Urban-Klein, B., Martens, T., Lamszus, K., Bakowsky, U., Hobel, S., Czubayko, F., and Aigner, A. (2006) RNA interference-mediated gene silencing of pleiotrophin through polyethylenimine-complexed small interfering RNAs in vivo exerts antitumoral effects in glioblastoma xenografts, *Hum. Gene Ther.* 17, 751-766.
163. Dai, Y., Roman, M., Naviaux, R. K., and Verma, I. M. (1992) Gene therapy via primary myoblasts: long-term expression of factor IX protein following transplantation in vivo, *Proc Natl Acad Sci U S A* 89, 10892-10895.
164. Guo, Z. S., Wang, L. H., Eisensmith, R. C., and Woo, S. L. (1996) Evaluation of promoter strength for hepatic gene expression in vivo following adenovirus-mediated gene transfer, *Gene Ther* 3, 802-810.
165. Scharfmann, R., Axelrod, J. H., and Verma, I. M. (1991) Long-term in vivo expression of retrovirus-mediated gene transfer in mouse fibroblast implants, *Proc Natl Acad Sci U S A* 88, 4626-4630.
166. Hunninghake, G. W., Monick, M. M., Liu, B., and Stinski, M. F. (1989) The promoter-regulatory region of the major immediate-early gene of human cytomegalovirus responds to T-lymphocyte stimulation and contains functional cyclic AMP-response elements, *J Virol* 63, 3026-3033.
167. Sambucetti, L. C., Cherrington, J. M., Wilkinson, G. W., and Mocarski, E. S. (1989) NF-kappa B activation of the cytomegalovirus enhancer is mediated by a viral transactivator and by T cell stimulation, *EMBO J* 8, 4251-4258.

168. Stamminger, T., Fickenscher, H., and Fleckenstein, B. (1990) Cell type-specific induction of the major immediate early enhancer of human cytomegalovirus by cyclic AMP, *J Gen Virol* 71 (Pt 1), 105-113.
169. Sen, R., and Baltimore, D. (1986) Inducibility of kappa immunoglobulin enhancer-binding protein Nf-kappa B by a posttranslational mechanism, *Cell* 47, 921-928.
170. Karin, M., and Ben-Neriah, Y. (2000) Phosphorylation meets ubiquitination: the control of NF-[kappa]B activity, *Annu Rev Immunol* 18, 621-663.
171. Brivanlou, A. H., and Darnell, J. E., Jr. (2002) Signal transduction and the control of gene expression, *Science* 295, 813-818.
172. Loser, P., Jennings, G. S., Strauss, M., and Sandig, V. (1998) Reactivation of the previously silenced cytomegalovirus major immediate-early promoter in the mouse liver: involvement of NFKappaB, *J Virol* 72, 180-190.
173. Niller, H. H., and Hennighausen, L. (1991) Formation of several specific nucleoprotein complexes on the human cytomegalovirus immediate early enhancer, *Nucleic Acids Res* 19, 3715-3721.
174. Lang, D., Fickenscher, H., and Stamminger, T. (1992) Analysis of proteins binding to the proximal promoter region of the human cytomegalovirus IE-1/2 enhancer/promoter reveals both consensus and aberrant recognition sequences for transcription factors Sp1 and CREB, *Nucleic Acids Res* 20, 3287-3295.
175. Zhang, X. Y., Inamdar, N. M., Supakar, P. C., Wu, K., Ehrlich, K. C., and Ehrlich, M. (1991) Three MDBP sites in the immediate-early enhancer-promoter region of human cytomegalovirus, *Virology* 182, 865-869.
176. Zhang, X. Y., Ni, Y. S., Saifudeen, Z., Asiedu, C. K., Supakar, P. C., and Ehrlich, M. (1995) Increasing binding of a transcription factor immediately downstream of the cap site of a cytomegalovirus gene represses expression, *Nucleic Acids Res* 23, 3026-3033.
177. Kircheis, R., Schuller, S., Brunner, S., Ogris, M., Heider, K. H., Zauner, W., and Wagner, E. (1999) Polycation-based DNA complexes for tumor-targeted gene delivery in vivo, *J Gene Med* 1, 111-120.
178. Keberle, H. (1964) The Biochemistry of Desferrioxamine and Its Relation to Iron Metabolism, *Ann N Y Acad Sci* 119, 758-768.
179. Lee, Y. S., and Wurster, R. D. (1995) Deferoxamine-induced cytotoxicity in human neuronal cell lines: protection by free radical scavengers, *Toxicol Lett* 78, 67-71.
180. Maxwell, P. H., Pugh, C. W., and Ratcliffe, P. J. (2001) Insights into the role of the von Hippel-Lindau gene product. A key player in hypoxic regulation, *Exp Nephrol* 9, 235-240.
181. Hergovich, A., Lisztwan, J., Barry, R., Ballschmieter, P., and Krek, W. (2003) Regulation of microtubule stability by the von Hippel-Lindau tumour suppressor protein pVHL, *Nat Cell Biol* 5, 64-70.
182. Esteban-Barragan, M. A., Avila, P., Alvarez-Tejado, M., Gutierrez, M. D., Garcia-Pardo, A., Sanchez-Madrid, F., and Landazuri, M. O. (2002) Role of the von Hippel-Lindau tumor suppressor gene in the formation of beta1-integrin fibrillar adhesions, *Cancer Res* 62, 2929-2936.
183. Mack, F. A., Patel, J. H., Biju, M. P., Haase, V. H., and Simon, M. C. (2005) Decreased growth of Vhl^{-/-} fibrosarcomas is associated with elevated levels of cyclin kinase inhibitors p21 and p27, *Mol Cell Biol* 25, 4565-4578.
184. Young, A. P., Schlisio, S., Minamishima, Y. A., Zhang, Q., Li, L., Grisanzio, C., Signoretti, S., and Kaelin, W. G., Jr. (2008) VHL loss actuates a HIF-independent senescence programme mediated by Rb and p400, *Nat Cell Biol* 10, 361-369.
185. Thoma, C. R., Toso, A., Gutbrodt, K. L., Reggi, S. P., Frew, I. J., Schraml, P., Hergovich, A., Moch, H., Meraldi, P., and Krek, W. (2009) VHL loss causes spindle misorientation and chromosome instability, *Nat Cell Biol* 11, 994-1001.
186. Song, E., Lee, S. K., Wang, J., Ince, N., Ouyang, N., Min, J., Chen, J., Shankar, P., and Lieberman, J. (2003) RNA interference targeting Fas protects mice from fulminant hepatitis, *Nat Med* 9, 347-351.
187. Liu, F., Song, Y., and Liu, D. (1999) Hydrodynamics-based transfection in animals by systemic administration of plasmid DNA, *Gene Ther.* 6, 1258-1266.

188. Rossmannith, W., Chabicovsky, M., Herkner, K., and Schulte-Hermann, R. (2002) Cellular gene dose and kinetics of gene expression in mouse livers transfected by high-volume tail-vein injection of naked DNA, *DNA Cell Biol* 21, 847-853.
189. Crespo, A., Peydro, A., Dasi, F., Benet, M., Calvete, J. J., Revert, F., and Alino, S. F. (2005) Hydrodynamic liver gene transfer mechanism involves transient sinusoidal blood stasis and massive hepatocyte endocytic vesicles, *Gene Ther* 12, 927-935.

9 Acknowledgement

The present thesis closes another chapter of my life.

Before making the next move I want to take the time to thank all the people who supported me professionally and personally. Without you this work could not have been done.

First of all I would like to thank Prof. Dr. Eckard Wolf for the acceptance of this thesis at the veterinary faculty of the Ludwig-Maximilian-University Munich.

I am very grateful to Prof. Dr. Ernst Wagner for giving me the opportunity to perform this work in his laboratories. Thanks for the broad scientific support, helpful and fruitful discussions and the re-focussing on the overall aim that were essential for the success of this thesis.

A special thank goes to my direct supervisor Dr. Manfred Ogris for introduction into the world of *in vivo* imaging. Without his constant guidance, imperturbable optimism and easing jokes I would certainly have been lost somewhere in the depth between luciferin, luciferases and light emission.

Also, I would like to thank Dr. Martina Rüffer who backed me up in all troubles arising from the students training.

Thanks as well to those students, who helped me in the lab: Claudia Rauscher, Tim Tremmel, Sabine Hengge, Johannes Meyer and Silvia Rochlitz.

My special gratitude goes to Carolin Schweimer, who was not only of help, but did outstanding troubleshoots with balky experiments and never lost her dedication and patience. She and Mona Surma did a great job in dragging me back on track when I was at the brink of despair. Thanks for that.

I am deeply grateful to all of my colleagues for professional but foremost personal support.

Thanks to Ursula Biebl and Anna Kulinyak for taking care of all the laboratory consumables.

Thanks to Melinda Kiss and Miriam Höhn for scientific advice in molecular biology and cell culture but also for diverting discussions about non-scientific topics.

Thanks to Wolfgang Rödl for his patience and constant support in all the troubles a veterinarian can step into in a chemical laboratory, such as molarity calculations, life threatening chemicals, adverse machines and drug metabolism courses. An additional big

“thank you” for the unbending battle against all the adverse phenomena a working place can develop, such as “strange smells”, “freezing temperatures”, “in-door rainy days”, “bewitched computers”, “beeping telephones” and so on.

Thanks to Markus Kovac for the amicable cooperation in keeping the mouse house running. I appreciate his lessons on male perception, true friendship and the correct female dress code.

Last but not least thanks to Olga Brück for relieving us of all the administrative stuff whom scientists are not at all fond of.

I would like to thank all the PhD students and postdoctoral fellows I had the pleasure to work with.

First of all I owe my gratitude to Dr. Alenka Schwerdt and Dr. Nicole Tietze, who supervised my first steps in the laboratory and the mouse house and introduced me to everything/everybody I needed to know (including – and I highly appreciate that – to all of my new colleagues).

I was fortunate to work in the most crowded lab room together with the most inspiring and open-hearted people. Therefore I have to thank a lot of people, namely Miriam Höhn, David Schaffert, Dr. Nicole Tietze, Katarina Farkasova and Markus Kovac, for contributing to this great atmosphere.

Thanks to those colleagues who provided the basis for my thesis and worked in close cooperation with me, such as Christian Dohmen, Alexander Philip, Dr. Arkadi Zintchenko, Dr. Julia Kloeckner and Katarina Farkasova.

Without all of you this thesis could not have been done.

But additionally I would like to express my gratitude to all the people who supported me personally and thereby made me who I am today.

I will never forget the skiing holidays, including racy downhill with Manfred, Lili and Terese, “Schafskopfen” with Andy, Thomas, Christian and Christian and quite spicy and exotic dinners cooked by our foreign colleagues.

The various free time activities conducted by the “hard core” of those who are not even tired of each other after working time, like “T-G-I-F-beer”, running with Lili and Nicole, summer triathlon and swim exercises with Andy, “Munschkin” battles with David and Eva and betting battles with Andy and Kevin, “Dirndl” shopping with Arzu, Katarina, Melinda and Prajakta, “Wiesn” and “Nockherberg” visits and Munich nightlife experiences with all of them (to quote just some examples) made my time in Munich memorable.

But as important as sharing the fun parts are good advice in troublesome times. All of you repeatedly listened to my troubles. But my special thank goes to David, Michael, Andy, Nicole and Lili for extensive “smoking”, “hot chocolate” or “ice cream” discussions.

Beside my colleagues there are of course more people who had and still have a high impact on my performance.

I am very grateful to all of my friends, but especially to Angelika, Anna and Bianca, for their friendship over all these years.

A very special and cordially thank goes to Sesu for his trust in me, the altruistic support and all the perspectives he shows me.

Finally, I want to thank my family, especially my parents and Gerrit, for their never-ending love and support.

Without all of you I could not have done this thesis.